New Jersey Geological Survey

Bulletin 77

Contributions to the Geology and Hydrogeology of the Newark Basin

State of New Jersey
Department of Environmental Protection
Water Resource Management
New Jersey Geological Survey
2010

For product and ordering information:
World Wide Web: www.state.nj.us/dep/njgs/pricelst/pubsinfo.htm
PDF download: www.state.nj.us/dep/njgs/pricelst/njgsrprt.htm
Telephone: 609-777-1038

The NJ Geological Survey (NJGS) is a public service and research agency within the NJ Department of Environmental Protection. Founded in 1835, the NJGS has evolved from a mineral resources and topographic mapping agency to a modern environmental organization that collects and provides geoscience information to government, consultants, industry, environmental groups, and the public.
For more information on the NJGS visit us on the World Wide Web at: www.njgeology.org.

Front cover. Geophysical logging of the Springdale Golf Course, Princeton University, Mercer County, NJ by the NJ Geological Survey in December 2003. The Princeton University Carillon (Class of 1892 Bells) looms in the distance.

Contributions to the Geology and Hydrogeology of the Newark Basin

Edited by Gregory C. Herman and Michael E. Serfes, N.J. Geological Survey

Prepared in cooperation with
the U.S. Geological Survey,
Oberlin College, Lafayette College and
Michalski and Associates.

This volume is published as chapters A through F and Appendixes 1 to 4.

N.J. Geological Survey Bulletin 77

State of New Jersey
Department of Environmental Protection
Water Resource Management
New Jersey Geological Survey
2010

Conversion Factors and Datums

Multiply	By	To obtain
	Length	
micrometer (μm)	0.00003937	Inch (in.)
millimeter (mm)	0.03937	Inch (in.)
centimeter (cm)	0.3937	Inch (in.)
meter(m)	3.281	foot (ft)
kilometer (km)	0.6214	mile (mi)
	Area	
square kilometer (km^2)	0.3861	square miles (mi^2)
	Fluid volume	
1 gallon	231	cubic inches (in^3)
1 gallon	0.134	cubic feet (ft^3)
1 liter	0.264	gallon (gal)
	Flow rate (volumetric)	
1 liter per second (L/s)	15.85	gallons per minute (gpm)
1 cubic meter per day (m^3/d)	0.183	gallons per minute (gpm)
1 cubic meter per day (m^3/d)	35.3107	cubic foot per day (cfd)
1 cubic foot per second (cfs)	449	gallons per minute (gpm)
	Hydraulic conductivity	
1 centimeter/second (cm/sec)	1.97	feet per minute (ft/min)
1 centimeter/second (cm/sec)	2837	feet per day (ft/day)
1 centimeter/second (cm/sec)	21200	gallons per day per foot squared (gpd/ft^2)
1 meter/day (m/day)	24.5	gallons per day per foot squared (gpd/ft^2)
1 meter/day (m/day)	3.281	feet per day (ft/day)
	Transmissivity*	
meters squared per day (m^2/day)	**10.765**	feet squared per day (ft^2/d)
	Volume of water in wells	
h = height of water column (ft)	2” well	V = 0.16 h
	4” well	V = 0.65 h
	6” well	V = 1.47h
	8” well	V = 2.61 h
	10” well	V = 4.08 h

Temperature in Fahrenheit (^oF) = (1.8 x ^oC) + 32

*Standard units for transmissivity (T) are cubic foot per day per square foot times foot of aquifer thickness "[(ft^3/d)/ft^2]ft" or cubic meters per day per square meter times meter of aquifer thickness "[(m^3/d)/m^2]m." These mathematical expressions reduce to foot squared per day "ft^2/d" or meter squared per day "m^2/d."

Horizontal coordinate information is referenced to the North American Datum of 1983 (NAD83) unless otherwise stated. Vertical coordinate information is referenced to the North American Vertical Datum of 1988 (NAVD 88) unless otherwise stated.

Contents

[1]US Geological Survey, [2]Oberlin College, [3]West Virginia Dept. of Environmental Protection, [4]Lafayette College, [5]Michalski & Associates, Inc., [6]NJ Geological Survey, [7]Rutgers University

Appendix Contents

Borehole Geophysics and Hydrogeology Studies in the Newark Basin, New Jersey

Photos of organizers and panelists at the hydrogeology workshop at the New Brunswick campus of Rutgers University, November 11-12, 2004.
Workshop organizers (from left to right): Glen Carleton (USGS), Pierre Lacombe (USGS), Ying Fan Reinfelder (Rutgers University), Michael Serfes (NJGS), Zoltan Szabo (USGS), Lisa Senior (USGS), Gregory Herman (NJGS). Not shown are Laura Toran (Temple University), and Andrew Michalski (Michalski Associates).

Panel Discussion, Day 1. From left to right: Pierre LaCombe (USGS), Joseph Smoot (USGS), Paul Olsen (Lamont Doherty Earth Observatory), Roy Schlische (Rutgers University), Robert Bond (Langan Engineering), Andrew Michalski (Michalski & Associates), MaryAnn Malinconico (Lafayette College), and Gregory Herman (NJGS).

Panel Discussion, Day 2. From left to right: Daniel Goode (USGS), Joseph Smoot (USGS), Glen Carleton (USGS), Zoltan Szabo (USGS), Michael Serfes (NJGS), Donna Fennell (Rutgers University), and Danielle Rhine (Rutgers Uinversity). Photographs by Yuri Mun (Rutgers University).

Introduction

New Jersey Geological Survey Bulletin 77 is an outgrowth of a group discussion that took place in early 2004 following a Henry Darcy distinguished lecture given by Dr. Alan Shapiro of the U.S. Geological Survey at the New Brunswick campus of Rutgers University. This discussion focused on hydrogeological work being conducted in the Newark basin, an Early Mesozoic basin filled with fractured sedimentary and igneous bedrock located in eastern Pennsylvania, central New Jersey, and southwest New York State. The basin underlies some of the most densely populated areas in the country, and therefore, is increasingly subject to environmental stresses including increasing groundwater demand and pollution. Discussion revealed that there is a large amount of information being collected by investigators, but there is a lack of awareness and availability of this information, including the diversity of processes studied, the competing views concerning major controls on groundwater flow, flux, and quality, the various advanced tools and techniques currently used to understand these controls. A regional workshop subsequently was convened to address some of these needs on November 11-12, 2004 at the New Brunswick campus of Rutgers University. Participation of various government agencies, universities, and the private sector provided an initial forum for exchanging and integrating ideas and findings (see photos on the opposite page). At this workshop, a NJ Geological Survey publication was proposed to provide a synthesis of the cumulative body of work.

The result, Bulletin 77 contains six articles and four appendixes detailing geological research conducted in the Newark basin during the past 30 years. The purpose of this bulletin is to provide geologists and environmentalists with a more thorough understanding of how the basin formed and evolved, and how these developments affected present day groundwater storage, transmission, and chemistry. The first two articles (chapters A and B) focus on traditional geological aspects including the stratigraphic framework and bedrock composition, and detailed analyses and descriptions of the secondary minerals filling aquifer pores. These are critical aspects of how the basin aquifers formed and evolved into their present state, and provide a sense of dimension, geometry and composition for aquifers throughout the basin. The remaining four articles (chapters C through F) focus on hydrogeological topics. Chapter C addresses basin-scale groundwater movement in early stages of the basin's history using vitrinite-reflectance thermal-alteration indexes for the three primary formations in the basin, together with reported fission-track geothermometry, geochronology, and radiometric-age controls. With respect to modern groundwater issues, chapter D summarizes practical methods of characterizing groundwater flow in the shallow subsurface at contamination sites and discusses conceptual flow models for the fractured-bedrock aquifers. Chapter E focuses on arsenic in groundwater, a recognized public health issue, and summarizes the state of knowledge of its geologic sources, and its mobilization and transport in organic-rich black and gray beds and other red mudstone and siltstone beds. Chapter F summarizes the results of research conducted by NJGS on the types and distribution of subsurface water-bearing features (WBFs) penetrated by water wells throughout the basin. The WBFs are identified, photographed, measured, classified, and related to other aquifer properties using geophysical logs for each well. Detailed results of each project are summarized in the appendixes.

Appendixes 1 to 4 include study results from more than 30 hydrogeology studies of hundreds of water wells in the New Jersey part of the Newark basin from 2001 to 2008. The appendixes provide location maps, borehole-televiewer photographic records of borehole walls and features, and hydrogeological sections detailing the different types and occurrences of WBFs in the subsurface water-bearing zones of each aquifer. The appendixes are based on aquifer groups, including: 1) diabase and basalt igneous rocks, 2) Brunswick aquifer coarse-grained rocks, including conglomerate and sandstone, 3) Brunswick aquifer fine-gained rocks, including mudstone and siltstone and 4) Lockatong argillite and Stockton sandstone. Each appendix includes multiple entries, with each entry detailing the results for a single project.

We are thankful to have had the opportunity to work with the contributors and editors to see this bulletin to completion. This work provides a modern understanding of how the basin aquifers formed, how groundwater is stored and flows in these fractured-bedrock aquifers, and the sources, mobilization, and transport of naturally-occurring arsenic in the basin's groundwater.

Hydrogeology and Borehole Geophysics of Fractured-Bedrock Aquifers, Newark Basin, New Jersey

By Gregory C. Herman, NJ Geological Survey

Chapter F of

Contributions to the Geology and Hydrogeology of the Newark Basin

N.J. Geological Survey Bulletin 77

State of New Jersey
Department of Environmental Protection
Water Resource Management
New Jersey Geological Survey
2010

Contents

Figures

Tables

Chapter F

Hydrogeology and Borehole Geophysics of Fractured-Bedrock Aquifers, Newark Basin, New Jersey

Gregory C. Herman[1]

Abstract

This report summarizes the results of 36 hydrogeologic projects in which fractured-bedrock aquifers in the Newark basin were studied by the NJ Geological Survey from 2001 through 2008. These studies utilized geophysical logs of 128 water wells to determine the character, spatial distribution and continuity of geologic features that store and transmit groundwater. These water-bearing features (WBFs) are stratigraphic and structural in nature and were identified using an optical televiewer, a heat-pulse flowmeter, traditional geophysical logs, rock cores and other data. The geophysical records of each study are detailed in appendixes as hydrogeologic sections that chart WBFs in each well and aquifer.

The New Jersey part of the Newark basin includes the Stockton, Lockatong, Brunswick, and diabase aquifers. The Stockton, Lockatong and diabase aquifers correspond directly to the respective geologic formations. The Stockton is of alluvial origin and consists of arkosic sandstone with lesser amounts of siltstone and mudstone. The Lockatong is of lacustrine origin and is consists of gray, red and black argillite. The Stockton and Lockatong locally include alluvial fanglomerate and sandstone near the northwest, faulted margin of the basin. Diabase is of igneous origin and it intruded the Stockton, Lockatong and Passaic Formations as thick sills and thin dikes. The Brunswick aquifer includes rocks of lacustrine, alluvial and igneous origin that are, in ascending order: the Passaic, Orange Mt. Basalt, Feltville, Preakness Basalt, Towaco, Hook Mt. Basalt and Boonton Formations. The Brunswick consists of seven aquifer zones that differ in composition and texture in various parts of the basin. Four zones in the central part of the basin are underlain by fine-grained sedimentary beds of the Passaic Formation. These are the lower and middle, gray and red zones respectively, and consist of red and gray siltstone and mudstone and gray and black shale, arranged in stacked, cyclical sequences. These rocks were formerly mud, silt and sand deposited in shallow to deep lakes during alternating dry and wet climate cycles. Gray zones contain proportionately more gray and black shale than the red ones. Three other Brunswick zones in the peripheral margins of the basin contain coarse-grained sedimentary rocks mapped in the Passaic and Boonton Formations. These are conglomerate, conglomerate-and-sandstone, and sandstone zones and consist of red beds of alluvial and shallow lacustrine origin. The sedimentary and basalt formations of Early Jurassic age are included in the Watching zone. The basalt formations in the Watchung zone are designated basalt units in the Brunswick aquifer, rather than basalt aquifers.

WBFs in 119 of the 128 wells in the study were identified using optical and acoustic borehole televiewer images. Three types of WBFs were identified:

1) bedding planes and layers,
2) fracture planes, and
3) linear intersections of bedding and fracture planes.

Type 1 WBFs include planar fractures resulting from mechanical breaking along stratigraphic contacts between beds of varied texture and thickness. Type 1 also includes sedimentary beds and igneous layers that are highly porous and permeable owing to the dissolution and removal of secondary sparry minerals from fracture interstices and/or the rock matrix by interaction with weakly-acidic groundwater. Type 2 WBFs includes transmissive extension and shear fractures not parallel to the stratigraphic plane. Fractures are grouped here by gentle (1^o to 29^o), moderate (30^o to 59^o) and steep (60^o to 89^o) dip angles. Most conductive fractures are steeply-dipping tectonic extension fractures, including ordinary joints with fracture interstices that are free of secondary authigenic minerals that seal gaps. Type 3 features are intersections of strata and fracture planes that channel water along linear conduits. Examples of WBFs and their physical link to geological strata and structures are illustrated using two- and three-dimensional diagrams, photographs, and hydrogeologic sections, most of which are included in a set of appendixes.

Measured geophysical responses and types of

[1]NJ Geological Survey
29 Arctic Parkway, Box 427
Trenton, NJ 08825
greg.herman@dep.state.nj.us

WBFs in each aquifer and aquifer zone are summarized in tables. All types of WBFs occur in all bedrock aquifers. However, type 1 WBFs are most common in basalt (52 percent) and red, coarse-grained sedimentary units (48 percent). Type 2 features are most common in all aquifers (54 percent) and the highest percentage is in Brunswick fine-grained, gray units (70 percent). Type 3 features are the least common in all aquifers (about 12 percent) but are most common in the red, coarse-grained sedimentary beds (26 percent) including coarse-grained sandstone (24 percent) and conglomerate (48 percent).

Closely spaced wells make it feasible to construct hydrogeologic sections illustrating subsurface and topographic conditions. These sections include interpretations of the shallow and deep aquifer sections. The shallow section includes weathered bedrock to depths of about 60 to 100 ft below land surface (bls) in areas having less than 20 ft overburden. Groundwater flowing in shallow bedrock under natural, nonpumping conditions is generally controlled by local topographic gradients and nearby surface-water drainage. Topographic gradients stem from the differential erosion of gently-dipping strata. Groundwater flowing in deep bedrock is semiconfined. Deep wells tapping semiconfined strata have complex, nonpumping cross flows with water entering and leaving uncased parts of the boreholes at different depths and flow rates. Hydrogeological sections normal to the strike of bedding demonstrate how these nonpumping cross flows result from gently-dipping, semiconfined beds cropping out at various elevations with differing hydraulic potentials.

Stratigraphic unconformities within thick accumulations of red mudstone locally include mineralized paleosoil. These horizons commonly have dense accumulations of authigenic minerals subsequently removed locally from the rock matrix by mineral dissolution to form highly-transmissive, type 1 WBFs and strata-parallel water-bearing zones. Paleosols also form stratigraphic pinchouts where strata are cut off at gentle angles by superjacent beds forming hydrologic boundaries that locally retard groundwater recharge in poorly productive aquifers.

Introduction

Bedrock aquifers of Early Mesozoic age in the Newark basin (figs. F1 and F2) underlie some of the most densely populated and heavily industrialized areas in the United States. They also supply vast quantities of groundwater for domestic, commercial, and industrial needs (Hoffman and Lieberman, 2000). Protecting these aquifers from pollution and overpumping requires an understanding of the hydrogeological framework, that is, the configuration of the various bedrock strata and fractures that store and transmit groundwater.

The purpose of this report is to provide a fuller understanding of the hydrogeologic framework of fractured-bedrock aquifers in the Newark basin by summarizing the types, spatial distribution and continuity of water-bearing features (WBFs) identified in water wells in the New Jersey part of the basin (fig. F3). Identification of these features relies on borehole geophysical data that were collected, analyzed and catalogued for 36 hydrogeologic projects involving 128 water wells drilled into the Stockton, Lockatong, Brunswick and diabase aquifers (table F1, figs. F2 and F3, and appendix table A1). These projects were conducted by the NJ Geological Survey (NJGS) in support of publicly-funded pollution investigations and water-supply-permit activities by the NJ Dept. of Environmental Protection (NJDEP), or were NJGS research projects funded by the NJDEP Hazardous Waste Spill Fund. Most of the geophysical data were collected by the NJGS in water-supply and water-monitoring wells with uncased, open boreholes of 6- to- 8 inch diameter, appendix table A1). Most wells are less than 600 ft deep and were drilled into bedrock overlain by thin (< 20 ft) overburden. Some borehole records were generated by secondary parties and donated to the NJGS or were part of third-party geotechnical investigations that were reanalyzed and incorporated here. The hydrogeologic effects of thick unconsolidated deposits overlying bedrock are not considered in this report.

Identification of WBFs relies on the use of borehole imaging systems, including optical and acoustical televiewer probes, and a multidirectional video camera. Of these, the optical televiewer (OPTV) is the most useful because it provides an oriented, digital photographic record of the strata penetrated in a well plus secondary structures such as fractures and faults. The digital data files are processed and interpreted for structural analysis of the aquifer as seen in the borehole walls. A tally is kept of the types of WBFs within the various aquifer units and zones, and the ranges of observed geophysical responses for the various types of geophysical logs employed in these analyses. Photographs and schematic diagrams of the OPTV used by the NJGS are included in a section

Table F1. Number of projects and wells for each major aquifer.

Aquifer	Projects	Wells
Diabase……..	4	7
Brunswick……..	24	102
Lockatong……..	4	9
Stockton…….	5	12
Total*……..	**36**	**128**

* Some projects and wells cover more than one aquifer so that total values are less than column totals.

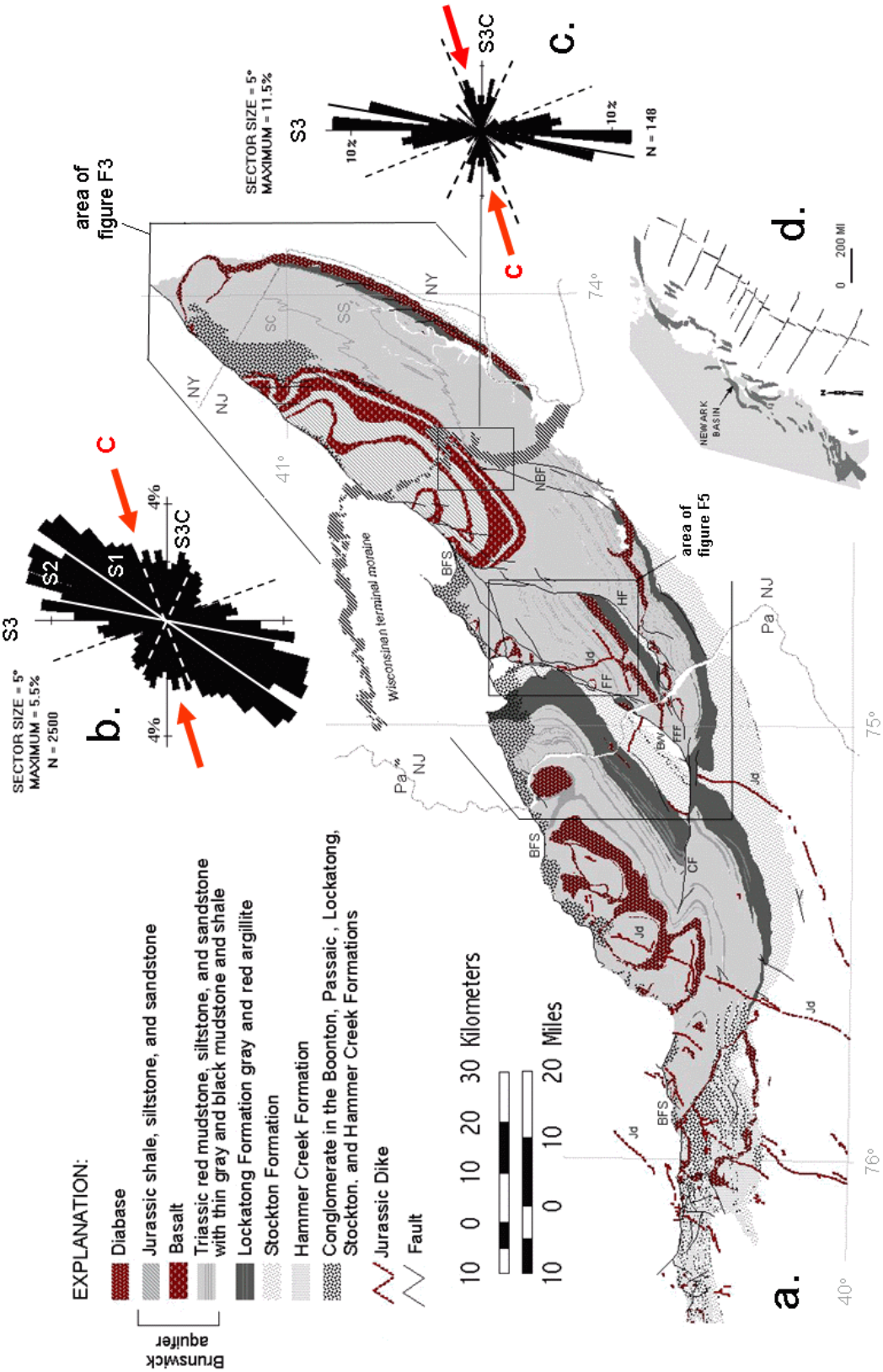

Figure F1. Bedrock geology of the Newark basin (**a.**) showing stratigraphic formations, sedimentary facies, faults, dikes, and circular histograms of extension fractures. Bedrock map compiled from geographic information system shape files for New Jersey (http://www.state.nj.us/dep/njgs/geodata/dgs04-6.htm), New York http://www.nysm.nysed.gov/data/lhud_bedr1a.zip), and Pennsylvania (http://www.dcnr.state.pa.us/topogeo/map1/bedmap.aspx#entirestate). Histogram **b.** shows plane strike for 2500 sets of tectonic extension and shear fractures in about 1300 outcrops in the center of the basin. Extension fractures in Late Triassic rocks predominantly strike N20°E to N65°E whereas those in younger Early Jurassic rocks strike more northerly (histogram (**c.**). adapted from Monteverde and Volkert (2005). SC – sandstone and conglomerate facies, SS – sandstone and siltstone facies, NBF – New Brunswick fault, HF – Hopewell fault, FF – Flemington-fault, FRF - Furlong fault, CF - Chalfont fault, RF - Ramapo fault. Index map of Mesozoic basins on the East Coast (**d.**) adapted from Schlische (1992).

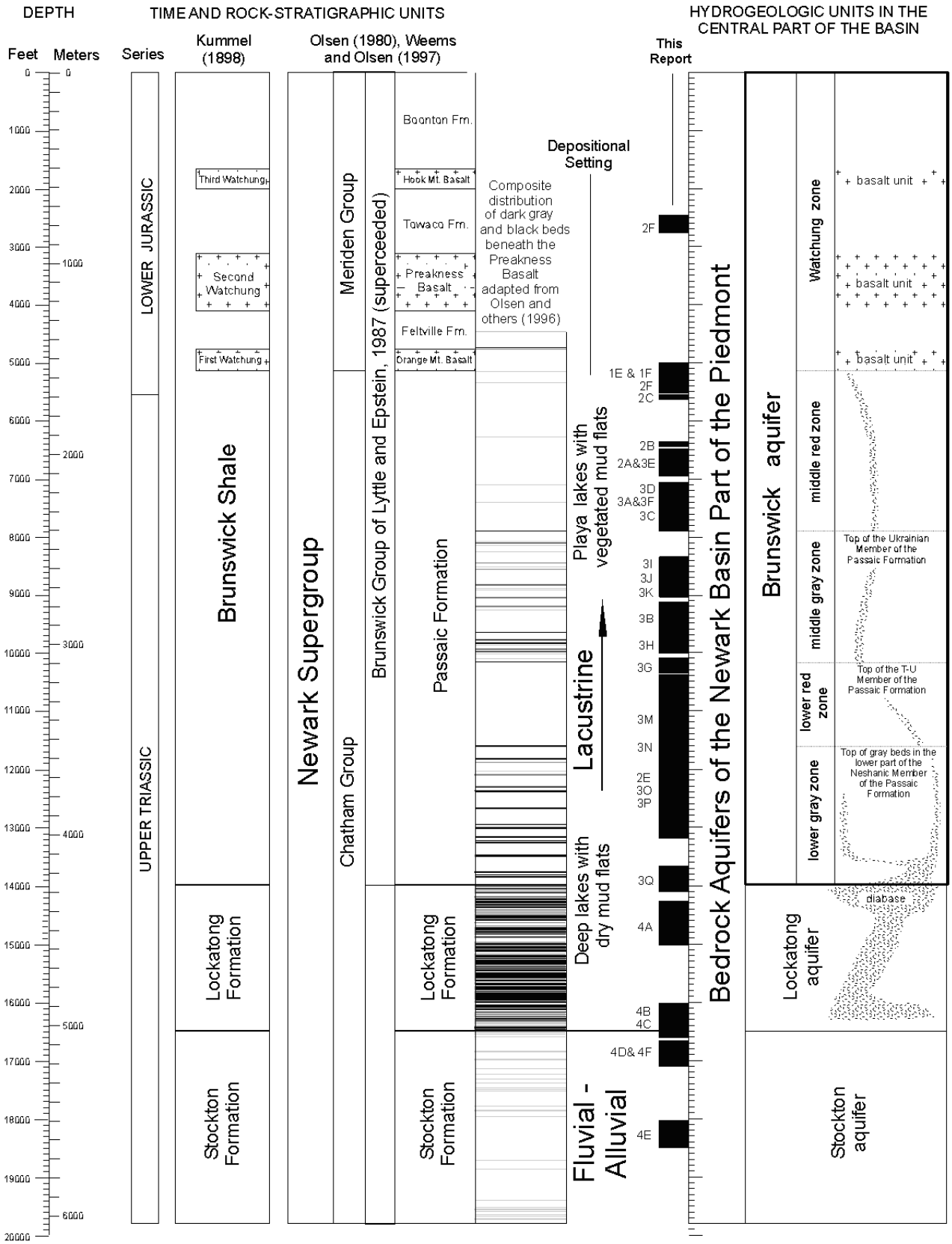

Figure F2. Summary of time, rock and hydrogeologic units in the central part of the Newark basin showing approximate stratigraphic intervals covered in this report and earlier studies.

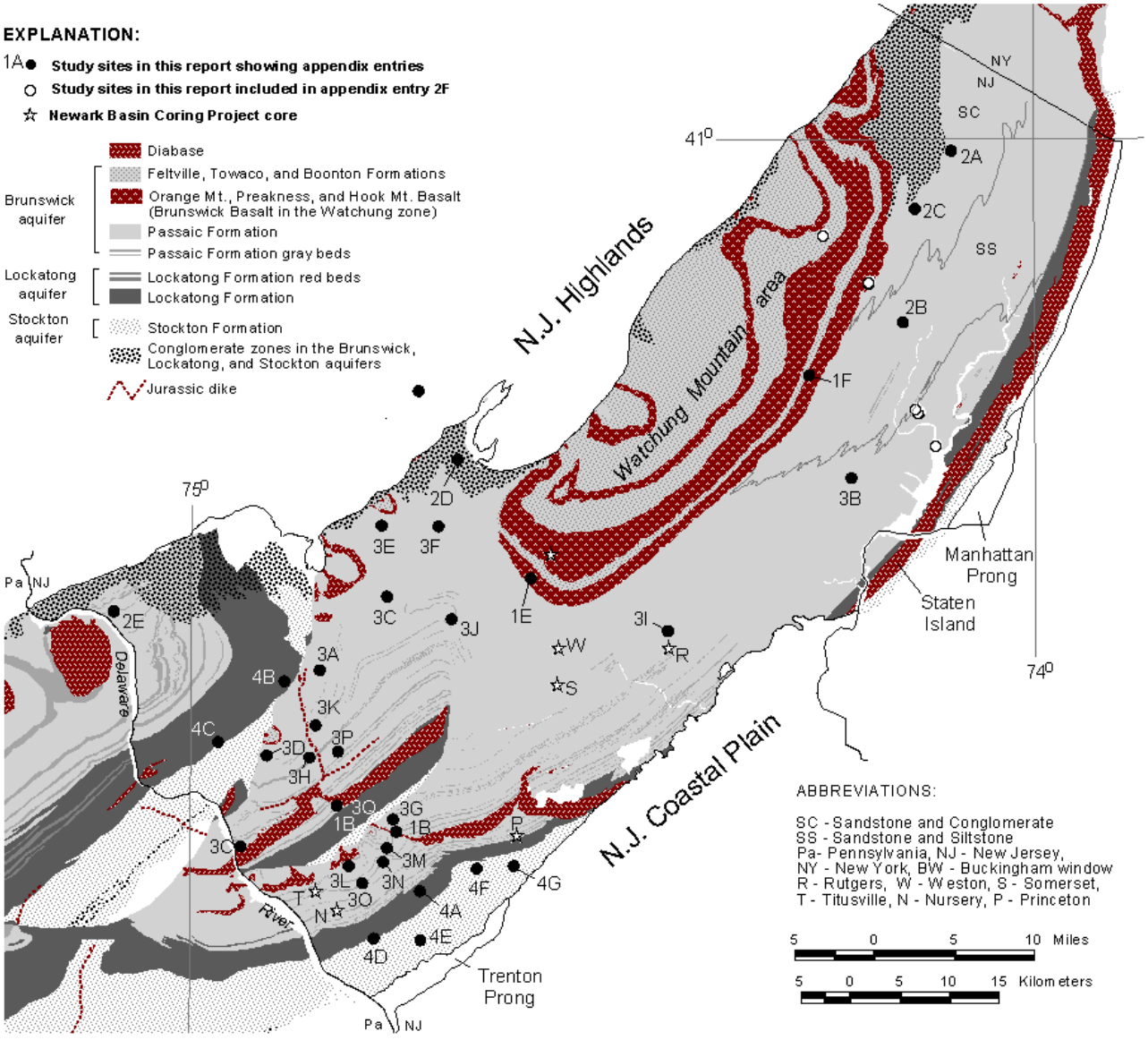

Figure F3. Map of study locations showing core locations for the Newark Basin Coring Project (Olsen and others, 1996). Geology compiled from sources listed in figure F1.

on borehole geophysics.

Each borehole analysis is unique. The WBFs in each well differ from one another in their characteristics and spatial distribution. Some WBFs are simply bedding planes whereas others are tectonic fractures or intersections of bedding and structural features. Where two or more boreholes are closely spaced, their WBFs can be compared and represented in profile, or in 3D perspective, as a hydrogeological framework. This delineates the continuity and orientation of the WBFs and bedrock features constituting the stacked set of aquifers and less-permeable layers in a multilayer aquifer system.

Other data collected for this report include heat-pulse flowmeter (HPFM) studies of borehole cross flows, bedrock core samples, and straddle-packer tests with information on groundwater yield for specific bedrock intervals. Local differences in land elevation are also shown to affect the direction and rate of borehole cross flows in different areas. Cross flows were mostly measured under nonpumping conditions but some projects include flow measurements that were taken while pumping.

This work builds on fracture mapping (Herman, 1997) and uses customized computer programs (Herman, 2000; 2001a) to represent geological structures and hydrogeological data in map,

profile and three-dimensional (3D) perspectives. Computer-generated, 3D models may be used to illustrate the spatial distribution and geometry of interpreted hydrogeologic features, and how they locally interact to transmit groundwater or result in borehole cross flows.

Detailed records for each project are presented in appendixes 1 to 4. These records include a location map of logged wells, detailed structural analyses of stratigraphic layering and fractures from OPTV records, and hydrogeologic sections based on geophysical logs that illustrate specific examples of the types and distributions of WBFs. The appendixes are used throughout the report to illustrate relationships.

Geologic setting

The Newark basin is a sedimentary basin of Early Mesozoic age formed on the eastern North American continental margin during tectonic rifting and breakup of the supercontinent Pangea prior to the onset of sea-floor spreading and formation of the Atlantic Ocean (Dietz, 1961; Sanders 1963). The basin covers about 2900 mi^2 extending from southern New York across New Jersey and into southeastern Pennsylvania (fig. F1). It is filled with as much as 20,000 ft of Upper Triassic to Lower Jurassic sedimentary and igneous rocks (fig. F2) that are tilted gently northwestward, faulted, and locally folded (Schlische and Olsen, 1988, Schlische 1992; and Olsen and others, 1996). Multiple tectonic movements have affected the basin (Lucas and others, 1988; de Boer and Clifford, 1988; Schlische, 1992; Herman, 2005). Tectonic extension peaked from the latest Triassic to the earliest Jurassic with widespread igneous activity (tholeiitic basalt and diabase) and a marked increase in sediment-accumulation rates (Schlische, 1992). Tectonic deformation and synchronous sedimentation continued at least into the Middle Jurassic (Schlische, 1992) when extensional faulting and associated tilting and folding were succeeded by periods of contraction, uplift and erosion, similar to events in other areas of the continental margin (de Boer and Clifford, 1988; Withjack and others, 1995; Olsen and others, 1992). Coastal plain sediment deposited on the underlying Mesozoic rocks resulted in flexural loading of the continental margin during the Late Mesozoic through Early Cenozoic (Owens and Sohl, 1969; Owens and others, 1998). Late Cenozoic glacial and fluvial deposits and erosion landforms in the Newark basin form buried valleys, till plains, upland surfaces, fluvial terraces and scarps (Stanford, 2000; Stanford and others, 2001).

The Newark basin is underlain by three sedimentary formations of Late Triassic to Early Jurassic age and overlying and discontinuous sedimentary rocks of early Jurassic age interlayered with basalt flows (figs. F1 and F3). The primary bedrock units include in ascending order: the Stockton, Lockatong, and Passaic Formations (fig. F2). The Stockton Formation unconformably overlies basement rocks of Proterozoic and Paleozoic age. Basal conglomerates of the Stockton fine upward into sandstone and progressively thicker mudstone interbeds. The unit reaches a maximum thickness of about 4000 ft. The Lockatong Formation includes black, gray, and red argillite (highly indurated shale), and gray mudstone and siltstone; the red units are progressively more abundant higher in the sequence. The formation reaches a maximum thickness of about 3500 ft. The Passaic Formation in central parts of the basin is mostly red mudstone and siltstone with lesser amounts of gray and black shale (Olsen and others, 1996). These fine-grained facies grade laterally into sandstone and conglomerate in the southwest and northeast margins of the basin. The maximum thickness of the Passaic Formation is about 11,800 ft.

The sequence of interlayered basalt and clastic sedimentary rocks of early Jurassic age includes in ascending order: the Orange Mt. Basalt, Feltville Formation, Preakness Basalt, Towaco Formation, Hook Mt. Basalt, and Boonton Formation. Each basalt formation consists of several basalt flows (Tollo and Gottfried, 1992) that were fed by diabase sheets and dikes that intruded and thermally metamorphosed older sedimentary deposits in the basin. The sedimentary rocks of Jurassic age are fluvial-deltaic sandstone, siltstone, and lacustrine mudstone. The combined maximum thickness of Jurassic bedrock in the Newark basin is about 4920 ft. All sedimentary formations in the center of the basin grade into alluvial fanconglomerate to the northwest along the border fault system (figs. F1 and F3).

The succession of lacustrine sedimentary rocks in the Lockatong and Passaic Formations reflects a gradual climatic change during a 30-million-year period from arid conditions in a narrow basin to subhumid ones in a broad basin (Smoot and Olsen, 1994). Sediment deposited in deep lakes bordered by dry, saline mud flats was gradually succeeded upwards by sediment deposited in shallow lakes flanked by wetter, vegetated mud flats (Smoot and Olsen, 1985; 1988). Included in this succession is a series of graduated sedimentary cycles that reflects the rise and fall of lake level (Van Houten, 1962), largely in response to periodic and cyclical climatic changes occurring over tens of thousands to millions of years (Olsen, 1986; 1988). The detailed stratigraphy of the Newark basin is based on outcrop mapping and an extensive, regional rock-coring program referred to as the Newark Basin Coring Project (fig. F1, and Olsen and others; 1996). The basic rock-stratigraphic cycle of sedimentary units in the basin is the 'Van Houten' or 'precession' cycle (Olsen,

1986). It marks the successive, gradational accumulation of mudstone and siltstone during transgressive, highstand, and regressive lake stages controlled by a 21,000-year precession cycle of the earth's axis. Precession cycles are arranged in a series of large-order compound sedimentation cycles resulting from orbital variations occurring over 109,000-, 413,000-, and ~2,000,000-year periods. A typical Van Houten cycle in Late Triassic sedimentary bedrock includes a middle high-water sequence marked by fine-grained shale, mudstone and siltstone sandwiched between other sequences of mudstone, siltstone, and sandstone deposited in shallow transgressive, then regressive waters. The upper unit reflects lowstand periods when the lake was at least occasionally dry, with incipient soil development in a subaerial environment.

Sedimentary beds and igneous layers dip gently 1° to 29° northwest in the basin except near faults and folds, where strata dip more moderately (30° to 59°) to steeply (60° to 89°) as a result of tectonic strain. Gently-dipping strata commonly are cut by secondary bedrock fractures that dip steeply and are mapped as joints (fig. F4). In those areas containing more moderately-to-steeply-dipping strata, these secondary fractures dip more gently, suggesting that most extension fractures formed early in subhorizontal strata, then were locally tilted together with bedding during later stages of deformation. Herman (2001) reported that the average dip of extension fractures (joints) in pre-tilted beds in the center of the basin is about 70°, the ideal angle of inclined shear failure reported for extended rocks (Xiao and Suppe, 1992; Dula, 1991; Withjack and others, 1995).

Figure F4. Joints in the Passaic Formation (location 3Q, fig. F3). Joints are elliptical, systematic extension fractures that form in clustered sets. They dip steeply and form in conjugate arrays. Photograph provided by Matthew Mulhall.

Four groups of faults and steeply- to moderately-dipping extension fractures have been mapped in the basin (Herman, 2005). The groups are differentiated by structural strike and relative age. The first and oldest set (S1) strikes N.35°E. to N.70°E. subparallel to the basin's northwestern, faulted margin (fig. F1). The group of faults defining the northwest margin is referred to as the border-fault system (BFS of Schlische, 1992). Individual fault segments generally show a progressive counterclockwise change of strike from about E.-W. in the southwest part of the basin to N.40°E. in the northeast. Fault dips steepen from about 25° to 30°S.E. near the Delaware River (Ratcliffe and others, 1986) to about 60° to 70°S.E. in the northeastern parts of the basin (Ratcliffe, 1980). The BFS displays a right-stepping geometry of individual fault segments in map view (fig. F1). Parts of the northwestern margin lacking mapped faults are interpreted to be underlain by buried and hidden, or 'blind' fault splays covered by younger sediment (Schlische, 1992; Drake and others, 1996). Fault movement along the BFS is thought to be predominantly normal dip-slip with a maximum stratigraphic offset exceeding 3.5 miles in the northeast. Detailed studies of fault slip from core drilling along the BFS show complex fault movements with oblique dip-slip commonly reported (Burton and Ratcliffe, 1985; Ratcliffe and others, 1990).

The second structural group (S2) includes intrabasinal faults and associated extension fractures striking ~N.10°E. to N.35°E. (fig. F1). S2 intrabasinal faults include isolated and interconnected splay faults that cluster into fault systems separated by 10 to 20 miles along the basin's transverse axis (fig. F1). In New Jersey, from west to east, they are referred to as the Flemington (FF), Hopewell (HF), and New Brunswick (NBF) faults. These faults decrease in stratigraphic displacement eastward, the FF having the greatest displacement and the NB the least. The FF links up with the Furlong (FRF) and Chalfont (CF) faults in Pennsylvania (Schlische, 1992). The CF-FRF-FF system of faults displays a curved map trend veering from about E.-W. in Pennsylvania to N.-S. in New Jersey before connecting with the BFS (Houghton and others, 1992). A window of Paleozoic bedrock crops out midway along its trace at the point of maximum curvature (fig. F1). The FF has component faults interpreted to dip about 40° to 70°E. with predominant normal slip and lesser right-lateral oblique slip (Drake and others, 1996). Maximum stratigraphic

offset exceeds 2.5 miles near Flemington. The HF is interpreted as dipping 50° to 70°E, with normal and right-lateral oblique slip (Drake and others, 1996; Laney, 2005; Laney and others, 1995). Some of the western faults in the HF system are normal faults with westerly dips of about 70° (Monteverde and others, 2003). The NBF is interpreted to have predominantly normal slip on steeply-inclined faults (Stanford and others, 1998) and maximum stratigraphic offset of about 1.5 miles near New Brunswick (Owens and others, 1998).

The third structural group (S3) includes faults and fractures striking from about N.20°W. to N.15°E. in the northeast part of the basin near the Watchung Mountains (Monteverde and Volkert, 2005; Volkert, 2006). A fourth group of extension fractures (SC3) and oblique-slip faults strikes about E.-W. in complimentary directions to S3 structures. S3C mineralized cross fractures in New Jersey occur southeast of the HF and north of the Trenton Prong (Herman, 2005). They may represent late-stage dilation and mineralization of earlier, curviplanar, nonsystematic cross fractures optimally aligned for reactivation and growth in the present compressive-stress field (C in fig. F1). The interactions between the different fault, fold, and fracture sequences record episodes of extension and collapse followed by periods of compression and uplift (de Boer and Clifford, 1988; Schlische 1992; Herman, 2006;2008).

Hydrogeologic units and the leaky, multi-unit aquifer system

Hydrogeologic units in the New Jersey part of the Newark Basin reflect local stratigraphy and consist of four principle aquifers including the Stockton, Lockatong, diabase and Brunswick (fig. F2). The Stockton, Lockatong and diabase coincide with the respective geologic formations. The Stockton is of alluvial origin and consists of arkosic sandstone with lesser amounts of siltstone and mudstone. The Lockatong is of lacustrine origin and consists of gray, red and black argillite. The Stockton and Lockatong locally include alluvial fanglomerate and sandstone near the northwest, faulted margin of the basin. Diabase is of igneous origin and it intruded the Stockton, Lockatong and Brunswick as thick sills and thin dikes (figs. F1 and F3). The Brunswick is of lacustrine, alluvial and igneous origin and includes, in ascending order: the Passaic, Orange Mt. Basalt, Feltville, Preakness Basalt, Towaco, Hook Mt. Basalt and Boonton Formations.

Shale is typically used by well drillers and geologists working in the basin to describe many of the fine-grained red beds in the Brunswick, but Van Houten (1965) and Smoot and Olsen (1988) have shown that most of it is massive mudstone and siltstone. Much of the fissility of the red beds has been destroyed by repeated episodes of wetting and drying of sediment on mud flats, by bioturbation, and by the accumulation and growth of secondary authigenic minerals, including gypsum and calcite, in the shallow subsurface during diagenesis. Shale-like bed partings commonly develop in these massive rocks following prolonged weathering near the surface. The term shale is historically embedded in the literature and existing databases, but ‘mudstone and siltstone’ are used here to refer to red fine-grained beds. ‘Gray’ and ‘black’ beds in the Brunswick aquifer consist of gray mudstone and shale, dark gray shale, and black, laminated to thin-bedded shale rarely exceeding 6 ft in stratigraphic thickness. Other colors recorded for these beds, such as brown, yellow and green, are called gray here as they commonly represent weathered gray and black beds. Black beds are mapped as part of the ‘gray beds’ on geologic maps but it is important to note them separately in subsurface investigations. For example, unusually high radioactivity, radon and concentrations of arsenic have been found in dark gray and black shale in the basin (Szabo and others, 1997; Serfes and others, 2005). These beds typically act as units confining adjacent red-bed aquifers. This is apparent where fluid electrical conductivity and resistivity logs show stepped values at contacts between red and gray beds (appendix 3G8, 3H2, 3I2, 3I3, 3K3, 3K6, 3K7, 3M10, 3N5, 3N13 and 3P4).

The Brunswick is subdivided into eight aquifer zones to facilitate aquifer mapping and cataloguing of aquifer parameters. These zones reflect variations in bedrock composition and texture in the different formations and parts of the basin. A conglomerate zone is used for the northwestern, faulted margin of the basin containing cobble fanglomerate in the Passaic Formation and the sedimentary formations of Jurassic age in the Watchung Mountain region (figs. F2 and F3). A second zone is used for this same region for the fine-grained sedimentary rocks and interlayered basalt formations (figs. F2 and F3). This Watchung zone also occurs as small stratigraphic outliers along the Flemington fault system (Houghton and others, 1992; Drake and others, 1996). The remaining six zones are used for areas underlain exclusively by the Passaic Formation. Of these, two occur in the northeast margin of the basin underlain by pebble conglomerate and sandstone red beds of alluvial origin (figs. F2 and F3). The four remaining zones are used for the central part of the basin underlain by fine-grained sedimentary beds of lacustrine origin. They are, in ascending order: the lower gray, lower red, middle gray and middle red zones (fig. F2). The middle zones were previously defined to be upper zones (Herman, 2001b) but are redefined here because they physically occupy middle sections of the aquifer, and also to avoid confusion

when referring to red strata of Jurassic age in the upper part of the Brunswick. These four zones show a pronounced stratigraphic cyclicity (Olsen and others, 1996) that facilitates aquifer subdivision where distinct sets of bed-strike-parallel topographic ridges formed as a result of differential erosion of the red, gray, and black strata (fig. F5). Hard beds of siltstone, mudstone and shale form ridge tops whereas softer or extremely fractured mudstone and shale underlie valleys. Typically, in areas underlain by fine-grained lacustrine beds, stratigraphic sequences having abundant black and gray shale form prominent ridges with dark shale underlying northwest-facing hill slopes (Appendix 3G1, 3H1, 3K1, 3N1, 3N2 and 3P1).

The lower gray zone of the Brunswick aquifer consists of red and gray mudstone and siltstone, and gray and black shale. It correlates with the lower part of the Passaic Formation, from the top of the Lockatong Formation to the top of two, thick gray-bed sequences in the bottom of the Neshanic Member (fig. F2). These gray beds form a prominent topographic ridge in the center of the basin. The upper contact of the lower gray zone is mapped at the base of this ridge (fig. F5). The lower red zone consists of red mudstone and siltstone with minor gray mudstone and shale, and includes the remainder of the Neshanic Member upwards to the base of the Kilmer Member (fig. F2). The middle gray zone consists of red mudstone and minor siltstone, gray mudstone, and gray and black shale. It correlates with the middle part of the Passaic Formation, including the Kilmer Member, upward to the top of gray beds in the bottom of the Ukrainian Member (fig. F2). The middle red zone consists of red mudstone and micaceous siltstone, with minor amounts of gray mudstone and shale. It includes the remainder of the Ukrainian Member and the Passaic Formation upward to the base of the Orange Mt. Basalt.

Figure F5. Shaded relief map of the Amwell Valley showing four zones in the Brunswick aquifer with contacts following pronounced topographic ridges. db – diabase, sf – Stockton Formation, lf – Lockatong Formation, ba - Brunswick aquifer, cg – conglomerate, rv – Round Valley reservoir.

The directional hydraulic property of fractured sedimentary bedrock aquifers in the Newark basin has been repeatedly demonstrated since Herpers and Barksdale (1951) first reported that wells aligned along bedding strike could affect one another. During the past twenty years, Andrew Michalski and colleagues have defined the *Leaky Multi-Layer Aquifer System* (LMAS) model for Triassic mudstone and siltstone in the basin along with an outline of useful approaches for conducting hydrogeological investigations at groundwater pollution sites (see Chapter D and Michalski, 1990; Michalski, 2001; Michalski and Klepp, 1990; Michalski and Gerber, 1992; Michalski and Britton, 1997). The LMAS model describes the tendency of groundwater to flow along gently inclined bedding fractures in deep, multi-unit bedrock (fig. F6). These transmissive, bed-parallel features are nonuniformly distributed in a vertical direction by distances ranging from about 30 ft to more than 150 ft. They are separated by thick, leaky stratigraphic layers with subvertical extension fractures that are developed throughout the basin but differ spatially in density and orientation (Herman, 1997; 2001). These fractures are locally open and conductive and they provide pathways for groundwater to infiltrate and flow between highly transmissive units. In some instances, the steeply dipping fractures have been reported to be the principle conduits for groundwater recharge, storage and flow (Knapp, 1904; Vecchioli, 1965; Spayd, 1985). Both bedding and fracture components of the LMAS are discussed in detail below and illustrated in the appendexes.

Overburden and weathered bedrock overlie LMAS components and provide storage and pathways for groundwater to recharge deeper aquifers. Permeable fractures in weathered bedrock include the steeply-dipping extension fractures from which secondary cements such as calcite have been removed by weakly acidic, recharging groundwater (Herman, 2001b). Deep flow zones are recharged with groundwater where transmissive beds extend upward to shallow depths (Michalski and Britton, 1997).

Groundwater infiltrates fracture apertures in the weathered bedrock that may extend from the surface to depths exceeding 60 ft in parts of the basin with thin

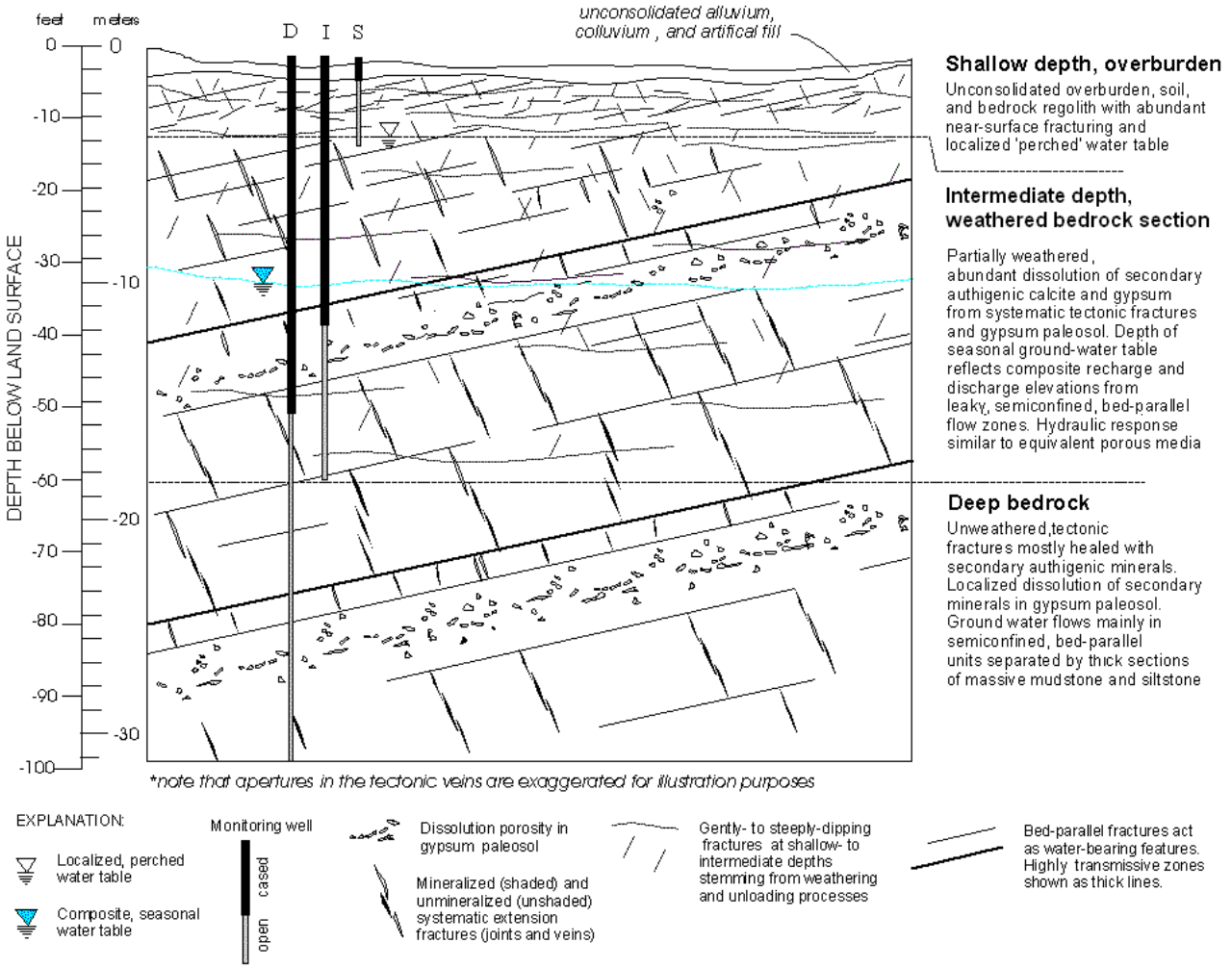

Figure F6. Profile view of a three-tiered conceptual framework of fractured sedimentary aquifers in the Newark basin as modified from the leaky, multi-unit aquifer system (LMAS) model of Michalski and Britton (1997) for areas lacking thick (>50 ft) overburden. Steeply-dipping extension fractures occur as joints near land surface where they are open and permeable. They are mostly plugged by secondary minerals in the subsurface except where these were removed by dissolution. Transmissive WBZs mostly occur along fractures developed between stratigraphic layers, shown above as dipping gently right-to-left. Other layer-parallel WBZs occur as permeable fracture sets preferentially developed within specific strata or as tabular strata with abundant secondary porosity resulting form the dissolution of secondary, authigenic minerals from the bedrock matrix. The latter are referred to as gypsum paleosoil that increases in abundance in the lower and middle red zones of the Brunswick aquifer. Gently-dipping fractures stemming from weathering and unroofing are common near land surface to intermediate depths in weathered bedrock. Groundwater flow is progressively more anisotropic at depth, reflecting the gradual change from many open, interconnecting flow conduits near land surface to very few, widely spaced conduits in deep bedrock that lie along bed partings or in paleosol horizons. Layered WBZs in deep bedrock are generally separated by thick confining beds. Deep (D), intermediate (I) and shallow (S) wells are used to monitor each tier.

overburden (Herman, 2001b). In contrast, buried-valley aquifers are thick accumulations of glacial sediment locally overlying bedrock that can store and transmit significant volumes of deep water. These aquifers commonly are saturated and overlie weathered bedrock. The depth and hydrogeological properties of weathered bedrock underlying buried-valley aquifers in glaciated terrain are not well documented.

Borehole geophysics

The identification and classification of WBFs rely on the use of slim-line geophysical tools to measure the various physical properties of the formation and its water. Most of the geophysical logs detailed in the appendixes were collected by the NJGS. Logs collected by others are so noted in appendix table A1 along with

NJGS project names and well parameters, including location coordinates, uses and construction details. Conventional geophysical logs typically include borehole diameter (caliper-inches), single-point electrical resistance (ohms), natural gamma-ray emissions (counts per second - cps), water temperature (^{o}F), fluid electrical conductivity (microsiemens/cm) and resistivity (ohm-m). Oriented borehole images were acquired using optical and acoustical borehole televiewer (BTV) systems manufactured by Robertson Geologging Ltd.. The basic design and components of the OPTV system are shown in figure F7. The OPTV provides a continuous, orientated, 360º digital image of the strata and structures in the borehole wall. Figure F8 shows how OPTV data are processed and displayed as digital records. The cylindrical image is processed and transformed into rectangular coordinates using Robertson Geologging Ltd. proprietary computer software (fig. F8a). Planar structures penetrated by the borehole are interpreted on the 'unwrapped and flattened' image (fig. F8b). Hard-copy outputs of the interpreted images are generated at 1/12 (fig. F8c) and/or 1/8 scales using the Joint Photographic Experts Group (JPEG) image format and are then catalogued as NJGS library records. Structural interpretations include the description and 3D location and orientation of planes intersecting the borehole, including plane dip and strike (Fig. F8c and Table F2).

The structural analysis of WBFs using BTV technology is based on a selective-sampling procedure of imaged borehole features. Stratigraphic layers and fractures were measured in ~16-ft stacked intervals such

A

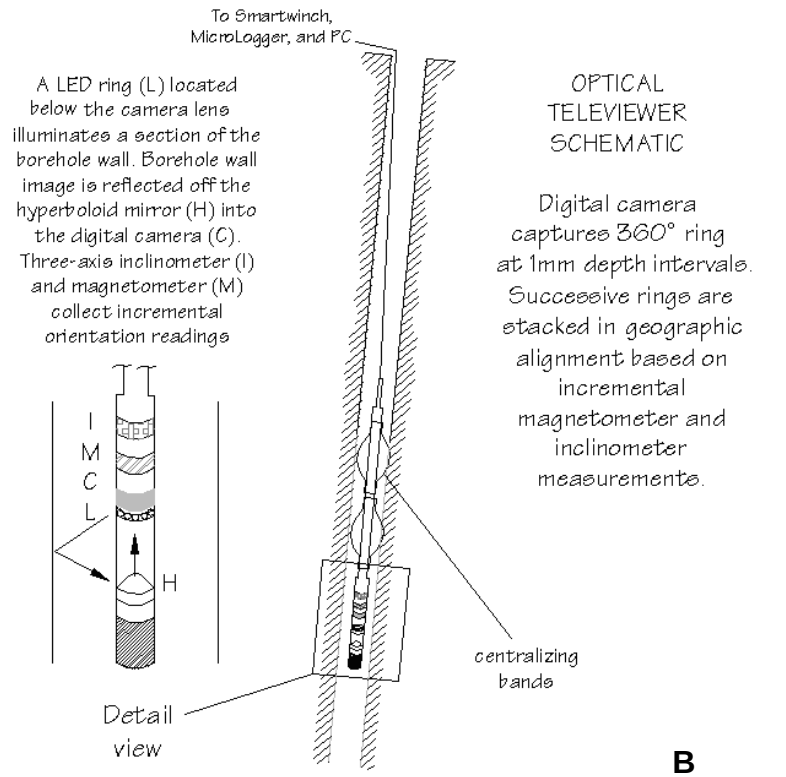

B

Figure F7. The NJGS OPTV is used for mapping subsurface geological features in 6- and 8-inch water wells. A. Photos of the sonde assembly showing how the tool is deployed. B. Illustrations show that light from the diode source (L) illuminates the borehole wall and reflects the wall image off the hyperbolic mirror (H) into the digital camera (C). Cabled-depth readings together with magnetometer (M) and inclinometer (I) incremental readings provide a 3D orientation for each pixel. Data are transmitted up a coaxial cable for data storage and processing on a personal computer.

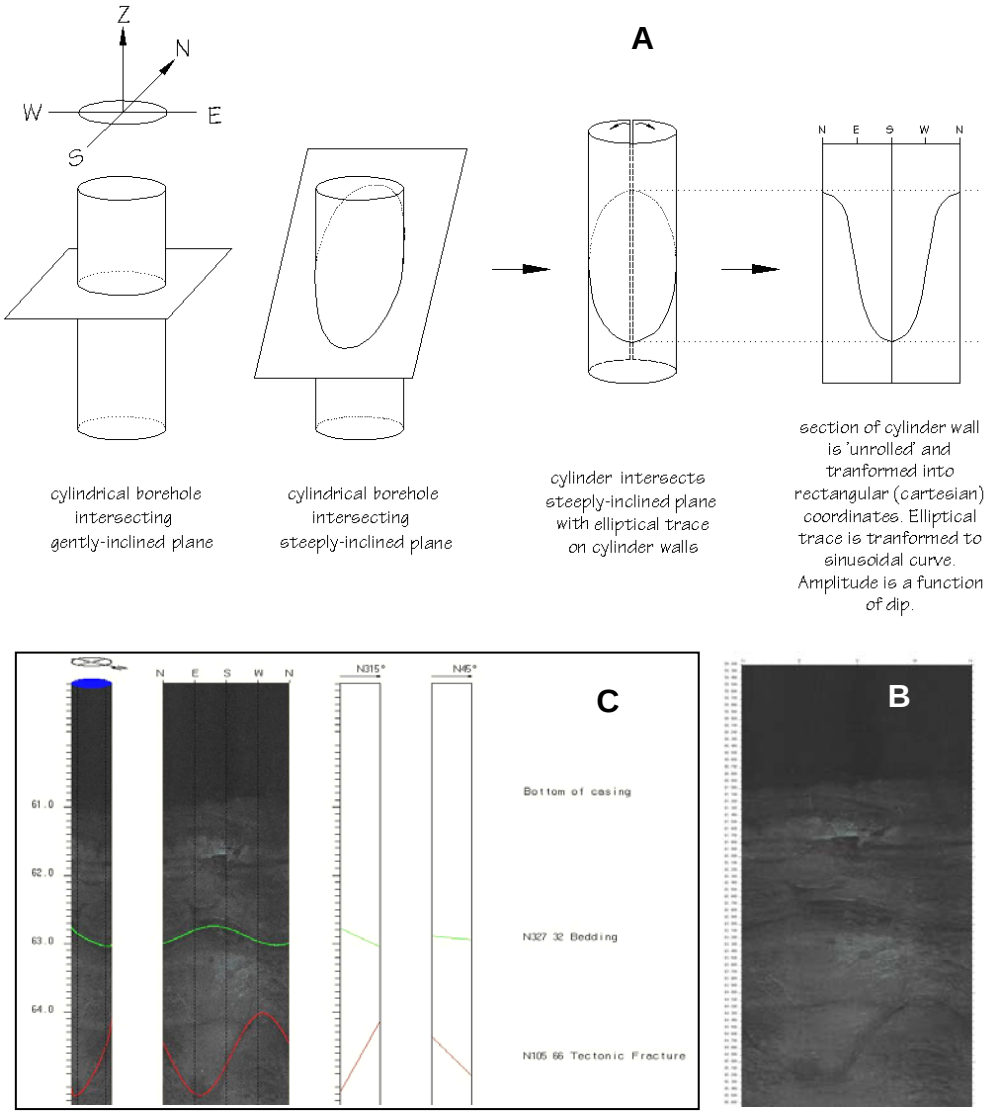

Figure F8. BTV diagrams and images showing how OPTV records are processed interpreted, and output as data records. A. Schematic diagram showing how a cylindrical BTV image is 'unrolled' for display during data processing. B. Uninterpreted OPTV record. C. Interpreted OPTV record including stick diagrams and feature parameters output at 1/12-scale using a JPEG image format.

Table F2. Example of data fields and parameters for interpreted geological features output using BTV processing software. Column headings are explained below.

ID	DEPTH	INC	BRG	CODE	AZM	DEV	CO	C1	C2
1..	28.388	23	188	2	213.99	3	Fracture	Gently-inclined	Vein
2..	32.138	34	25	0	208.00	3	Bedding		
3..	33.403	52	198	2	211.40	3	Fracture	Moderately-inclined	Conductive
4..	35.922	15	19	0	218.66	4	Bedding		Conductive
5..	43.290	77	185	2	220.06	4	Fracture	Steeply-inclined	Vein

ID – Feature-identification sequential integer
DEPTH – Depth (feet) below log reference datum to center of measurement point
INC - Inclination or dip (degrees) of the measured plane
BRG - Bearing or dip azimuth (degrees) of measured plane
CODE - Integer used to differentiate between stratigraphic layering and fracturing
AZM - Azimuth bearing (degrees) of borehole drift
DEV - Angular deviation (degrees) of borehole from vertical
C0, **C1** and **C2** – Text variables for classifying geological features

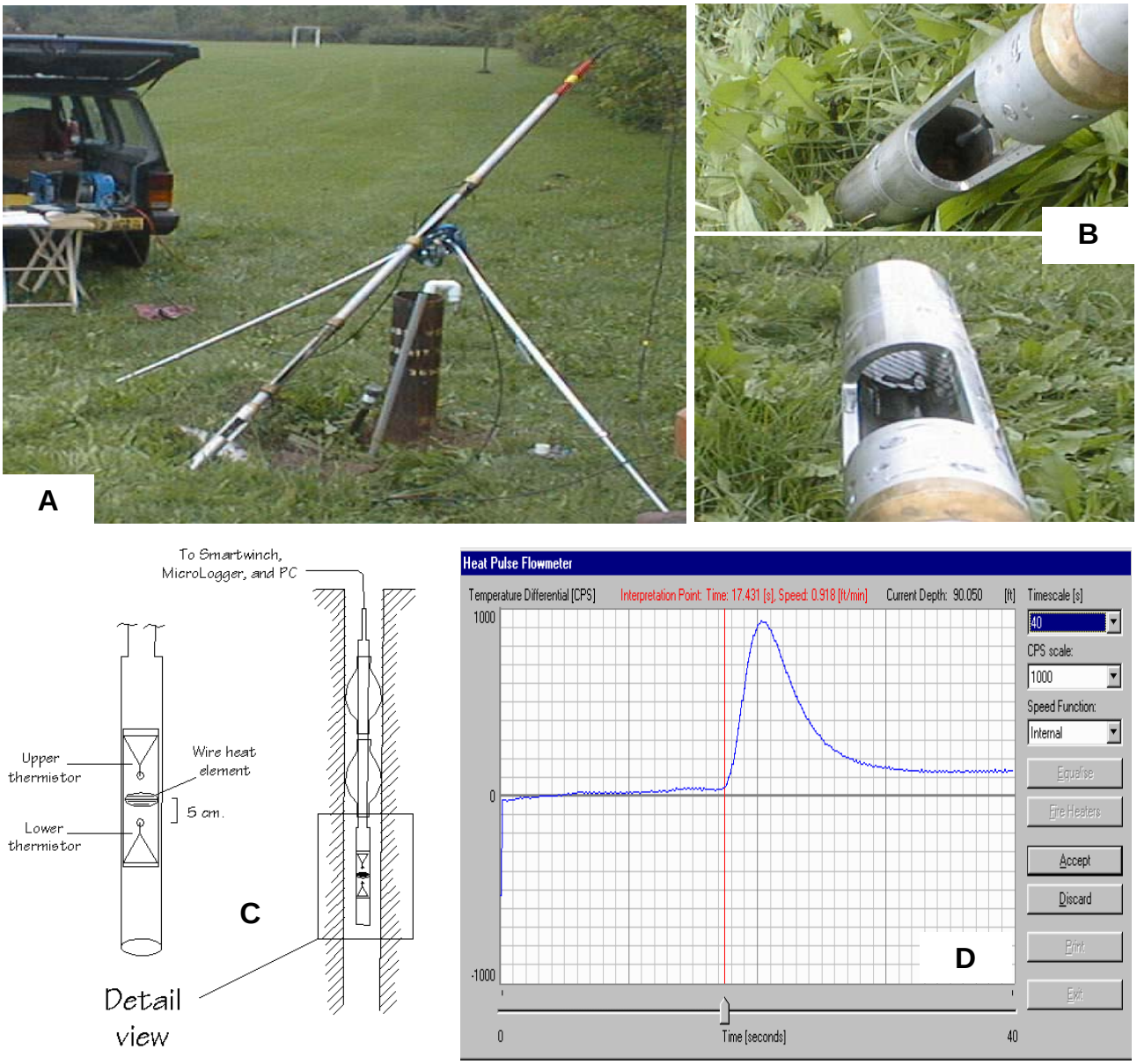

Figure F9. Photos and diagrams of the Robertson Geologging, Ltd. HPFM used by the NJGS. A. Photo of the sonde resting on the tripod/pulley and connected with a coaxial cable to the winch located in the Jeep. B. Details of the sonde assembly including the tool aperture, upper thermistor and heating grid. C. Schematic diagram illustrating the details of the sonde assembly and a profile of the instrument as deployed in a well. D. The data-acquisition interface showing a graph of the HPFM response time (x-axis, seconds) and the temperature differential between upper and lower thermistors (y-axis, counts-per-second (CPS)). Graph axes are scaled using pull-down menus shown on the upper right part of the display. The HPFM response time and fluid speed values (ft/min) are determined by sliding the cursor control along the base of the x-axis to the first deflection point where the arriving heat pulse produces a large positive-count differential for the upward thermistor as charted above. A downward-deflected curve indicates downward flow.

that a particular, measured feature was commonly taken to represent closely-spaced sets of subparallel features within the sample interval. For example, elliptical fracture surfaces cluster in spaced sets within stratigraphic intervals (fig. F4). For BTV interpretations, a single fracture measurement represents a fracture set if strikes or dips of multiple fractures are within 5° of each other. Five-degree histogram bins are the basis of graphical structural analyses reported in the appendixes. Structural planes identified in BTV records as stratigraphic layers, fractures, or faults are included in output tables using an ASCII text-file format (table F2). Data fields in these text files include depth of a feature, plane inclination (dip) and bearing (dip

azimuth). The azimuth bearing and deviation of the borehole from vertical is also recorded for each feature. These data tables are used for subsequent structural analysis of feature orientations and for investigating subsurface spatial relationships of geological features and well-field components using GIS (NJ Geological Survey, 2001).

Water flow rates in some boreholes were measured using a heat-pulse flowmeter (HPFM). HPFM technology was developed in the early 1970's and is in widespread use today. Unlike other probes used in this study, the HPFM is deployed in a well in a stationary mode at specific depths rather than actively trolling upward or downward in the well at a constant rate (fig. F9). The HPFM is selectively positioned to bracket potential WBFs identified using OPTV records, trace anomalies from fluid logs, or enlarged openings in the borehole indicated by caliper logs. The data-acquisition assembly of the HPFM probe contains a horizontal wire-grid heating element and thermistors positioned above and below it (figs. F9B and C). Apertures in the device (fig. F9B) permit the free flow of well fluid through the assembly. The flow velocity of the fluid column is determined when a pulse of electric current is emitted to the heating grid, which in turn warms the water column in the vicinity of the grid. The warm-fluid front migrates within the moving fluid column past a thermistor where it is detected, then registered as a response curve on a system display of the sonde log (F9D). Depending on the direction of flow in the borehole, either the upper or lower thermistor detects the warm fluid front first. An upward-flow response is measured at the first break point of an upward deflection (fig F9D) and vice versa for downward flow. Response time is computed in seconds and calculated fluid speed in feet per minute (ft/min). The HPFM is repeatedly equalized and fired at a specific depth until reproducible or similar results are obtained (table F3). Multiple values of traveltime and fluid velocity are measured and recorded at each depth, then combined later to determine an average time and fluid velocity at each depth of measurement (table F3). These values are then compared to other geophysical and geological records to construct profiles of borehole flow as part of the hydrogeologic interpretation of geophysical logs (table F3 and appendixes 1 to 4). The HPFM used by the NJGS has been tested and found to be about 75 percent accurate for measuring fluid velocities ranging from 0.3 to 17.0 ft/min (~0.5 to 25 gpm in a 6-inch well). Flow velocities below the 0.3 ft/min minimum threshold value are reported as no measurable flow.

Fractures, bedding in sedimentary rocks, and layering in basalt and diabase, are described as hydraulically conductive in illustrations titled

Table F3. Heat-pulse flowmeter data for well 4 (appendix 1B5)

Multiple heat-pulse arrival-time measurements at various depths[3]		**Average heat-pulse arrival time (HPAT) and calculated fluid velocity and flow rates at various depths. Average arrival time > 14 sec and < 32 seconds**			
Depth[1] (ft)	heat-pulse arrival time (seconds)	Depth[1] (ft)	HPAT (seconds)	Calculated fluid velocity[2] (ft/min)	Calculated flow rate[3] (gpm)[4]
85.10	26.880	85.10	26.88	0.20	0.30
99.95	20.625	99.95	21.72	0.38	0.56
99.95	22.813	119.60	18.18	0.53	0.79
119.60	15.000	160.00	16.98	0.59	0.87
119.60	17.569	200.00	16.50	0.62	0.91
119.60	18.472	240.00	18.09	0.54	0.79
119.60	20.417				
119.60	20.417				
160.00	16.979				
200.00	15.885				
200.00	17.656				
200.00	15.313				
200.00	17.135				
240.00	16.771				
240.00	18.229				
240.00	19.271				

[1]Depths are below land surface

[2]Calculated fluid velocity = ((-.85*(Log(HPAT)+3)) modified from Herman (2006)

[3]Rate calculated for a 6-in. well

[4] gpm - gallons per minute

The average results are charted to the right.

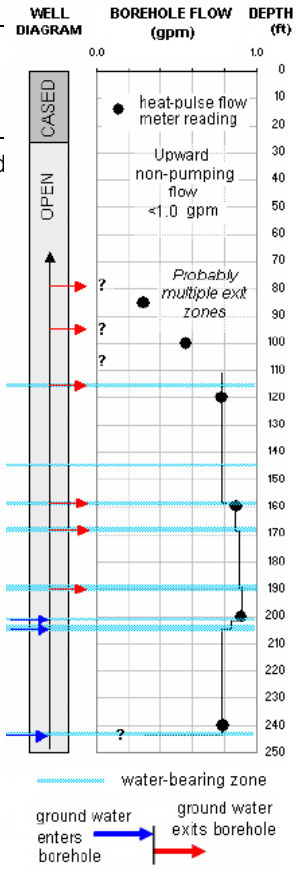

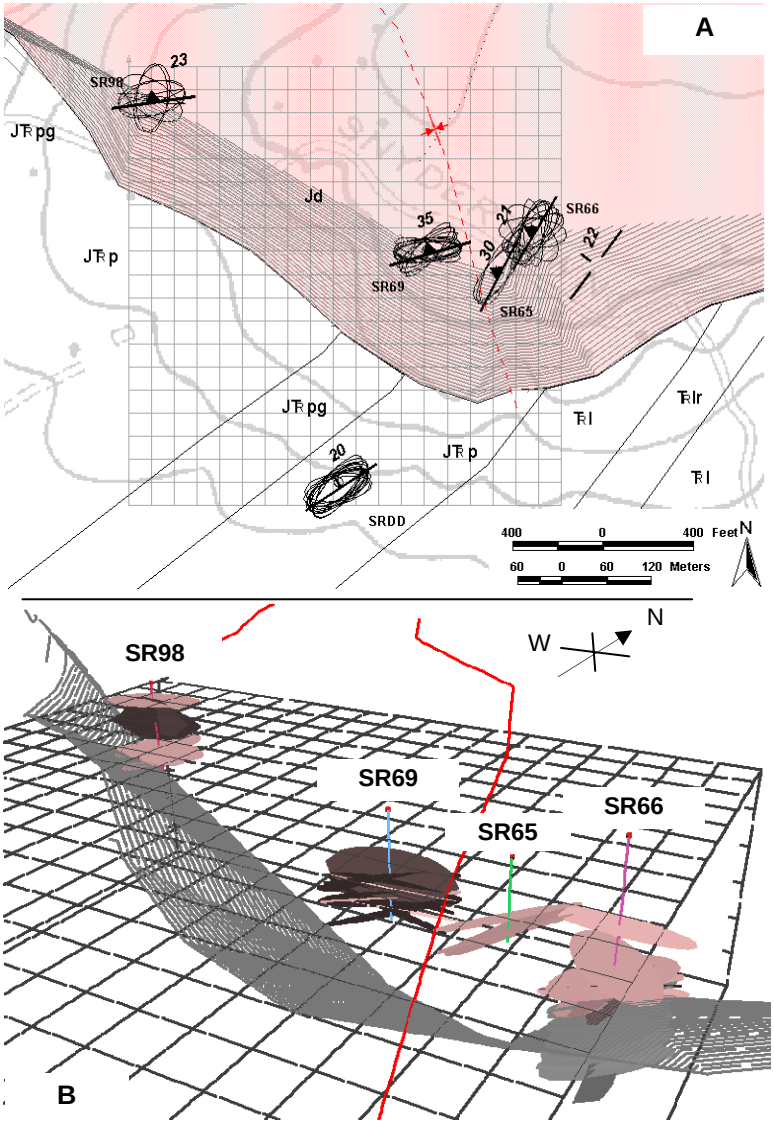

Figure F10. Geologic map (A) and 3D display (B) of the Snydertown Road domestic-well study (appendix entry 1B). The map view shows average strike and dip of compositional layering in diabase (Jd) and bedding in underlying mudstone and shale (wells SR66 & SRDD) determined from the five OPTV surveys. The bottom contact of the diabase sill with the underlying Passaic Formation was penetrated in well SR66.Compositional layering (pink) and sedimentary bedding (gray) are shown using 3D ellipses in B. An elliptical plane was generated at the point of interpretation of each structure and plotted along its borehole trace. Planes have 300-ft major axes oriented along strike and a 2:1 strike-to-dip aspect ratio. The orientations of layer ellipses in diabase are outlined on the map. Ellipses plot on top of one another when projected to the land surface and show that compositional layering varies considerably in strike in the vertical direction over small distances. The 3D perspective is viewed looking slightly down and a little West of North. Grid cells and tick marks are 100ft. Part of the sill base is mapped above using 5 ft contours and represented below in 3D. Axial traces of nearby folds are dashed red lines in the map and solid red lines below. The folds are gentle warps in the diabase layering and therefore postdate intrusion.

"Hydrogeologic interpretation of geophysical logs" in appendixes 1 to 4. A water-bearing zone (WBZ) is identified as a continuous section of the open hole where two or more WBFs intersect, based on visual evidence in OPTV records (appendix 3A3, 3D4, 3J4 and 3N7). Flow in and out of these zones typically produces trace fluctuations on fluid temperature, electrical conductivity/resistivity and flow logs (appendix 3D7, 3D9, 3K3 and 3K5). These anomalies are used to position the HPFM and straddle-packer assemblies for measuring the section fluid velocity and volumetric flow rates.

Groundwater chemistry within each WBZ or WBF commonly differs from that in the other isolated subsurface flows but mixing takes places in the open borehole. Dissolved minerals from inflows may sometimes precipitate on the borehole wall adjacent to the entry point in response to the chemical mixing of formerly isolated waters. Examples of borehole stains originating from WBFs are shown in the appendixes for the following units:

Diabase – figs. 1A3 and 1B6
Brunswick basalt units – 1E6 (left)
Brunswick sedimentary units – figs. 2E6, 2E7, 3C2, 3D13 (well 53), 3G5, 3H3, 3J4 (well 84), 3M12 and 3M18
Lockatong – 4B3 (left) and 4B7

Staining originating from WBFs may sometimes indicate both upward and downward flow directions (appendix 1A3) caused by the combined influence of natural cross flows and pumping that temporarily reverses borehole flow directions. Staining from pumping-induced flows appears subordinate to that stemming from natural, nonpumping cross flows, based on consideration of where the pump is set relative to the conductive feature. Nonpumping cross-flow velocities

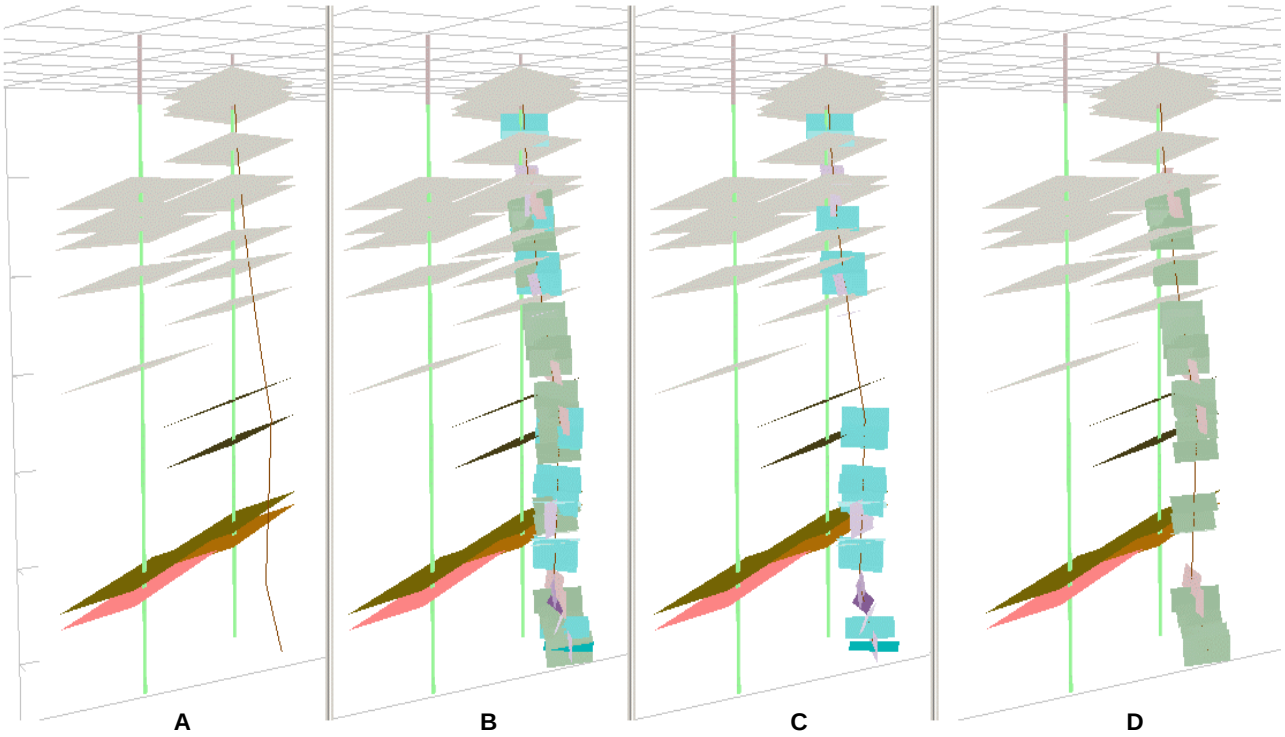

Figure F11. Paneled views from a 3D-GIS computer model of two wells in the lower part of the Passaic Formation (appendix entry 3P). Grid cells at the top of each panel and tick marks to the left mark 100-ft. intervals. Driller-reported WBZs are shown to parallel sedimentary bedding and are plotted along the vertical projection of two wells with cased (pink at top) and open (green) intervals . WBZs dip gently northwest (right-to-left). Dark planes at bottom represent high-yield zones. The actual borehole geometry of the well on the right is shown with a thin, crooked line that was generated using an OPTV record. It shows that the well has an irregular shape that drifts in a direction opposite to bed dip (A). All measured fracture sets are plotted along the borehole trace in B. Fractures are rectangular with a 50 ft strike and 25 ft dip length. One set of fractures (S1) is plotted in C whereas a different fracture set (S2) is plotted in D. This demonstrates that specific fracture sets may be local only, or may overlap. Borehole drift is affected by fracture distribution; major deviations in the borehole trace coincide with the distribution of different fracture sets. Highest-yielding WBZs correspond to sections containing overlapping fracture sets.

in poorly productive units are generally below about 0.3 gpm, the instrument detection limits of the NJGS HPFM (Herman, 2006). Low flow rates may cause more uniform log responses for the fluid column because only one or two entry streams are mixed.

Each BTV survey and interpretation generates structural geological data for the set of interpreted OPTV records and borehole-orientation information (table F2). Computer programs are used to statistically analyze these structural data and visualize their interrelationships using geographic information systems (GIS) and other computer-aided drafting software (figs. F10 and F11). Structural analyses of BTV data in the appendixes include circular histograms and stereonet diagrams that show map trends and 3D orientations, respectively. Mean strike, dip, and/or dip direction (azimuth) of bedding, layering, and fractures are included in these analyses for individual wells or groups of wells in a well field. Statistical maximums are interpreted for the 3D stereonet diagrams then used to represent primary map orientations of stratigraphic layering and secondary fractures on project-site maps throughout the appendixes.

Water-bearing features

WBFs have been identified in all four major aquifers, all zones in the Brunswick aquifer and in groups of igneous and sedimentary rocks (tables F4 and F5). A total of 650 WBFs are identified in the hydrogeologic sections, based on geophysical logs for 35 of the 36 projects and 119 of the 128 wells detailed in the appendixes. Detailed examples of diverse types of WBFs are presented using OPTV records for each study. Each project summary includes examples of interpreted features for at least one well. Some projects include multiple wells, and some feature interval-flow data derived from HPFM logs and/or from

straddle-packer tests. Projects having the most complete data include a hydrogeological profile and/or a 3D graphic interpretation showing the spatial distribution of WBFs in the subsurface. Studies with hydrogeologic interpretations of multiple wells having detailed subsurface information are indexed as hydrogeologic framework studies. Of the 36 projects (table F1), 12 are presented as framework studies, with 10 for the Brunswick and one each for the Lockatong and Stockton aquifers. Of the 10 for the Brunswick, 3 involve basalt units in the Watchung zone.

Three types of WBFs are identified including:

1) bedding planes and layers,
2) fracture planes, and
3) linear intersections of bedding planes and fracture planes

The assignment of a particular WBF to a specific group based on borehole imagery is a highly subjective exercise. In many instances, a feature or set of features can be assigned to more than one group. For example, networks of hydraulically conductive fractures having the same orientation locally occur within specific stratigraphic horizons (appendix 3D13 and 3D14). In such cases, there are both stratigraphic and fracture controls on the occurrence of a WBZ and it is difficult to assign WBF classification to solely one feature. They are therefore identified as being both a conductive bed and conductive fractures. Primary considerations for classifying WBFs are: what specific feature stores and conducts groundwater, and, if features are nonlayering fractures, is there good evidence showing stratigraphic control of their occurrence and distribution? In the examples noted above, the features are included as type 3, layer-fracture intersections, though arguments may be made for both stratigraphic and structural control. A common problem is that these relationships are demonstrated locally for a single well, but the continuity of features within a specific stratigraphic interval in a specific area requires BTV coverage in many wells with overlapping stratigraphic coverage; this however is not common. Designation of a feature simply as a ‘conductive tectonic fracture’ may not capture its essence as part of a group of features restricted to a particular stratigraphic horizon and lying just beyond the physical limits of the borehole record. In general, hydraulically conductive intersections of both strata and fracture planes are probably undermeasured in the summary geostatistics listed in tables F5 and F6.

Type 1 WBFs – Bedding planes and layers

WBFs classified as bedding planes and layers include planar features and tabular units lying parallel to sedimentary beds or compositional layering in igneous basalt and diabase. No distinction is made between the planar and tabular varieties in the hydrogeologic interpretations of borehole geophysical logs included in the appendixes; WBFs are simply noted as either conductive bedding (cb) or conductive layering (cl). However, the different varieties of these features are discussed here to promote an understanding of how groundwater is stored and conveyed in the Newark basin aquifers.

The permeable geological features related to stratigraphic layering include bed partings, or simple, planar mechanical breaks along contacts between strata composed of differing grain size and bed thickness. Examples from the different aquifers listed below are referenced to figures in the appendixes:

Diabase – 1B4-left, 1B6 and 1C3-left
Basalt – 1E6 and 1F3
Brunswick – 2A2 (well 15), 2A3, 2BC2, 2C2, 2D3, 2D4-left, 2E6-left, 2E7-right, 3C2, 3C5, 3J4-right, 3J5-right, 3M17-right, 3N6-left, 3N10-left, 3N12-right, 3P2 and 3E6-left
Lockatong - appendix 4B3-left and 4C3
Stockton – appendix 4C4 and 4D3.

Features having millimeter thickness are commonly noted by logging technicians as bedding fractures or ‘hairline’ fractures lying in the stratigraphic plane. They can be locally enlarged as a result of weathering and drilling operations to appear on BTV records as being a few centimeters thick (appendix 4D3 and 2E6-left and 2E-right). The lateral continuity of these mechanical breaks can be seen in BTV surveys of closely-spaced wells, and their subsurface continuity and capacity to be conductive planes extends hundreds to thousands of feet (appendix 4F9-left, 3N11-left and 3N12-right). Conductive bed partings commonly occur near stratigraphic contacts between gray and black beds with massive red mudstone and siltstone (appendix 3E6-left and 3H3)). Two additional types of WBFs noted as conductive bedding or layering include tabular units with thickness of as much as a few feet and lateral continuity over distances of hundreds of feet. These tabular units include highly-fractured transmissive strata lying between adjacent, confining mudstone and siltstone layers (appendix 3D13 and 3D14) and fine-grained sedimentary beds containing mineral-dissolution zones within gypsum paleosoil horizons (appendix 3F4--right and 3M7).

Massive mudstone beds make up a large part of the Brunswick aquifer (Smoot and Olsen, 1985; 1994). They list three types of massive mudstone common in the Newark basin including burrowed, mud-cracked and root-disrupted varieties. Each represents an end member having dominant, distinctive fabrics that denote specific depositional environments (Smoot and Olsen,

Table F4. Summary of projects, wells and WBFs, geophysical logs collected and ranges of log values

PROJECTS, WELLS AND WATER-BEARING FEATURES							GEOPHYSICAL LOGS COLLECTED												LOG-RESPONSE VALUES				
Appendix Entry	NJGS Project	Aquifer or aquifer zone(s)	no. of wells	number of WBFs by type			Imaging			Fluid				HPFM		Formation				fluid resistivity (ohm-m)	fluid conductivity (μs/cm)	HPFM borehole flow (np) (gpm)	formation natural gamma bswl (cps)	formation single-point resistance bswl (ohms)
				1	2	3	O	A	B	FC	FR	FT	PA	np	pu	C	G	SP	SL					
1A	258 S. Franklin AGW	diabase	1	7	3	1	X		X	X	X	X		X	X		X	X		14-30	328-700	0.3	20-105	1595-2074
1B	Snydertown Rd AGW	diabase	4	3	18	1	X		X	X	X	X		X		X	X	X		12-56	185-900	0.9	4-55	370-2900
1C	Crusher Rd.WS	diabase	1	1	4		X			X		X									205-475			
1D	Block 38, Lot 16 WS	diabase	1		7		X		X	X	X	X				X	X	X		7-71	141-1410		5-86	2920-2994
1E	Essex County CC WS	BWB	3	15	4	3	X		X	X	X	X		X				X		18-40	257-545	5.6	7-61	70-1550
1E	Essex County CC WS	BSS	1	3	1	1	X		X	X	X	X		X				X		22-36	280-285	0.5	30-160	123-300
1F	1163 Delaware AGW	BWB	1		6	1	X		X	X	X	X		X		X	X	X		7-28	354-1385	ND	6-42	500-2270
1F	1163 Delaware AGW	BMR	1				X		X	X	X	X		X		X	X	X		28-29	349-354	ND	15-195	140-234
2A	Ridgewood Shell GWI	BSC	9	4			X																	
2B	Sandos-Clariant GWI	BSS	2	6	4		X																	
2C	Hoffman-LaRoche GWI	BSC	3	3	6		X																	
2D	Hamilton Farms WS	BC	3	8	7	14	X			X		X		X							120-234	0.3		
2E	Milford Boro WS	BLGSC	5	22	8	8	X		X	X	X	X		X		X	X	X		15-43	230-1370	ND	44-560	1240-4288
2F	Passaic Flood Tunnel GI	BWS-BMR-BLR	9								X	X	X			X	X		X	1-41			20-234	
3A	Flemington Boro WS	BMR	1	12	3		X		X	X	X	X				X	X	X		1-10	345-15000		52-208	1514-1564
3B	Hillside Car Wash WS	BMR	1	2			X			X		X									1742-1820			
3C	Readington Twp GWI	BMR	5	18	12	1	X		X	X	X	X		X		X	X	X		28-103	65-290	3.8		
3D	Delaware Twp AGW	BMR	5	6	7		X		X	X	X	X		X			X	X		22-38	200-211	2.5	40-220	150-1020
3E	Potterstown Rt 22 GWI	BMR	6	10	10		X		X	X		X			X					2-28	300-576	ND	17-320	120-450

Aquifer abbreviations: BWB - Brunswick Watchung basalt, BWS- Brunswick Watchung sedimentary rock, BC - Brunswick conglomerate, BSC - Brunswick sandstone and conglomerate, BLGSC - Brunswick lower gray zone with sandstone and conglomerate, BMR - Brunswick middle red zone, BMG - Brunswick middle gray zone, BSS - Brunswick sandstone, BLR - Brunswick lower red zone, BLG - Brunswick lower gray zone

Water-bearing feature (WBF) key: Type 1 - bedding planes and layers, Type 2 - fracture planes, Type 3 - linear intersection of bed and fracture planes

Geophysical log abbreviations: O - optical televiewer, A - acoustic televiewer, B - borehole video camera, FC - fluid conductivity FR - fluid resistivity, FT - fluid temperature, PA straddle packed, HPFM - heat-pulse flow meter, np - nonpumping, pu - pumping, C - caliper, G- natural gamma, ND - not determined, SP - singe-point resistance, SL - short-long normal resistivity

Log-response abbreviations: μs/cm - microsiemens per centimeter, gpm - gallons per minute, cps - counts per second, bswl - below static-water level

(continued on next page)

(continued from previous page)

Table F4. Summary of projects, wells and WBFs, geophysical logs collected and ranges of log values

PROJECTS, WELLS AND WATER-BEARING FEATURES							GEOPHYSICAL LOGS COLLECTED													LOG-RESPONSE VALUES				
Appendix Entry	NJGS Project	Aquifer or aquifer zone(s)	no. of wells	number of WBFs by type			Imaging			Fluid				HPFM		Formation				fluid resistivity (ohm-m)	fluid conductivity (μs/cm)	HPFM borehole flow (np) (gpm)	formation natural gamma bswl (cps)	formation single-point resistance bswl (ohms)
				1	2	3	O	A	B	FC	FR	FT	PA	np	pu	C	G	SP	SL					
3F	Trump National GC WS	BMR	7	1	32		X																	
3G	Hopewell Boro AGW	BMR	7	21	15	4	X		X	X	X	X	X	X	X	X	X	X	X	15-44	79-325	0.5	80-200	125-340
3H	Larison's Corner GWI	BMG	1	2	9	1	X			X	X	X	X			X	X		X	28-36	870-895		58-300	103-386
3I	Home Depot GWI	BMG	3	6	8	2	X			X	X	X		X		X	X	X		1-31	325-12000	ND	55-240	250-675
3J	Branchburg Rt202 GWI	BMG	6	8	24		X																	
3K	Heron Glen GC-QNS WS	BMG	4	5	7		X		X	X	X	X			X	X	X	X		29-44	230-336	8.0*	75-320	630-760
3L	Harbat Farms WS	BLR	1		5		X		X	X											220-228			
3M	Stony/Honey Brook WS	BLR	10	20	29	9	X	X		X	X	X	X	X						9-60	264-448	2.4	50-367	47-933
3N	Bristol Meyers-Squibb GWI	BLG		4	33	9	X	X		X		X	X	X							230-950	ND		
3O	Pennington Boro WS	BLG	1	2	7		X			X		X		X							325-335	ND		
3P	The Ridge GC WS	BLG	2	3	8		X			X		X					X				250-850		15-4012	
3Q	Snydertown Rd GWS	BLG-L	2		2	1	X			X	X	X				X	X	X		18-38	263-538		30-2686	310-1685
4A	Terhune Orchards GWS	L	2	2	3	3	X			X		X				X	X	X			225-390		50-960	439-1717
4B	Hilltop Development WS	L	5	2	24	2	X			X		X		X		X	X	X			255-820	ND	50-1750	350-1400
4C	29 Pine Hill Rd. AGW	L-S	1	6	5	1	X			X	X	X	X	X			X	X		14-24	431-690	0.9	75-650	10-1250
4D	Ewingville Rd & Rt31 GWI	S	3		1		X																	
4E	Green Acres CC WS	S	2	3	12	3	X			X	X	X		X	X	X	X	X		14-55	280-857	3.8	5-540	540-860
4F	Springdale GC WS	S	3	8	11	7	X			X	X	X		X		X	X	X	X	14-55	250-425	15.0	50-600	100-600
4G	Princeton Plasma Physics	S	3					X												1-103	2-15000	ND	1-4012	10-4288
		Totals	128	213	335	72																		

Aquifer abbreviations: BMR - Brunswick middle red zone, BMG - Brunswick middle gray zone, BLR - Brunswick lower red zone, BLG - Brunswick lower gray zone, L - Lockatong, S - Stockton

Water-bearing feature (WBF) key: Type 1 - bedding planes and layers, Type 2 - fracture planes, Type 3 - linear intersection of bed and fracture planes

Geophysical log abbreviations: O - optical televiewer, A - acoustic televiewer, B - borehole video camera, FC - fluid conductivity
FR - fluid resistivity, FT - fluid temperature, PA straddle packed, HPFM - heat-pulse flow meter, np - nonpumping, pu - pumping,
C - caliper, G- natural gamma, ND - not determined, SP - singe-point resistance, SL - short-long normal resistivity

Log-response abbreviations: μs/cm - microsiemens per centimeter, gpm - gallons per minute, cps - counts per second, bswl - below static-water level

* flow measured while two irrigation wells were pumping nearby

1994). Cycle thickness also increases from the hinged and lateral basin margins inward toward the center (Schlische, 1992). The basic Van Houten precession cycle thickens upward in the basin, reflecting a gradual upward increase in sediment-accumulation rates throughout time (Schlische, 1992). Generally, the Lockatong precession cycles are about 5 to 20 ft thick. The Passaic cycles range in thickness from about 10 to 30 ft. The Jurassic lacustrine cycles are the thickest, ranging from about 30 to 75 ft (Schlische, 1992). Identifying precession cycles in the lower and middle red zones of the Brunswick aquifer is complicated by the abundance of red beds and the scarcity of gray and black marker beds (fig. F2). Thick red beds were deposited during prolonged arid conditions resulting from the overlapping effects of larger-order climate cycles. Cycle thickness of a stratigraphic section differs in different parts of the basin, probably in response to a combination of tectonic and climatic controls (Schlische and Olsen, 1990; Schlische, 1992).

Mud-cracked and burrowed mudstone is mostly restricted to the Lockatong aquifer and lower gray part of the Brunswick aquifer and indicates deposition of sediment on dry or occasionally wetted mud flats (Smoot and Olsen, 1994). Root-disrupted mudstone is progressively more abundant in the middle-to-upper-red zones in the Brunswick aquifer (Herman, 2005) and results from deposition on wet mud flats having periodic, fresh, groundwater tables (Smoot and Olsen, 1994). All varieties of mudstone locally contain assemblages of millimeter-to-centimeter scale crystal casts and linear to ovate syndepositional sedimentary features filled with secondary, sparry cements locally including calcite ($CaCO_3$), gypsum ($CaSO_4 \cdot 2H_2O$), analcime [$Na_{16}(Al_{16}Si_{32}O_{96}) \cdot 16H_2O$)], albite ($NaAlSi_3O_8$), potassium feldspar ($KAlSi_3O_8$), and dolomite ($CaMg(CO_3)_2$)(Van Houten, 1965; Smoot and Olsen, 1994; Tabakh and Schreiber, 1998). Secondary, authigenic calcite and gypsum are most abundant in the middle part of the Brunswick aquifer where sedimentary vesicles, evaporite-crystal casts, desiccation cracks, and root structures form networks of type 1 conduits (fig. F12 and appendix 3M7).

Dense accumulations of calcite and gypsum grew locally in relict soil horizons, but and are now partially dissolved in bedrock to depths exceeding 400 ft below the land surface, leaving vuggy, tabular beds of siltstone and mudstone capable of storing and transmitting significant quantities of water (appendix 3M7, 3M8, 3M12-right, 3G5-right, 3G7-right). These horizons are collectively referred to as gypsum paleosols. This term is also applied to red beds whose appearance and hydraulic properties are inherited from past accumulations of evaporite minerals in a subsurface stratigraphic horizon. These horizons may be cemented with salts of carbonate, sulfate and other evaporites in

Table F5. Types[1] of WBFs by aquifers, zones, units and groups of rocks

Aquifer	Zones, units and groups	No. of Wells	Type 1	Type 2	Type 3	Total	%1	%2	%3
Diabase…..	……	7	11	32	2	45	24	71	4
Brunswick...	……	93	181	247	54	482	38	51	11
Lockatong..	……	10	8	31	6	45	18	69	13
Stockton…..	……	12	13	25	10	48	27	52	21
TOTAL[2]…..	……	**119**	**213**	**335**	**72**	**620**	**34**	**54**	**12**
Brunswick	Basalt units in the Watchung zone (BWB)……..	4	15	10	4	29	52	34	14
Brunswick	Conglomerate and Sandstone (BC and BSC)…..	20	37	21	22	80	47	26	26
Brunswick	Sandstone (BSS)……..	3	9	5	1	15	60	33	7
Brunswick	Middle Red zone (BMR)……..	33	70	79	5	154	45	51	3
Brunswick	Middle Gray zone (BMG)……	14	21	48	3	72	29	67	4
Brunswick	Lower Red zone (BLR)……	11	20	34	9	63	32	54	14
Brunswick	Lower Gray zone (BLG)……..	10	9	50	10	69	13	72	14
Brunswick	Coarse-grained units (BC, BSC and BSS)……	23	46	26	23	95	48	27	24
Brunswick	Fine-grained units (BMR, BMG, BLR and BLG)..	68	120	211	27	358	33	59	8
Brunswick	Red Units (BC, BSC, BSS, BMR and BLR)……..	67	136	139	37	312	43	45	12
Brunswick	Gray Units (BMG and BLG)……	24	30	98	13	141	21	70	9
	Igneous rocks (diabase and basalt)……..	11	26	42	6	74	35	57	8
	Sedimentary rocks……	110	187	295	67	549	34	54	12

[1]Type 1 – bedding planes and layers, type 2 – fracture planes, type 3 – linear intersections of bed and fracture planes

[2] Some wells penetrate more than one aquifer, group or unit so that the total number of wells and WBFs may not equal column totals.

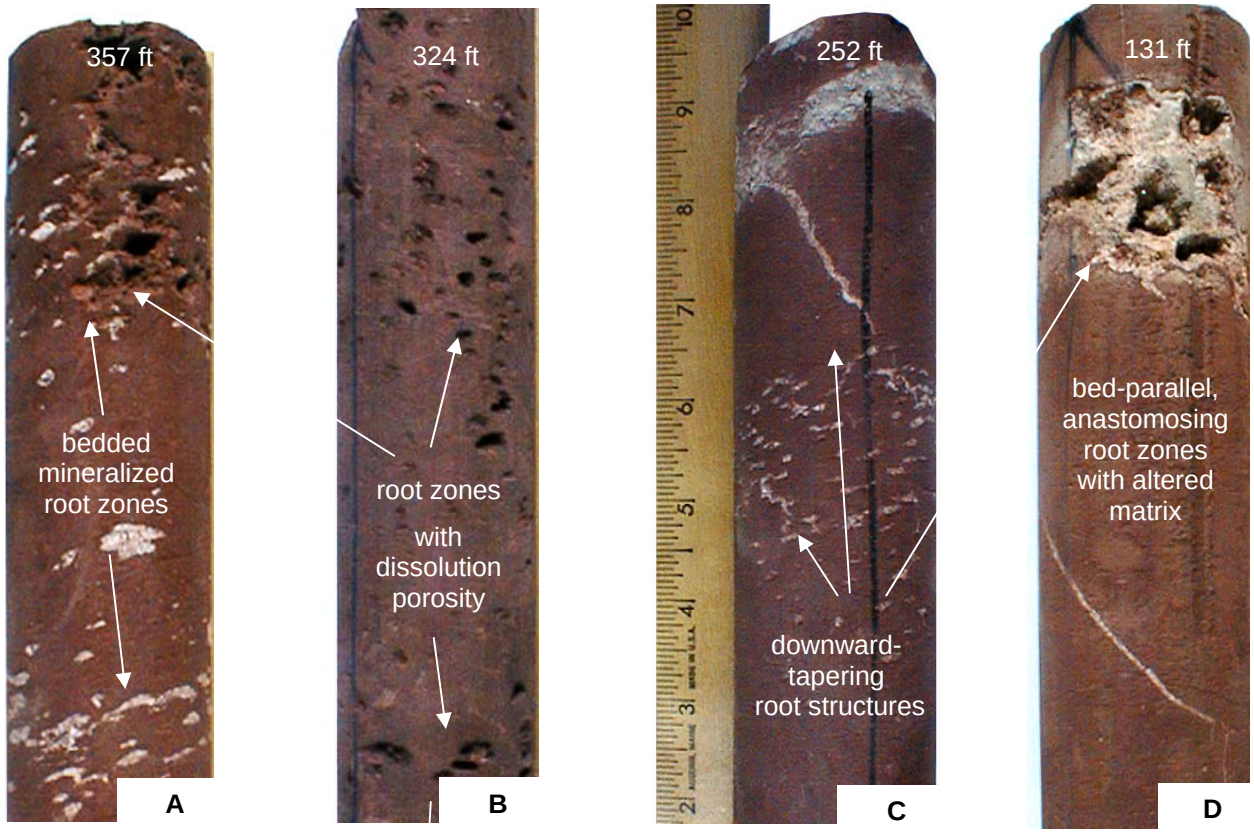

Figure F12. Examples of cores showing stratified gypsum paleosols from the lower red zone of the Brunswick aquifer. A, B, and D show beds having effective secondary porosity stemming from dissolution of soluble minerals from matrix pores. C and D show downward-tapering root structures within these soil horizons. Secondary tectonic vein cuts the lower part of D from upper left to lower right. Ruler shows scale in inches.

arid settings, such as those on margins of deserts and playa lakes (Retallack, 2001). Such minerals are readily soluble in fresh water. In many beds, all that remains of these ancient evaporite beds are pseudomorphs of crystals or breccia layers where the sediment collapsed into the dissolved salt layers producing breccia and 'crumb' fabrics during diagenesis (Smoot and Olsen, 1985). In other beds, mineralized nodules and root tubes form anastomosing networks of secondary authigenic minerals (appendix 3M7). Their hydrogeological significance is illustrated in appendix entries for the Stony Brook-Millstone Watershed Association research well field (3M), the Hopewell Borough Supply Well 6 study (3G) and Trump National Golf Course (3F) as previously described by Herman (2001).

Layering in diabase and basalt is more varied in strike over small distances than sedimentary bedding. For example, compositional layering in diabase in the Sourland Mt. sill has a wider variety of orientations (fig. 1B1) than underlying mudstone and shale in the Passaic Formation (fig. 3Q1). Basalt layers are more varied in strike than adjacent sedimentary beds (appendix 1E2). The variation in compositional layering reflects the complex flow paths followed during the injection and extrusion of magma into and onto other strata. Their varied orientations reflect limited subsurface continuity of layering, with the likelihood of adjacent layers being onlapped and truncated. This limits continuity in the subsurface in an average strike direction and decreases horizontal conductivity. Complex layering contributes to the 3D heterogeneity of these igneous aquifers except where layer boundaries are more continuous along contacts of major sills and flows resulting from large magma pulses, or the development of thick cumulate layers during fractionation and cooling processes. These stratigraphic intervals have varied textures, colors and/or fracture densities (appendix 1A2, 1B3, 1B5, 1B7, 1C2 and 1D2, 1E3, 1E5, 1E7, 1E9 and 1F2). Increased structural heterogeneity results in decreased horizontal and vertical conductivity and in groundwater recharge potential in comparison to the fine-grained sedimentary beds having continuity in the basin subsurface over distances of miles (Olsen and others, 1996).

Type 2 WBFs: Fracture planes

WBFs classified as conductive fractures (cf) are those that have visible secondary porosity along most or the entire entire fracture plane that is not oriented parallel to the bedding plane. All fractures in bedrock are secondary geological features postdating sedimentary bedding and igneous layering. Natural fractures occur as a brittle strain response in the Earth's crust from deep-seated tectonic stresses or as a response to near-surface stresses stemming from the removal of overburden by erosion and weathering. Other bedrock fractures can be artificially induced in rock cores (Kulander and others, 1990) and in well boreholes following drilling and hydrofracturing. However, this section is focused on sets of naturally-occurring, systematic, tectonic fractures that store and transmit groundwater in deep, relatively unweathered bedrock, as seen in wells having uncased sections ranging from about 20 to 50 ft bls. Fractures are considered systematic where they occur in sets that are parallel or subparallel (Hodgson, 1961).

Systematic fractures in the basin include sets of steeply- to moderately-dipping extension fractures and gently- to moderately-dipping tectonic shear fractures. Of these, the steeply-dipping extension fractures, commonly referred to as joints in outcrop (figs. F6, F13, F14a, F15 and F16), are the most abundant in the Newark basin and are shown below to be an important part of the aquifer framework.

Sets of steeply-dipping extension fractures formed in basin bedrock as a brittle strain response to tensile stretching of the crust along what is now the eastern margin of North America during the Early Mesozoic (Herman, 2005; 2008). These fractures are classified as 1) joints if the two sides of the fracture show no differential displacement to the naked eye, 2) as healed joints if the fracture walls are completely or partially joined together by secondary crystalline minerals or 3) as tectonic veins if secondary minerals completely fill the space between fracture walls (Ramsay and Huber, 1987). Extension fractures are mostly or entirely filled with secondary albite (fig. F14b) and calcite (fig. F18) in bedrock excavations (figs. F4, F13b, F14a, F15 and F16a, b and d), rock cores (figs. F12, F17 and F18) and BTV records. obtained below near-surface depths (~6 ft bls). However, these fractures are typically mapped as joints because any secondary minerals that formerly filled them are weathered out (Herman, 2001b). Their tensile origin is confirmed by their characteristic markings in outcrop that include plumose (feather) patterns, rib marks and hackles (Pollard and Aydin, 1988; Herman, 2005). Multiple sets of steeply-dipping extension fractures of different orientations occur throughout the basin so that two to four different fracture sets occur at a single location (figs. F11, F14b, F17a, F18; Herman, 2005). The spacing, arrangement, and density of these fractures also differ as a result of mechanical layering of strata (fig. F15) and proximity to large normal faults (Herman, 1997). Fracture spacing and fracture-strike lengths vary with layer thickness so that fracture

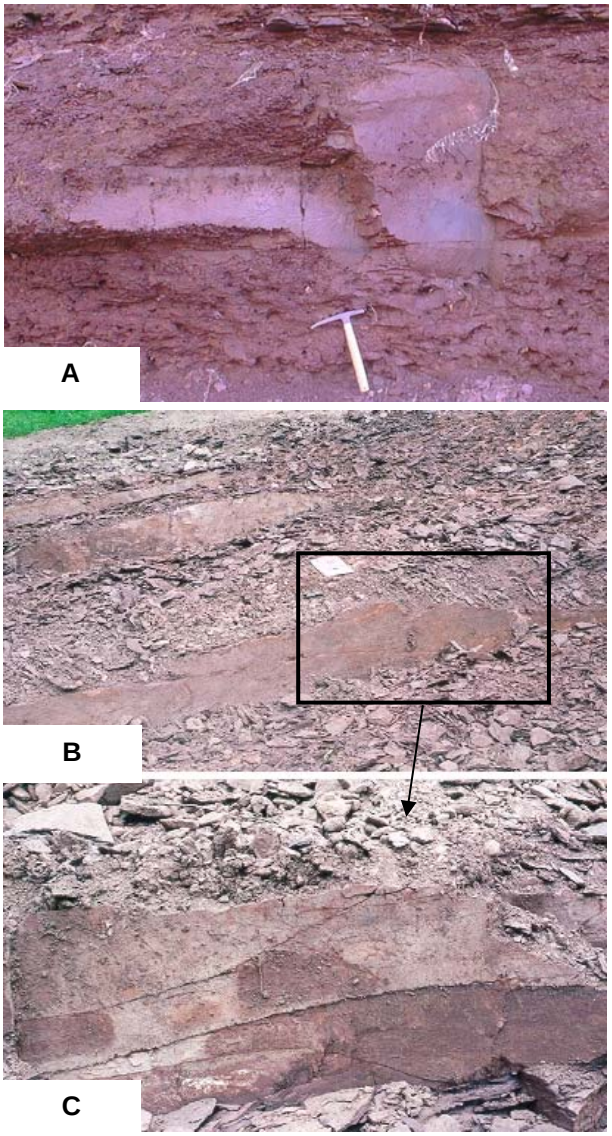

Figure F13. Extension fractures in Passaic Formation mudstone red beds. A. Stream-bank outcrop showing a pitted paleosol horizon overlain by a fractured mudstone (near appendix entry 3F). Note how the two joints span different heights within the fractured layer. B and C show a shallow bedrock excavation (appendix entry 3P). The rectangle in B approximates the area covered by C. The latter highlights a steeply-dipping fracture face having a trace length of about 3 meters and a height of about 3 feet for the fractured stratigraphic interval. Two, gently-dipping, curviplanar fractures intersecting the steep face are typical of gently-dipping fractures in shallow bedrock stemming from stratigraphic unroofing and weathering.

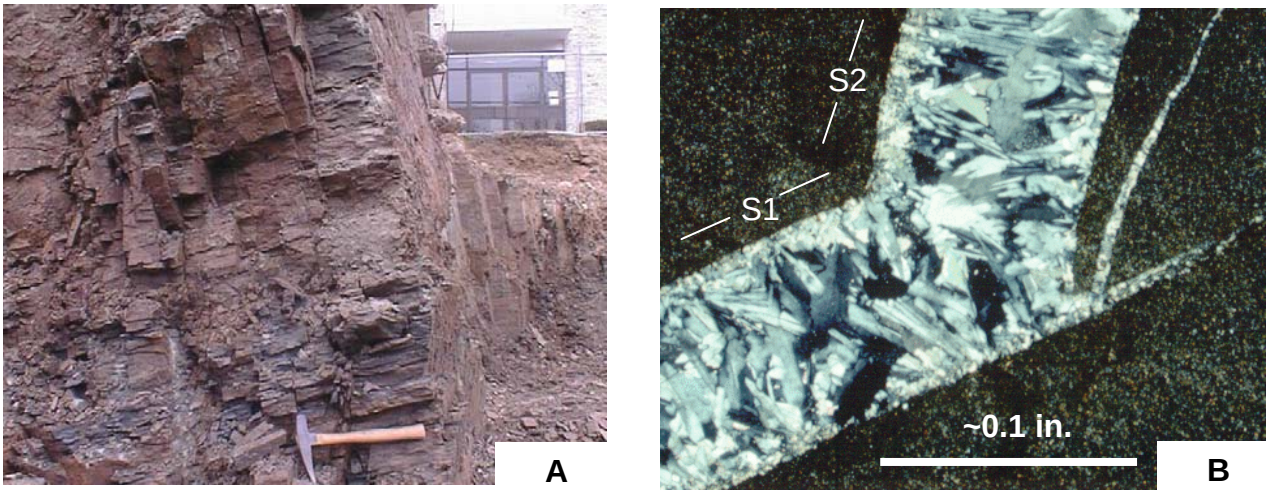

Figure F14. Extension fractures in the Lockatong Formation exposed in a foundation excavation (A) along Route 31N in Ewing, NJ. B. Photomicrograph (crossed nicols) of a tectonic vein from A showing sodium-silicate (albite) filling fracture interstices having both S1 and S2 fracture orientations.

Figure F15. Extension fractures in mudstone and siltstone of the Passaic Formation (Brunswick Middle Red zone) exposed in vertical face cuts during excavation of a commercial pipeline, Somerset County. Plastic netting on the upper benches is about 4 feet in height. Note the difference in thickness between bedding and fractured layers and how fracture density and dimensions differ. Photograph courtesy of Don Monteverde, NJGS.

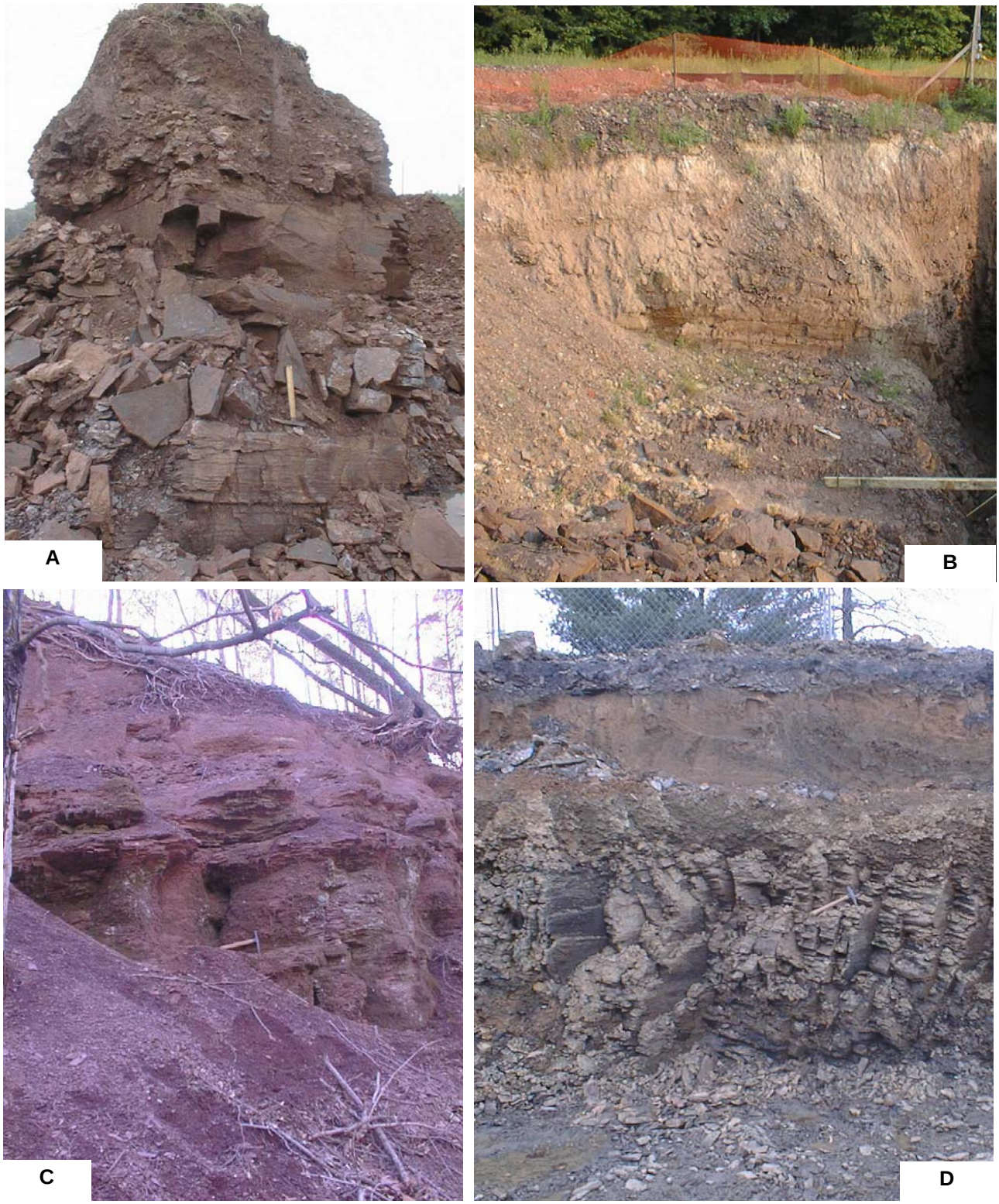

Figure F16. Photographs showing regolith overlying weathered bedrock in the lower gray (A) and middle red (B and C) zones of the Brunswick aquifer, and the Lockatong aquifer (D). A, B and D are in excavations whereas C is a stream-bank outcrop.

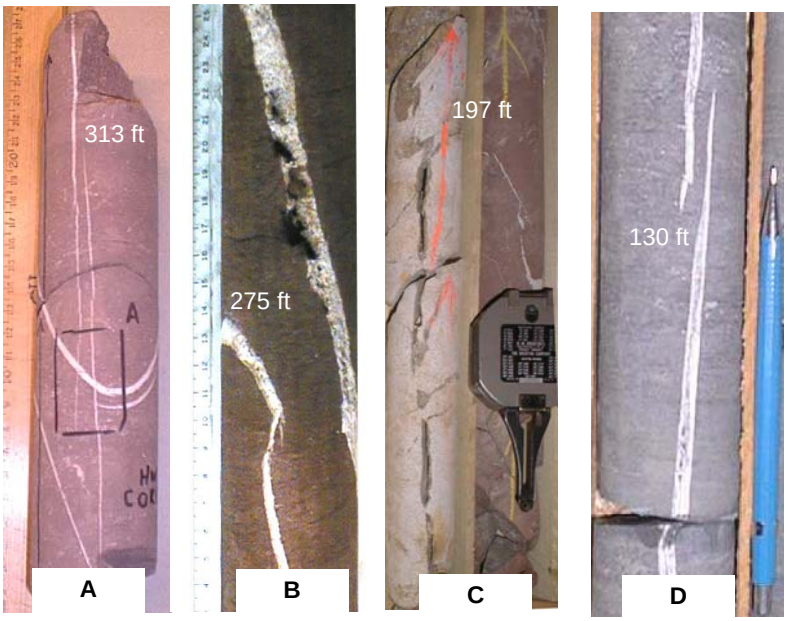

Figure F17. Core photos showing mineralized extension fractures (tectonic veins) that are locally conductive. Fractures are permeable where secondary minerals that otherwise fill veins are dissolved out. A and B are from Hopewell Boro (appendix 3G). A shows multiple sets of crosscutting veins. B shows where secondary minerals are locally dissolved from veins that are hydraulically conductive. C shows open and conductive extension fractures in the Stockton Formation, Mercer County. D shows tectonic veins in gray mudstone of the Brunswick aquifer in Mercer County. Approximate depth to top of core sample indicated on each photo. Ruler shows centimeter scale for A and B.

density generally increases as the thickness of the fractured layer decreases as shown by fracture-spacing studies conducted in sedimentary rocks elsewhere (Pollard and Adyin, 1988; Huang and Angelier, 1989; Narr and Suppe, 1991, Gross, 1993). Fracture density also increases from an average of <1 fracture per meter in areas remote from faults to >50 fractures per meter near large fault traces (Herman, 1997).

Secondary fracture-fill minerals are locally dissolved and removed from extension-fracture interstices in deep bedrock (figs. F17b and F17c) by weakly-acidic groundwater. Notable examples of conductive extension fractures are included in the appendixes for the following aquifers:

Diabase – 1A3-right, 1B4-right, 1B8, 1D3-right and 1D4-left
Basalt – 1E6-right
Brunswick – 2B3-left, 2D3, 2D5, 2E7-left, 2E8-right, 3C2, 3C3, 3C4, 3C5-left, 3D8, 3D10, 3D12, 3D14, 3E6-right, 3F5-right, 3F6-right, 3H3-right, 3I4-left, 3J3, 3J4, 3J6, 3M6, 3M11, 3M17, 3M18, 3N6-right, 3N7, 3N10, 3N14, 3O2 and 3P5
Lockatong – 4B6 and 4B7
Stockton – 4C3-left, 4E3, 4E5, 4E6, 4F4, 4F5 and 4F7.

Open, conductive, extension fractures occur randomly throughout Newark basin aquifer systems and commonly provide leakage between primary WBZs aligned with stratigraphic planes. Statistically, they act as primary WBFs in the gray units of the Brunswick aquifer and in the Lockatong aquifer (table F5). Overall, they make up just over half of the WBFs in this study (table F5).

Late sets of gently- to moderately-dipping, systematic, tectonic shear fractures and veins occur locally in areas of gently-folded rocks (appendix 3M2 and 3N3) and igneous intrusions (fig. 1B1). These fractures are also largely filled with secondary minerals, especially in the sedimentary units, but are less significant in providing cross-layer leakage than the steeply-dipping fractures because of their gentler dips

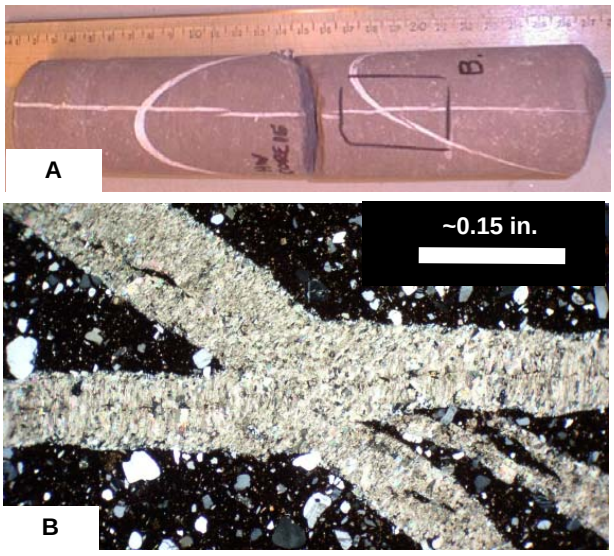

Figure F18. Photos of calcite-filled tectonic veins from Hopewell Boro (appendix 3G). Red mudstone core contains young veins striking/dipping N10^{o}W dipping 86^{o}E that crosscut older veins striking N45^{o}E dipping 66^{o}S and striking N75^{o}E dipping 62^{o}S. Black rectangle in A is the sample area of photomicrograph B. Fibrous calcite fills fracture interstices. Younger vein(horizontal in B cuts across older ones and helps establish the relative timing of fracturing in the basin. Photomicrograph taken using crossed nicols.

and limited vertical extent. Their restricted distribution also limits their hydrogeologic importance. Other nonlayering, nonsystematic fractures (Groshong, 1988) do not appear to contribute significantly to the hydrologic framework of unweathered bedrock, based on the inspection of the BTV records. Most are steeply-dipping cross fractures striking normal to the clustered arrays of systematic extension fractures. Cross fractures are irregular, curviplanar and discontinuous surfaces that commonly terminate against bedding and other fractures (Hodgson, 1961; Herman 2005). They also have little or no separation of the fracture walls and very few secondary mineral accumulations.

Another set of fractures in the subsurface includes subhorizontal gypsum veins reportedly originating from stratigraphic unroofing (Tabakh and others, 1998). They are filled with satin spar (gypsum) fibers that are commonly straight and oriented nearly normal to the fracture walls (fig. F19). They occur in the Passaic Formation at depths ranging from about 300 ft to 700 ft bls and range in thickness from less than an inch to several inches. Localized curved fibers indicate vein growth accompanying stratigraphic tilting and/or flexural slip (Tabakh and others, 1998). These veins are thought to have precipitated in a 'mixed phreatic zone' from saturated diagenetic brines originating in a shallow 'dissolution zone' (Tabakh and others, 1998; fig.8). These gypsum veins can reduce an aquifer's productivity. For example, packer-tested intervals in subsurface borings for the Passaic Flood Tunnel geotechnical investigation (appendix 2F) show that stratigraphic sections with these veins (appendix 2F3) have very low transmissivity in comparison to adjacent intervals that lack them. Subhorizontal gypsum veins were seen in only one well having an OPTV record as part of this study (appendix 3B). They strike and dip at very low angles to sedimentary bedding and mostly dip gently north (appendix 3B2). Their strike orientation parallels many other late-stage tectonic shear planes in diabase and suggests that they may have originated in response to late stage, compressive stresses resulting in basin inversion. More work is needed to identify their occurrence, origin, and hydraulic importance. Subhorizontal cracks stemming from basin exhumation and stratigraphic unloading also occur at shallow depths (fig. F13c) within the unsaturated and active phreatic zone but are difficult to detect and differentiate from other fractures due to the lack of secondary vein fill and small fracture apertures.

Bedrock weathers near the land surface because of the many physical, chemical and biological processes that alter it into regolith. These processes include freeze-thaw cracking, erosion, mineral precipitation and dissolution, alteration and transformation, and root growth. The deterioration produces networks of secondary pores that enhance groundwater storage and movement in the weathered bedrock interval that commonly reaches, and in some cases exceeds, depths of about 60 ft bls in areas poor in unconsolidated sedimentary cover (Herman, 2005). Other nonsystematic fractures in the shallow subsurface stem from freeze-thaw cracking, sedimentary and glacial unloading, and occur as intermittently permeable fractures of limited extent. The sum total of fracture systems interconnect at different densities and orientations in different places to form a network of hydraulically conductive planes and linear intersections of planes that generally channel shallow groundwater down topographic slope.

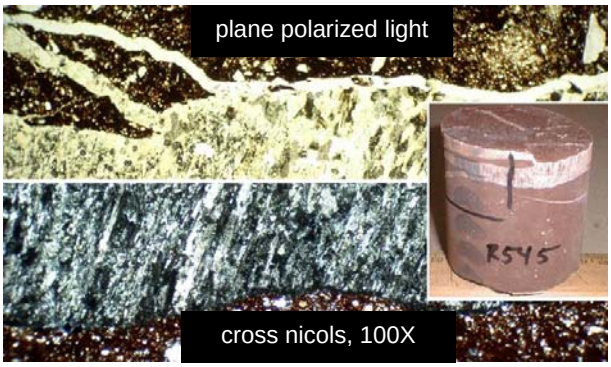

Figure F19. Photo and photomicrographs of gypsum veins from the Rutgers NBCP core (fig. F3) from 545 ft depth. Gypsum veins are as much as a few inches thick iin wells and rock cores from the Passaic Formation in northeast and central parts of the basin. They occur at depths of about 320 to 700 feet and are late structures oriented subparallel to land surface. Satin-spar gypsum fibers are subvertical and locally show shear fabrics. These structures tend to reduce an aquifer's productivity.

Type 3 WBFs: Linear intersections of bedding and fracture planes

A third type of WBF includes hydraulic conduits formed by the intersections of fracture planes with other fractures and with stratigraphic planes. The intersection of two planes forms a line that intersects a plane at a point. Therefore, many of these features appear as points of secondary porosity on the borehole wall (appendix 2E5-right @ 382 ft, 3H4-right @ 250 ft, 3M6 @ 52 ft and 3N10-left @ 176 ft). These features are also barely visible at the scale of the typical hydrogeologic section because they appear as points in the profile plane.

Potential permeable conduits situated at intersections of stratigraphic and fracture planes display a wide range of orientations. This is demonstrated in the appendixes using cyclographic stereonet plots of fracture planes measured in the BTV records (for example, appendix 3M2, 3N3 and 3N4). Hydraulically conductive plane-intersections are an important part of the hydrogeologic framework because they provide steeply-plunging pathways for groundwater to infiltrate and recharge deep bedrock. The trends and plunges of intersecting, potentially permeable structures in an area can be generated and plotted to visualize them on maps and 3D diagrams (fig. F20).

Other WBFs of this type include examples where secondary porosity has preferentially developed in fracture interstices within a specific stratigraphic horizon (appendix 3D13-left, 3D14, 3J3, 3J4 and 3M17-left), where fractures terminate against stratigraphic contacts (appendix 3P3-right and 4F5) and where fractures intersect other fractures of different orientations (appendix 3M11, 3M14-left, 3N7-left, and 4E3-left). In one case, sets of open, permeable fractures occur within a specific stratigraphic section that is continuous over a distance of more than 1000 ft (appendix 3D14).

Hydrogeologic analyses

The methods of developing hydrogeologic sections and 3D framework depictions included in the appendixes are described below. 2D and 3D visualization methods are used to illustrate standard and advanced hydrogeological concepts such as the development of stratigraphic unconformities in massive mudstone beds (appendix 3F2 and 3F3), and the influence of geological structures on the drift of well boreholes (fig. F11). Specific examples of framework interpretations for each major aquifer follow a discussion on groundwater recharge and discharge and

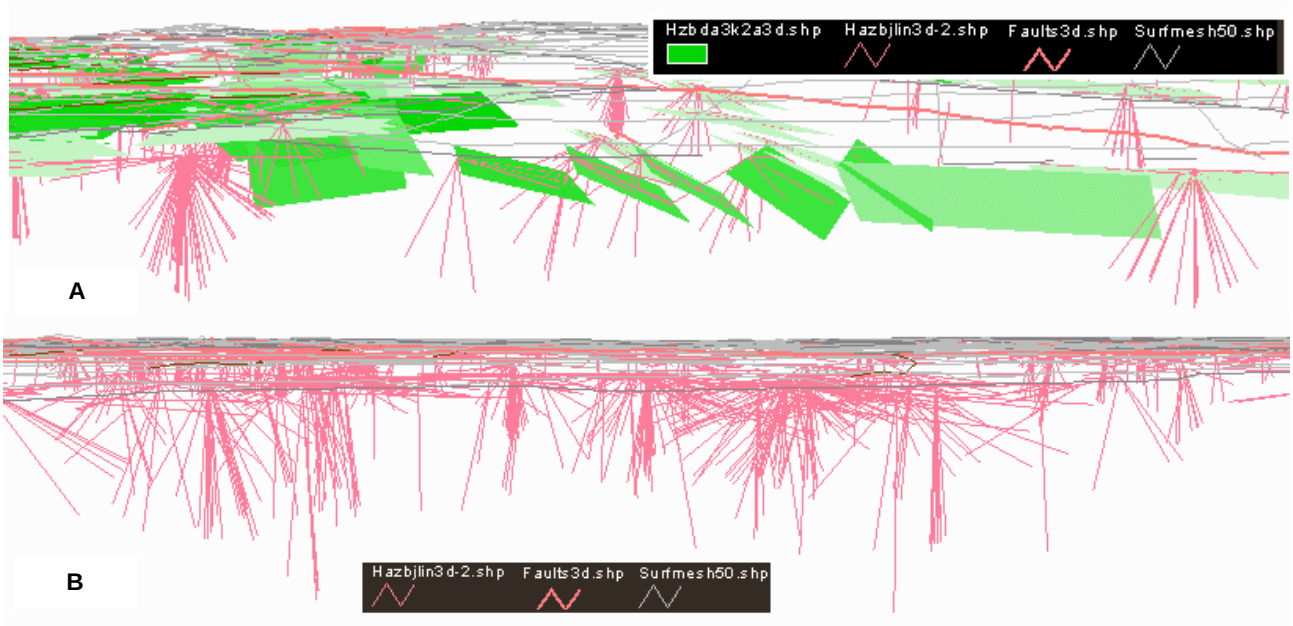

Figure F20. ArcView GIS 3D visualizations of layer-fracture and fracture-fracture intersections calculated for two areas of the basin based on structural measurements in outcrop. Linear intersections of two or more planes are potential permeable conduits, many of which plunge steeply and facilitate groundwater recharge to deep bedrock. A. Northeast view through part of the Flemington fault zone showing bedding (green, rectangular planes dipping left-to-right) and intersection lineation (pink lines) with respect to the trace of the Flemington fault (heavy red line). Planes are 3000 ft wide and 1000 ft long. Intersection lines are about 1000 ft to 1300 ft long. B. Northwest view through the Stony Brook-Millstone research well field (appendix entry 3M).

borehole cross flows. Stratigraphic descriptions included in figures stemming from OPTV interpretations rely on a description of unit color, textures, and layering characteristics. A list of the descriptive adjectives used here and in the appendixes is included in table F6.

Table F6. Lithologic description of geological features

Rock……..	shale, mudstone, siltstone, sandstone, conglomerate, basalt, diabase
Color……..	red, gray, black, orange
Textures...	fine (<.5mm), medium (.5-1mm)-, coarse (.5-1mm) very coarse (1-4mm), pebble (4-16mm), cobble (16-64mm)
Layering...	conductive, laminated (<0.5 in), thin (0.5-4 in), medium (4-12 in), thick (1-3 ft), very thick (>3 ft)
Fractures..	conductive, altered, mineralized, vein, dipping gently (1^o to 29^o), moderately (30^o to 59^o) and steeply (60^o to 89^o)

Map and cross-section components

The hydrogeological framework for the different aquifers is illustrated in the appendixes, using maps, hydrogeologic cross sections, and 3D diagrams. Map elements include the location of a well, or a group of wells, on a topographic or aerial-photographic base map together with the key planar features including stratigraphic contacts, structures such as fractures, faults, and folds and the line traces of cross sections. In some instances, lines extending from the wells normal to stratigraphic dip indicate the extent of the penetrated stratigraphic interval (for example, see appendix 2E1). Cross-section traces are aligned normal to stratigraphic strike to minimize distortions in the dip of strata-parallel WBZs. Features situated off the profile trace are projected into the plane of cross section. In these instances, apparent-dip angles of strata or structures striking at angles other than normal to the profile trace are calculated using trigonometric relationships derived from Ragan (1985).

Land surface is used as the uppermost boundary of the profile and is extracted from the topographic map along the profile trace using standard cross-section construction methods. The representative elevation of a projected well can vary depending upon the focus of the interpretation. Given the absence of subsurface control points that tie a well into another with identified stratigraphic markers, projected wells are drawn at their current surface elevations and therefore may lie above or below the land surface as depicted in cross section (appendix 3N2 and 3F3). The trace of a well in profile is ordinarily plotted vertically from the elevation of the top of casing to the total well depth (TD) as determined from geophysical logs, well-permit records, or from drillers' logs for those wells lacking geophysical logs. For the Brunswick, Lockatong, and diabase aquifers, weathered bedrock extends below overburden to about 60 ft bls unless direct evidence indicates otherwise. Weathered bedrock in the Stockton aquifer extends to a depth of 100 ft, as explained below. Hachuring makes it visually distinct (fig. F21). Other subsurface features represented in profile include WBFs oriented parallel to sedimentary bedding (fig. F21). Depths of WBFs and annotation of any observed borehole features are derived from the geophysical summaries for each well or set of wells in the appendixes. WBFs classified as stratigraphic planes and layers (type 1) are traced parallel to stratigraphic dip from control points identified and labeled on the geophysical log diagrams. Lengths of WBF traces are determined by interpolating between, and extrapolating from, control points to distances that are supported by the bulk of data. WBFs identified as fractures (type 2) are drawn using the same criteria but are shortened by a factor of ½ relative to type 1 features. This reflects their subordinate hydraulic role because they are smaller than stratigraphic planes. For the hydrogeologic section covering the Bristol-Meyers Squibb, Honey Brook Farm, and Stonybrook-Millstone Watershed Nature Reserve well fields (appendix 3N1 and 3N2) the interpretation includes the use of dip-domains. These are panels of parallel strata separated from others along sharp, subvertical lines (kink planes) bisecting panels of rock that dip at various angles. Boundaries between these domains are represented as flexures in an otherwise monoclinal stratigraphic sequence. Other map and profile components are added to reflect local conditions. For example, unconformity surfaces occur in gypsic mudstones near the border fault at Bedminster, NJ (appendix 3F2 and 3F3). Other framework elements may include the traces of gray and black beds in maps and cross sections with arrows indicating the direction of cross flows in wells (fig. F21). WBFs stemming from the intersection of layers and fractures are omitted on cross sections because most would appear as points rather than line traces.

Topographic controls on borehole cross flows

Surface water recharges groundwater in basin aquifers through the diverse, open and permeable features. Precipitation percolates downward under the

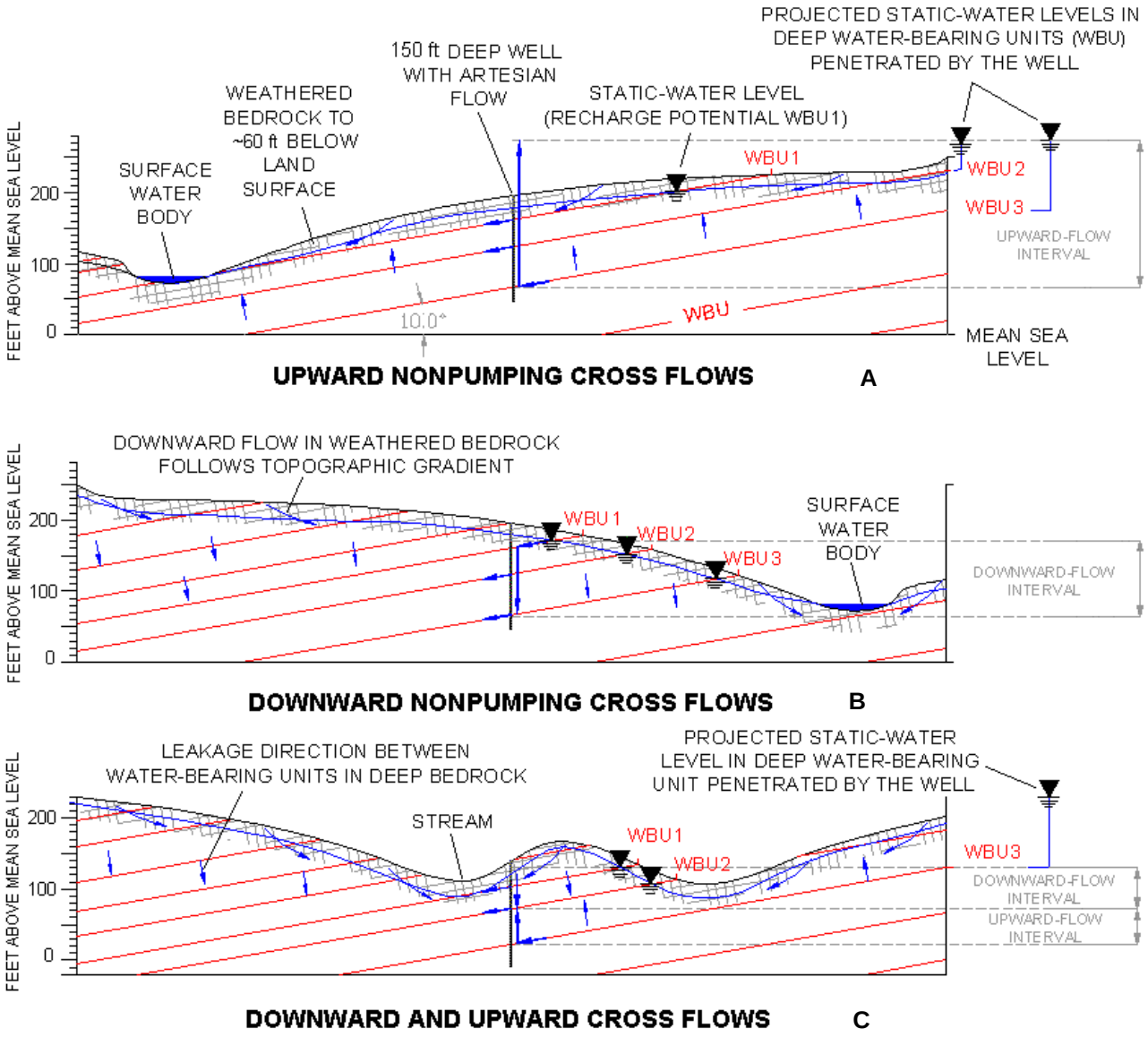

Figure F21. Profile diagrams illustrating the relationship between topographic grade and direction of cross flows in wells under natural (nonpumping) conditions. A. Upward cross flows occur in wells that penetrate deep aquifers with strata dipping in the same direction as topographic grade over long distances. B. Downward cross flows occur where strata dip in a direction opposite to long topographic grades. C. Wells that penetrate strata intersecting both recharge areas on hilltops and hill slopes and discharge areas in valleys can have both upward and downward cross flows. In general, cross flows can be expected to coincide with the direction of leakage in thick sequences of poorly conductive strata that confine bed-parallel WBZs.

influence of gravity into gently-dipping bedrock where permeable bed partings and layers are confined at depth by intervening thick, leaky and less permeable layers (fig. F6, Michalski and Britton, 1997; Michalski, 2001). Natural hydraulic gradients prevail between groundwater recharge and discharge areas in strata that crop out at different elevations in hilltops, hillsides and valleys. Cross flows between WBFs exist where natural flow systems are short-circuited by wells that penetrate different layers that are recharged at different elevations and so have different hydraulic potentials (figs. F21, F22 and appendix 3K2). Wells situated on large hilltops and hillsides sloping in a direction opposite to the dip of bedding have weak, downward cross flows (fig. F21B) that seldom exceed the minimum flow rate that the NJGS HPFM instrument can measure (~0.33 gpm in a 6-inch well). Wells situated in large valleys or hillsides sloping in a direction parallel to bedding dip tap pressurized, semiconfined water-bearing units with upward cross flows that are locally artesian (figs. F21A,

appendix 4C1 and 4C2). Wells in areas of many smaller ridges and valleys may produce upward and downward cross flows because they tap strata that crop out in both recharge and discharge areas (figs. F21C and F22B). For deep wells in hilly topography that tap several discharge and recharge areas, one may measure multiple cross-flow intervals in the well with different flow directions (appendix 3D7 and 3M10). The direction of cross flows may be based on knowledge of the vertical extent of the cased and open sections and on projection of the open sections to the surface.

Diabase

Seven wells in diabase were logged as part of four projects (table F1) in Mercer and Hunterdon Counties (fig. F3). The local surface-water drainage follows the measured fracture orientations in all projects (appendix 1A1, 1B1, 1C1 and 1D1). Groundwater flows mainly in tectonic fractures (71 percent) and to lesser extent along breaks between compositional layering (24 percent) and plane intersections (4 percent).

Diabase layering is thin to very thick and moderately inclined, probably about twice as steeply as

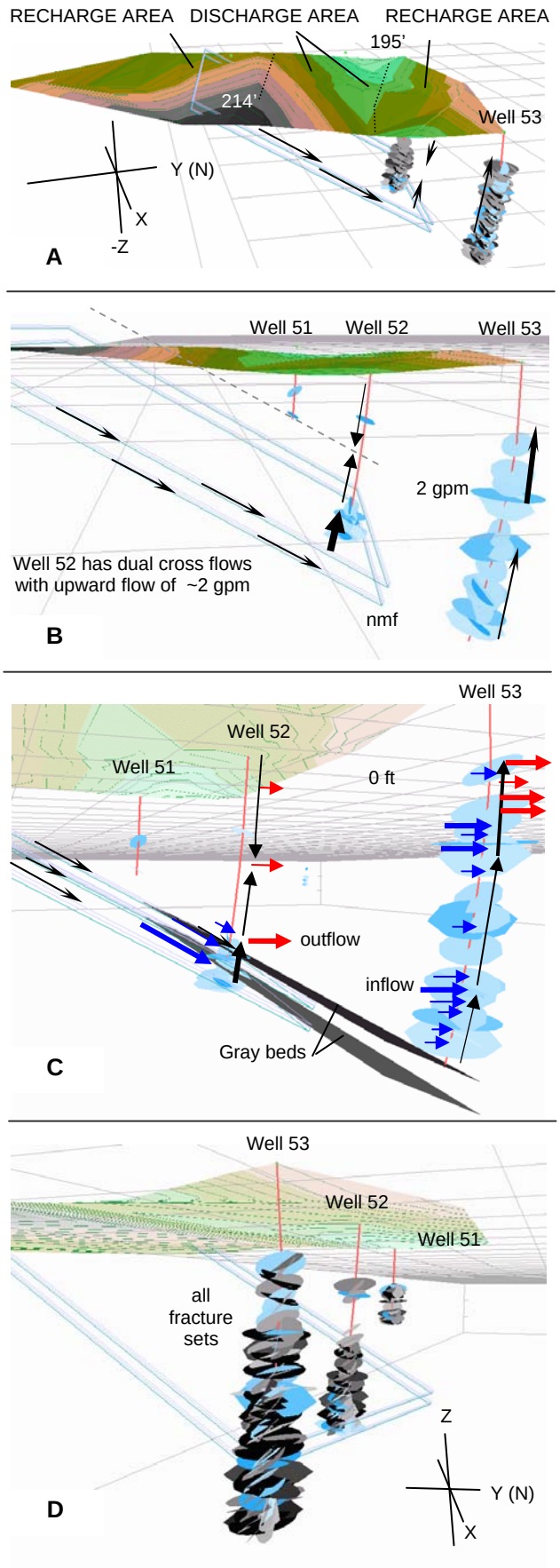

Figure F22 (right). West-looking 3D –GIS perspectives for an arsenic-in-groundwater study, Delaware Twp, Hunterdon County (appendix entry 3D). Topographic survey by Joe Rich and Walt Marzulli, NJGS. Well-field-grid cells are 100-ft and the wells range in depth from 175 ft to 250 ft. Sedimentary bedding and secondary fractures measured with the OPTV are plotted as elliptical planes along each borehole trace, shown as gently-curving, subvertical lines. Elliptical planes were generated using 50-ft major axes oriented along plane strike and using a 2:1 strike-to-dip aspect ratio. Hydraulically conductive bedding and fracture surfaces are shown as light-colored ellipses in B and C, but combined with all other measured fractures in A and D (dark ellipses). Bedding dips gently to moderately northeastward (left to right). Well 52 shows the cross-flow scenario illustrated in Figure F21C with dual cross-flow directions. Upward flows proceed from WBFs in fractured red beds that recharge at high topographic elevations and are confined by overlying gray beds. Downward flows occur in red beds that recharge at lower elevations with lower hydraulic potentials than other semiconfined units. Rates of nonpumping upward cross flows in well 52 reach about 2 gpm (C) in lower depths where water exits the borehole and units above begin to have weak downward cross flows. Cross flows are upward in well 53 because the well intercepts two recharge zones. Topography is modeled as a shaded surface ranging in elevation from 214 ft to 195 ft.

when originally intruded. Layering is locally complex as seen near the base of the Sourland Mt. sill (fig. F10) and in a thin sill at the west end of the Rocky Hill diabase sheet (appendix 1C1), with both NW and SE dips. Diabase layers alternate from light-gray to dark-gray with varying degrees of fracturing (appendix 1A2, 1B3, 1B5, 1B7, 1C2 and 1D2), but diabase shade is unrelated to the fracture density. Shaded layers range in thickness from about 2 ft to more than 100 ft whereas fractured layers range in thickness from a few feet to about 40 ft. The thickest set of fractures seen in BTV records is only about 6 ft in height but correlative fracture surfaces mapped in nearby diabase quarries exceed 20 ft in height and in width (Herman, 2005). The most densely fractured bedrock is near outcrops that show slickensided shear planes associated with nearby faulting (appendix 1C1). The strike of steeply-dipping extension fractures in diabase clusters in the S2 and S3 regional directions and reflects late ENE-WSW to E-W stretching in the basin (Herman, 2005).

Cross flows measured in diabase with the HPFM were less than 1 gpm (table F4). Fluid electrical conductivity and natural-gamma ray emissions are likewise low compared to other aquifers but formation electrical resistivity values are among the highest in the basin (table F4). Diabase is the least productive bedrock aquifer and has the poorest aquifer ranking in New Jersey (Herman and others, 1998).

Brunswick aquifer

Appendixes 1 to 3 include the results of 24 studies of the Brunswick aquifer, including 102 wells (table F1). Table F5 details the number of wells studied in the different zones and units. A detailed discussion of each of the zones in the Brunswick aquifer follows a brief discussion of the Passaic Flood Tunnel geotechnical evaluation summarized in appendix 2F.

An extensive borehole geophysical data set was generated for the Brunswick aquifer by the IT Corporation in 1995 as part of the Passaic Flood Tunnel geotechnical evaluation in the Passaic River valley. The results are on file at the NJGS office. Digital records of the borehole geophysical logs recompiled by the NJGS in 2003 are included in appendix 2F. These data are presented as a set of 4 geophysical log summaries based on data for 10 borings drilled near a set of 4 work shafts (appendix 2F1). The borings penetrated fine- to coarse-grained sedimentary units of the Brunswick aquifer in the northeastern part of the basin, and Lower Jurassic shale and siltstone in the Watchung Mt. area (fig. F3). The logs are the only records of geophysical responses from the Lower Jurassic sedimentary rocks in this study. The geophysical logs measure both formation and fluid properties and include some density logs and straddle-packer flow tests, in addition to detailed description of the drill cuttings. Gamma-ray logs and electrical-resistivity logs from nearby wells record lateral and vertical changes in the bedded mudstone, siltstone, and sandstone strata (appendix 2F2 to 2F6). Coaxial plots of logs of adjacent wells were made to compare changes in stratigraphy over short distances. The geophysical heterogeneity reflects the cumulative set of lacustrine and alluvial sedimentary processes resulting in the deposition of shallow-lake clay, silt and sand and massive mudstone on semi-arid mud flats. Descriptions of mineralized, vuggy mudstone and siltstone are assumed to mark gypsum paleosols. Records for workshaft 2B (appendix 2F3) show that deep parts of the aquifer below 320 ft have numerous horizontal gypsum veins and are poorly permeable, with transmissivity <1 gpd/ft, whereas vuggy beds above this depth are highly permeable, with transmissivity of ~30,000 gpd/ft.

Basalt units in the Watchung zone

Two studies were made of the Orange Mt. basalt in the Watchung zone of the Brunswick aquifer. One was on irrigation and monitoring wells at the Essex County Country Club (appendix 1E) where one well penetrated the base of the Orange Mt. basalt and finished about 150 ft in the uppermost Passaic Formation. The Orange Mt. basalt is the oldest, lowermost unit of the three in the Watchung Mountain area (fig. F3) and lies just atop the Triassic-Jurassic contact (fig. F2). The other study was on a domestic well in Somerset County (appendix entry 1F) that also penetrated the base of the Orange Mt basalt and 28 ft of the Passaic Fm. Although both studies involved wells that were finished in the uppermost Passaic Formation, the Essex study involved Brunswick sandstone whereas the Somerset study involved mudstone in the middle red zone (fig. F3). Sedimentary cross beds and cut-and-fill fluvial structures occur in fine-grained sandstone directly below the contact to the east (appendix 1E8) whereas massive mudstone underlies the contact farther west (appendix 1F4). At the latter, half-inch-sized ovoid accumulations of secondary minerals show hydrothermal alteration rinds that pock the shale. This contact is nonuniform in the basin and reflects both high-energy (sandstone) and low-energy (mudstone) sedimentary environments of deposition.

Analysis of WBFs of basalt shows that about half consist of type 1 fractures (table F5) between basalt layers of differing compositions and thicknesses. About one-third of the remainder are type 2 features, and type 3 features the least numerous at 14 percent. Cross flows measured with the HPFM reached more than 5 gpm in one 8-in-diameter supply well in the Essex study (appendix 1E3) but otherwise, measured flows were less

than 1 gpm. Gamma ray emissions from basalt are low in comparison to those from sedimentary units (table F4).

The geophysical results also show varied hydrogeology, reflecting stratigraphic heterogeneity and secondary structural controls. The Essex study (appendix 1E) showed that type 1 features were most abundant, whereas the Somerset study (appendix 1F) disclosed that type 2 WBFs can be locally dominant. In both locations, layering in basalt varies in thickness from laminated to thick-bedded, with textual and color changes. Measurable cross flows were found associated with both type 1 and 2 features (appendix 1E3 and 1E5) but flow rates in Well 11 for the Somerset study were considerably higher in the Passaic Fm than in the overlying basalt (appendix 1F2). This shows that basalt locally confines underlying sedimentary beds. Basalt has a poor aquifer ranking (Herman and others, 1998).

The local hydrogeological framework in basalt also depends on the proximity to local faulting and associated dense fracturing as seen elsewhere in the basin (Herman, 1997). Away from fault zones, bedding control of flow is strong, but within fault zones, fracture control is dominant. The N15^{o} to N30^{o}E strike of fracturing is the intermediate phase of extension fracturing in the basin (S2) and is the most common orientation of extension fractures in basalt and diabase in New Jersey; it is also a dominant regional trend (Herman, 2005).

Conglomerate, sandstone, siltstone, mudstone and shale

Coarse-grained units in the Brunswick aquifer occur in the conglomerate, conglomerate-and-sandstone, and sandstone zones mapped in the northwest and northeast margins of the basin (figs F1 and F3). About half (48 percent) of the WBFs in coarse-grained red beds are type 1 planes (table F5) resulting from mechanical parting along the interface between beds of differing thicknesses and grain sizes (appendix 2A2, 2A3, 2B2, 2B3, 2C2, 2C3, 2D3, 2D4, 2D5, 2E5, and 2E6). The remainder is about equally distributed among types 2 and 3 WBFs (table F5). Brunswick coarse-grained units have the highest proportion of type 1 and 3 WBFs of any sedimentary aquifer in the basin (table F5). Borehole cross flows in these units were measured in two projects (appendix 2D and 2E) and both had measured flows of less than 1 gpm (table F4). The vertical spacing of WBZs in sandstone ranged from about 2 ft to 50 ft (appendix 2D2, 2F2, 2E2, 2E3 and 2E4). The highest transmissivity of sandstone red beds was 700 gpd/ft from a straddle-packer test of a 20-ft section near workshaft 2C of the Passaic Flood Tunnel Geotechnical investigation (appendix 2F5).

Fine-grained units in the Brunswick aquifer include siltstone, mudstone and shale. They vary in the character, distribution, and continuity of WBFs in the red and gray beds. About 60 percent of all WBFs in siltstone, mudstone and shale are type 2 steeply-dipping extension fractures (table F5). Type 2 features are most common in all fine-grained units including those in the lower and middle zones (table F5). However, the middle red zone has the highest percentage (45) of type 1 WBFs, followed by the lower red zone (32 percent). Type 1 paleosol dissolution zones appear to locally transmit the most water of any features in sedimentary units: cross flows commonly reach 1 to 3 gpm (table F4; entries 3C, 3D and 3M). They first appear in thick red beds in the upper part of the lower red zone (fig. F12 and appendix 3G5 and 3G7) and are most abundant in the middle red zone (appendix 3A3, 3B3, 3C5, 3D4, 3D12, 3F4, 3F5, 3G5, 3G7, and 3G) where an overall upward increase in dissolution-enhanced WBZs coincides with the increase in root-disrupted, massive red mudstone in the Passaic Formation reported by Smoot and Olsen (1985). Layered dissolution zones in the middle red zone also coincide with elevated levels of sulfate in groundwater as noted by Michalski and Britton (1997) and signal a bulk chemistry change from a silicate and sodium-dominant depositional environment for the Lockatong Formation and the lowermost part of the Passaic Formation to a more calcium carbonate and sulfate environment for the playa lake deposits in the upper part of the Passaic Formation and middle red zone of the Brunswick aquifer (Smoot and Olsen, 1994; Herman, 2001b). A regional analysis of the quality of ambient groundwater from wells in the Passaic Formation part of the Brunswick aquifer showed that calcium-bicarbonate and calcium-sulfate waters dominate (Serfes, 1994).

Type 2 WBFs are most common in gray zones containing abundant gray mudstone and gray and black shale (table F5; BLG, BMG and gray units). Gray beds range from less than a few feet to about 50 ft in thickness. They locally include multiple, thin to thick red beds that transmit water principally through steeply-dipping extension fractures (appendix 3M18, 3N5, 3N8, 3N13, 3O2, 3P2, 3P4, and 3Q2). The effects of groundwater flow in these fractures are clearly seen in the Brunswick gray zones (table F5). Borehole geophysical data repeatedly show marked contrasts in fluid temperatures and electrical conductance/resistance between adjacent, thick red beds and thin gray and black beds (appendix 3K3, 3K6, 3K7, 3N5 and 3N13). This suggests that flow cells develop within thick sequences of red mudstone and siltstone separated by gray-bed sequences that act as regional confining layers. This interpretation is supported by outcrops where copper minerals locally occur in the base of some gray beds overlying thick red-bed sequences (Monteverde and others, 2003). Oxygenated groundwater circulating in

red beds may carry dissolved metals that precipitate out where they come into contact with overlying, confining gray beds in a reducing geochemical environment due to the elevated organic carbon content at or near the red-gray redox boundary. As seen in borehole imagery, permeable extension fractures within the red beds seldom penetrate adjacent gray and black layers which develop their own sets of fractures (appendix 3N6). Stratigraphic heterogeneity likely plays an important role in concentrating other metals, radionuclides, and elements such as arsenic in specific stratigraphic horizons.

Groundwater electrical resistivity/conductivity profiles of specific stratigraphic sequences also vary between wells within short distances (appendix 3N8 and 4B8) with anomalous log traces corresponding to where groundwater enters or exits boreholes through WBFs and WBZs. In some places, type 2 WBFs develop in specific, correlative stratigraphic horizons (appendix 3D13, 3D14 and 3N8). However, type 1 WBFs in gray beds typically develop along or near contacts with red beds (appendix 3N5, 3N8, 3O2 and 3P4) that appear to transmit groundwater over great distances through type 1 features. But in general, groundwater leaks through thick gray-bed confining units in the Brunswick gray zones that are largely disconnected from major strata-parallel WBZs. This may result from insoluble silica based matrix cements in deep lake beds (see Chapter B) and the high degree of compaction and hardening of the formation resulting from deep burial (see Chapter C). This is important because thick confining units separate a small number of type 1 WBFs that owe their permeability to fracture porosity along the interface of fracture layering. Consequently, vertical flux in fine-grained units containing many gray beds is weak and groundwater recharge is limited. However, certain beds are more prone to develop transmissive type 2 fractures than others (appendix 3D14).

The most extensive hydrogeologic studies involving BTV technology in New Jersey spanned 14 wells in three adjacent projects near Hopewell and Pennington in Mercer County. The projects cover the Bristol Meyers-Squibb Research Campus, the Honey Brook Organics Farm, and the Stonybrook-Millstone Watershed Association Preserve (appendix 3N1). The combined wells extend over the zsection between the lower red and gray zones (fig. F2) resulting in a map span of about 1 mile (appendix 3N1). The profile interpretation includes a series of marker beds in the OPTV data records that help establish area-wide stratigraphic correlation. The distribution and names of the geological formations and members mapped in these projects are based on Olsen and others (1996). Figure F23 illustrates how strike and dip in red beds in the lower red zone of the Brunswick aquifer vary in 3D at the Stony-brook-Millstone site and exhibit layering heterogeneity that limits hydraulic conductivity along the strike of bedding. This group of wells is also useful in demonstrating the depth of weathering in fine-grained, fractured sedimentary bedrock based on fluid-temperature differences in profiles of many close wells (fig. F24). These wells were drilled when regulations required only 20 ft of casing rather than the current requirement of 50 ft, and therefore enable measurements to be made of hydraulic responses in the weathered bedrock that are ordinarily unattainable with deeper casings. Fluid-temperature differences plotted in the vertical direction show many fluctuations of greater intensity in the upper 60 ft than at deeper sections. This indicates an enhanced connection between surface and groundwater in this upper, weathered section. This depth of weathering is supported by large fluid-temperature anomalies measured just below casing under pumping conditions in wells having only 50 ft of casing (fig. F25). In some locations, upward flows are lost into WBZs located directly below casing in the 50-to-60-ft interval (appendix 3D5, 3D9).

Lockatong aquifer

The Lockatong aquifer was studied in Hunterdon and Mercer Counties (figs. F2, F3 and appendix 3Q, 4A, 4B and 4C). Appendix entries 3Q and 4C involve Wells 108 and 116 that penetrated the upper and lower stratigraphic contacts with the Passaic and Stockton Formations. The other two projects involved two and five observation and test wells respectively (appendix 4A and 4B). More than two-thirds of all WBFs in the Lockatong are tectonic fractures (table F5; 69 percent). The remaining third is divided between type 1 (19 percent) and type 3 (14 percent). The Lockatong is similar to the lower gray zone of the Brunswick in most respects but with overall thicker gray beds and thinner red beds. BTV studies show that small-scale normal faulting is common in the Lockatong Formation; small faults strike N20^{o} to 50^{o}E in two separate fault blocks (appendix 4A4, 4A6, 4B4, and 4B6). The geophysical logs generally show that WBFs are scarcer and more widely spaced vertically than they are in the Brunswick aquifer. Fluid temperature and electrical logs typically display wavy gradients that gradually stabilize at depth into more uniform values with narrowly-focused sections having pronounced log-value shifts (appendix 4A2, 4A5, 4B2, 4B5 and 4C2) due to the small number of WBFs intersecting a well. This is consistent with the Lockatong aquifer having the lowest aquifer ranking of any sedimentary unit in the basin (Herman and others, 1998). Cross flows were below the minimum threshold of detection (~0.5 ft/min) with the NJGS HPFM (Herman, 2006).

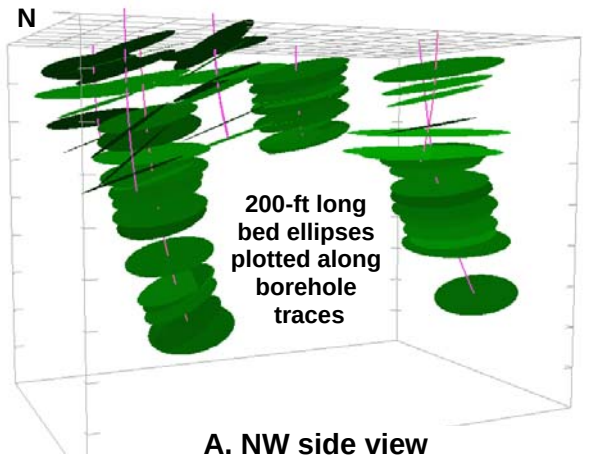

A. NW side view

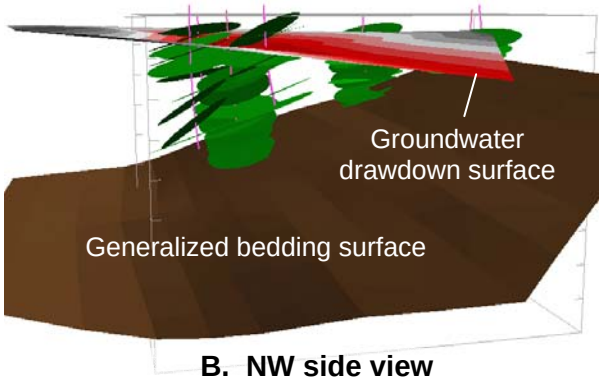

B. NW side view

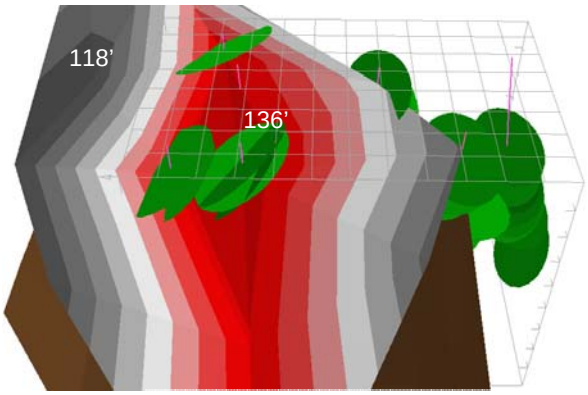

C. NW top-side view

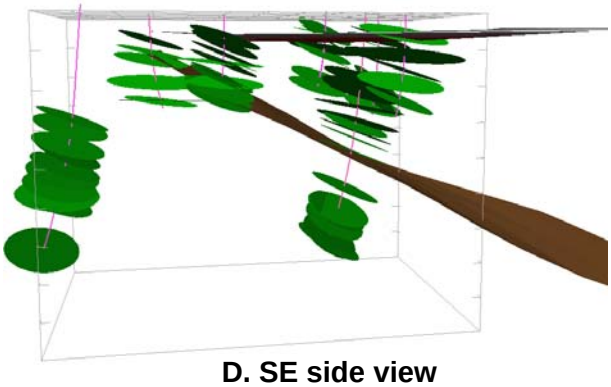

D. SE side view

Stockton aquifer

The Stockton Formation is the basal stratigraphic unit in the basin. BTV data for the Stockton aquifer are spotty and are mostly from north of the Trenton Prong between Trenton and Princeton, in Mercer County (fig. F3). The most extensive data stem from two framework studies using golf course irrigation wells and observation wells (appendix 4E and 4F). Other BTV analyses were made on third-party data from groundwater pollution investigations in Mercer County (appendix 4D and 4G). The upper contact with the overlying Lockatong aquifer was covered by an OPTV survey in Hunterdon County (appendix 4C). Analyses of WBFs in the Stockton show that just more than half are tectonic extension fractures and the remainder are about equally divided between types 1 (27 percent) and 3 (21 percent, table F5). HPFM data show that all types of WBFs may be highly transmissive (appendix 4E4, 4F3, and 4F5) and cross flows commonly exceed 3 gpm (table F4), and one 8-in-diameter well yielded about 15 gpm (appendix 4F5).

Geophysical logs of the Stockton aquifer generally show fluctuating hydraulic responses that commonly extend about 100 ft bls (appendix 4C2, 4E2, 4E4, 4F3, 4F5 and 4F7). Such responses are attributable to many WBFs intersecting the boreholes in the near-surface, weathered-bedrock section. This results from the removal of secondary authigenic minerals from fracture interstices, and the local weathering of bedrock along fracture surfaces to clay and silt. Fluid temperature and electrical logs typically display wavy gradients that gradually stabilize at depths below about 100 ft into more uniform values, with narrowly-focused sections having pronounced log-value shifts corresponding to WBFs and WBZs, as seen in other aquifers. High fluid temperatures above 100 ft depth in

Figure F23 (left). 3D-GIS perspectives of sedimentary bedding interpreted from OPTV records of part of the Stony Brook-Millstone Research well field (Appendix A entry 1C2). Cross-stratification of red beds is illustrated by bedding planes plotted as 3D ellipses along borehole traces, represented as gently-curving subvertical lines. Ellipses were generated using 200-ft major axes oriented along bedding strike and a 2:1 strike-to- dip aspect ratio. Grid tics and well-field grid cells are 50 ft. Top three views look southeast. The upper, shaded surface in figures B and C is a groundwater equipotential surface after a nine-day aquifer test conducted on the central well in the well field (Carlton and others, 1999). The lower surface is a generalized bedding surface representing average bedding orientations throughout the well field. Cross-stratification helps account for an irregular drawdown surface that is generally elongate along bedding strike but limited in its extent because of stratigraphic heterogeneity.

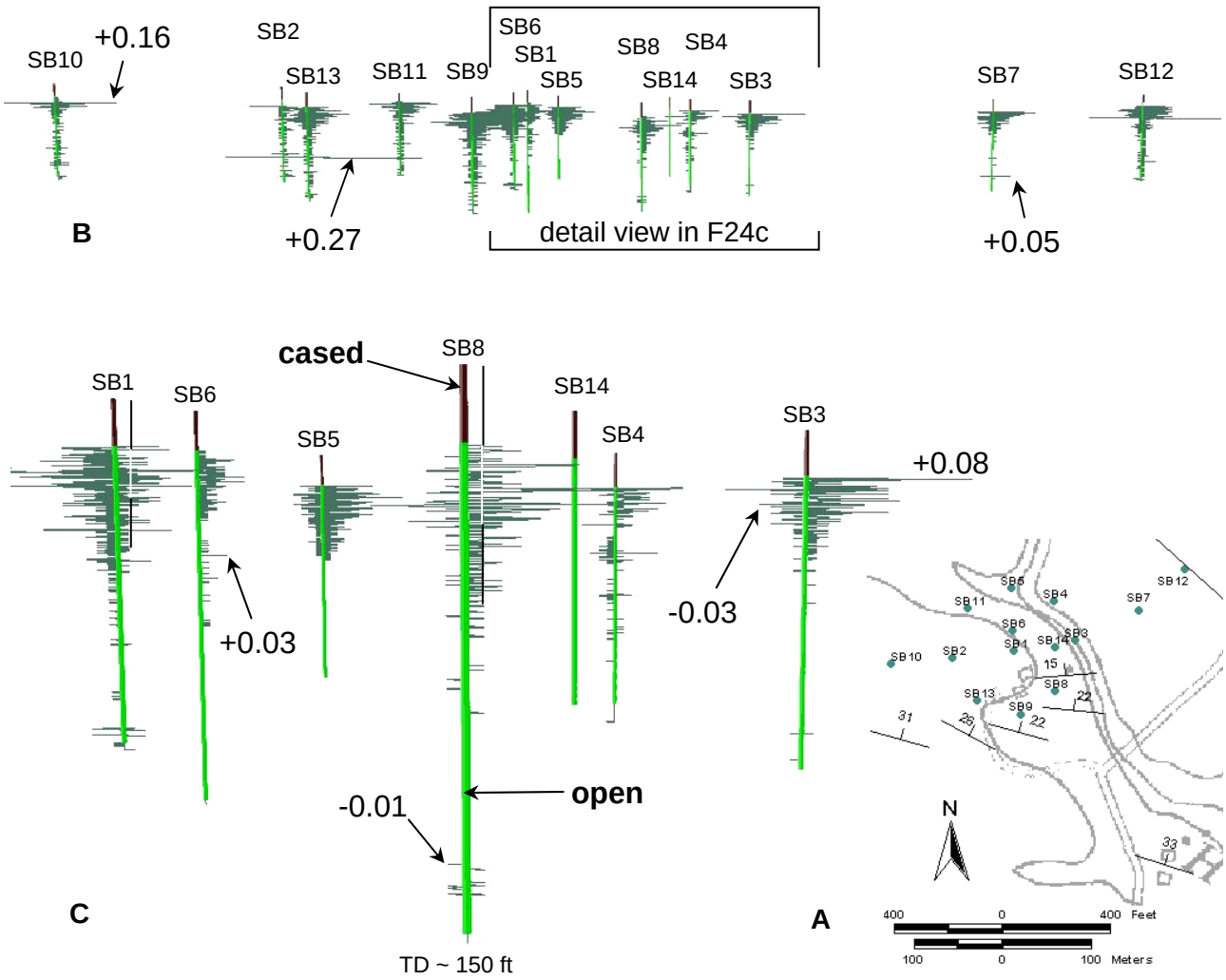

Figure F24. 3D-GIS perspective diagrams (looking northwest) showing fluid-temperature-difference profiles in the Stony Brook-Millstone Watershed Association preserve well field (Appendix 3M). A. Part of the US Geological Survey Hopewell, NJ 7-1/2' topographic map shows well locations and bedrock strike and dip. B. 3D perspective for the entire well field. The top of casing approximates land surface. Each well is about 150 ft deep with about 20 ft of casing. Horizontal spikes are fluid-temperature differences (^{o}F) plotted below casing. Temperature differences were calculated by subtracting successive readings taken at each 0.1-ft-depth interval. Line lengths are proportional to temperature differences that range from -0.45^{o} to +0.27^{o}. C. Detailed view of the part of the well field shown within bracketed area of B. Vertical black and white bar scales show 20-ft-depth increments for SB1 and SB8. The vertical distribution of temperature changes is used as a measure of entry and exit points of groundwater into and out of the open borehole and helps constrain the depth of the weathered zone in bedrock aquifers. Fluid-temperature differences decrease in frequency and magnitude downward to about 60 ft bls, near the base of the weathered zone. Intermittent temperature anomalies below this depth correspond to semiconfined-flow sections in deep bedrock. Well data and fluid-temperature logs provided courtesy of Glen Carleton, U.S. Geological Survey.

wells logged during warm summer months (appendix 4E4, 4F3 to 4F7) also suggest that the Stockton locally has a direct hydraulic connection between surface water and groundwater to that depth. The Stockton therefore has a deep water-table aquifer partly owing to its many fractured beds of deeply-weathered arkosic sandstone. The fractured layers provide highly permeable pathways for groundwater flow and, combined with secondary fractures, result in hydraulic gradients strongly reflecting topographic slope (appendix 4D1).

Outcrops of the Stockton in the southern Piedmont province near Trenton are scarce. Fractures are best characterized by use of BTV equipment. The strike of fractures in the Stockton is generally parallel and normal to bed strike (appendix 4D1, 4E1 and 4G1). Other, localized fracture sets reflect secondary structural strains near faults and folds. For example, fracture

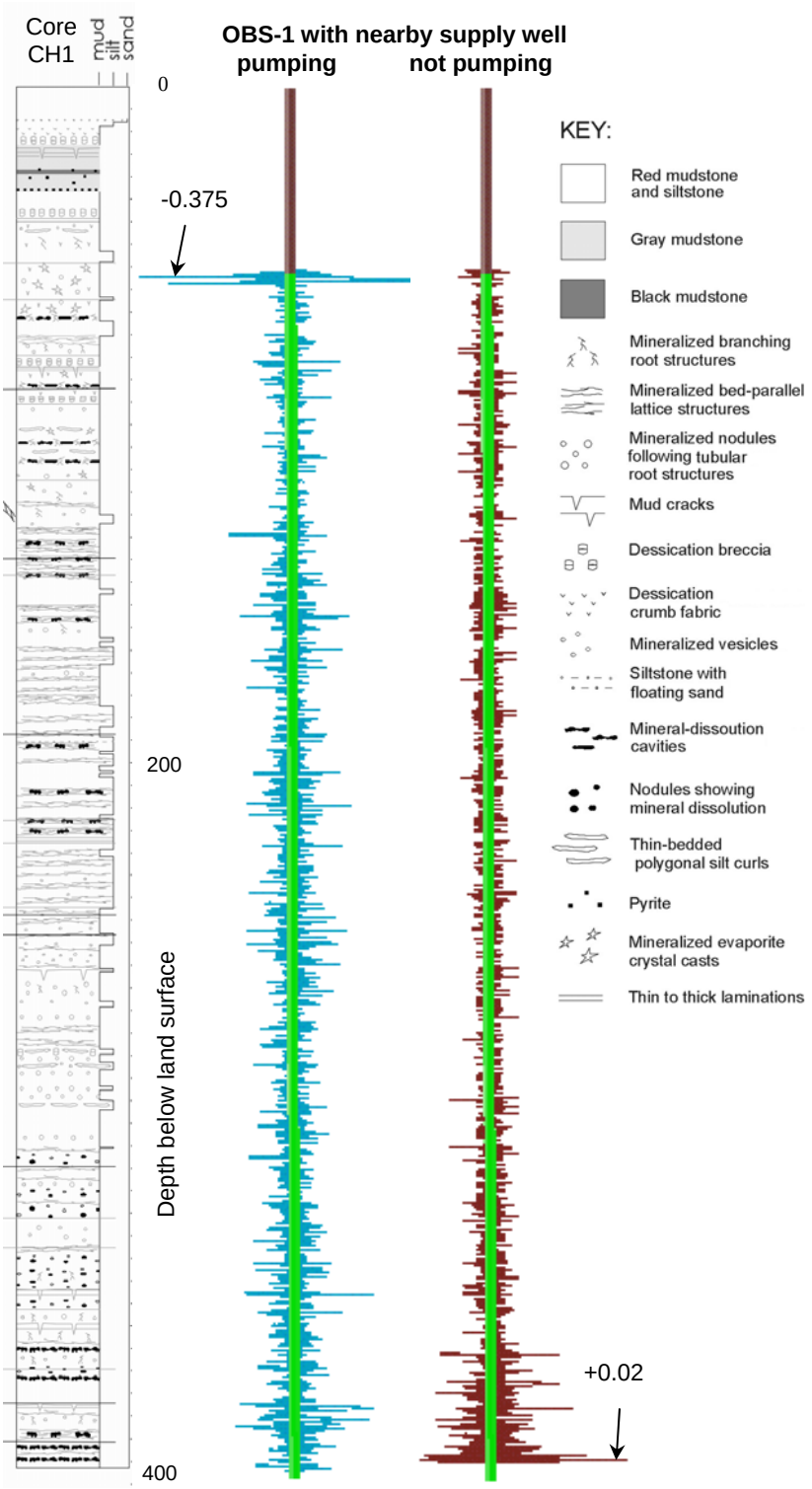

Figure F25. Diagrams comparing fluid-temperature differences (^{o}F) in Hopewell Borough well OBS-1 (Well 69, Appendix 3G) for pumping (left) and non-pumping (right) conditions. Diagrams are plotted next to stratigraphic diagram of nearby core (left). Temperature differences under nonpumping conditions are an order of magnitude lower than those for pumping conditions. Note the correlation between temperature anomalies and dissolution zones in the core and the pronounced temperature differences directly below casing under pumping conditions.

strikes for the Princeton study (fig. F26 and appendix 4F1) occur in all orientations but with strike maximums that agree with other, nearby but less fractured rocks. Concealed faults in this area are interpreted using surface-water drainage patterns, air-photo lineament analyses (fig. F26), and geophysical aeromagnetic coverage (Ghatge, 2004; Herman 2005). The Piedmont region was probably faulted and fractured during many incremental tectonic stages with faults and fracture zones striking in many directions (fig. F26).

BTV data of the Stockton show that cross bedding is common and bedding dip directions range over 180^{o} (appendix 4D1). Very thick sequences of alternating red and white sandstone are demonstrably continuous in the subsurface over hundreds of feet and include some stratigraphic pinch-outs interpreted by use of OPTV records and stratigraphic marker horizons for studies having two or more wells with overlapping stratigraphic coverage (appendix 4E6 and 4F2). These pinch-outs occur within larger belts of similar strata and do not appear to be as sharp in reducing horizontal conductivity in the Stockton aquifer as in the gypsic-paleosol unconformities in the Brunswick aquifer.

Open, permeable, steeply-dipping extension fractures penetrated by boreholes drilled into the Stockton reach maximum vertical dimensions of about 5 to 6 ft (appendix 4E3-right, 4F6-left and 4F8-left). Many type 1 WBFs in the Stockton occur at the contact between sandstone beds of different colors and compositions (appendix 4C2, 4C4-right, 4C3, 4E2 and 4F5). Many type 2 features also occur close to stratigraphic contacts (appendix 4C3 4C4-left, 4E2, 4E3, 4E5, 4E6, 4F4 and 4F5). The vertical spacing of water-bearing units is highly varied and ranges from inches to tens of feet of separation. The Stockton is typically able to supply hundreds of gpm of water to high-capacity wells and therefore has an intermediate-aquifer ranking in New Jersey (Herman and others 1998)

Relict hydrocarbon (bitumen)

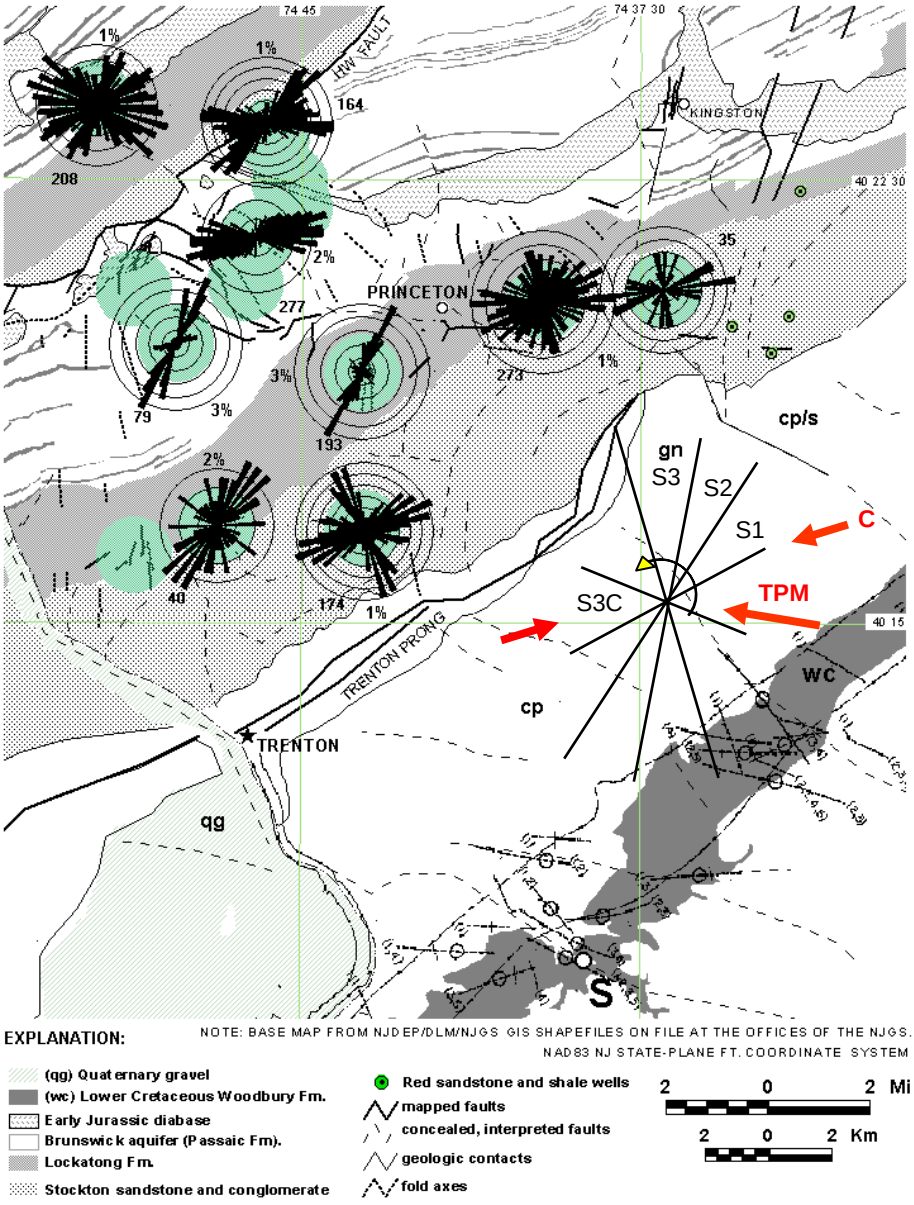

Figure F26. Bedrock geology of the Trenton area (modified from Drake and others, 1996; Herman 2005). Histograms show strike of nonbedding-plane fractures measured in OPTV records for selected projects detailed in figure F3. Histogram numbers indicate the number of measurements at each site; percentages indicate ring increments. Structural lineament analysis of the Woodbury Clay Formation (**wc**) by unpublished source on file at the NJGS. **S** – Site where overturned and contorted clay is reported in NJGS permanent notes. Histograms show different fracture strikes throughout the region. Diagram at center right summarizes the proposed sequence of extension-fracture development in the basin (S1 to S3, then SC3) in comparison to present-day, horizontal crustal compression determined from earthquake analyses (**C**; Goldberg and others, 2003) and current tectonic-plate motion (**TPM**) based on 12 years of GPS data NASA,2009). Abbreviations: qg – quaternary gravel, cp – coastal plain, cp/s coastal plain overlying Stockton Formation, gn – gneiss.

has been reported in authigenic mineral fill of tectonic fractures in the basin (Parnell and Monson, 1995; Herman, 2005, and Chapter C). OPTV images of bitumen clots and stringers in Stockton beds (appendix 4E3-left, 4E7-left, 4F6-lower right, 4F8-right, 4F9-right and 4F10-left) and in fractures (appendix 4F8-left) were collected in the area north of Trenton (fig. F3). The sedimentary matrix near bitumen accumulations is locally altered and stained by mineral-enriched fluids (appendix 4F5-right, 4F6-left and 4E7-left).

Discussion

Bedrock aquifers in the Newark basin, where unconsolidated overburden is generally thin (< 20 ft) include shallow, intermediate, and deep sections having variable hydraulic properties (fig. F6). Shallow overburden includes unconsolidated alluvium, colluvium, artificial fill, and regolith. Regolith in most sedimentary formations includes red, brown, orange, yellow, and gray silty clay to clayey silt residuum containing angular bedrock fragments above bedrock (fig. F16). Weathered conglomerate includes loose cobbles and gravel at the surface. The shallow section extends to depths of ~3 to 15 ft and commonly has a perched, transient water table near its base that discharges to streams and other surface-water bodies (fig. F6). Ackermann (1997) demonstrated a strong correlation between surface-water drainage patterns and the strike of fractures in bedrock overlain by thin cover. This relationship is further demonstrated by comparing

fracture strikes determined form BTV analysis to topographic trends (appendix 1A1, 1D1, 1E1, 1F1, 2E1, 3A1, 3D1 among others).

The intermediate or 'weathered' bedrock section is subject to prolonged episodes of weathering during wide fluctuations of climate, including permafrost during past glacial epochs. Conductive features in weathered bedrock included 1) gently dipping fractures resulting from erosion and pressure release (fig. F13c) in addition to those found in deeper bedrock including, 2) bedding fractures focused near stratigraphic contacts, 3) strata containing porous gypsum paleosols, and 4) fractured layers with secondary porosity stemming from mineral dissolution from both the rock matrix and fracture interstices. Abundant, connected pathways for groundwater flow in the weathered section commonly result in water-table or unconfined conditions and natural hydraulic gradients aligned down topographic slope (fig. F21 and appendix 2D1). Groundwater flow in the shallow bedrock is therefore more uniformly distributed than it is under the anisotropic conditions in deep bedrock that favor horizontal flow directions along stratigraphic strike (Vecchioli and others, 1969; Michalski and Britton, 1997; Carlton and others, 1999). Weathered bedrock commonly reaches depths of 60 to 100 ft in the Brunswick and Stockton aquifers respectively, based on groundwater temperature and electrical logs (see previous discussion for the Stockton aquifer. Also, Morin and others (1997 and 2000) reported high yields at depths of about 60 ft in basin wells. Water-temperature logs of the other aquifers, including the Lockatong, diabase, and basalt zones in the Brunswick aquifer, show no evidence of having as deep a weathered zone as that in the Stockton and therefore are assumed to have more shallow weathered sections like those in the Brunswick. Most wells in these other aquifers in this study have a minimum of 50 ft of casing that makes hydrogeologic evaluation of the weathered section difficult.

The hydrologic connection between open boreholes and weathered bedrock is an important consideration in addressing near-surface groundwater pollution because the depth of weathering may exceed the depths to which water wells are commonly cased. The weathered section in the Brunswick red beds and the Stockton Formation is shown here to range from about 60 to100 ft bls. As a result, about 10 to 50 ft of open borehole may be connected to the water-table aquifer and a likelihood of a strong hydraulic connection to near-surface waters, especially during pumping. This has been verified by large fluid-temperature and electrical log responses recorded directly below casing during pumping (fig. F25). Based on these findings, water-supply wells should be cased to a depth of at least 60 ft in all aquifers, and to about 100 ft in the Stockton aquifer.

The infiltration of water from precipitation through shallow fractures may be impeded in some places to less than it is in deep bedrock by silt and clay residuum of weathered rock in and along fractures (fig. F27 and Kasabach, 1966; Lewis-Brown and dePaul, 2000). However, vertical hydraulic-conductivity values of the weathered section exceed those in the deep zone by two orders of magnitude in nearby areas (Lewis-Brown and Jacobsen, 1995). This apparent anomaly points to the need for more hydrogeologic research on weathered bedrock to clarify aspects of groundwater recharge and contaminant transport in the shallow subsurface.

Groundwater exhibits anisotropic, confined-flow characteristics in deep bedrock mostly because gently-dipping strata exert primary control on the hydrogeologic framework. Groundwater is principally stored in myriad fractures but is transmitted long distances by bed partings and highly permeable layers between confining beds. Olsen and others (1996) demonstrated the continuity of lacustrine beds deposited in deep-water environments throughout the basin so that dark shale extended to distances of tens of miles. In comparison, the vertical fracture is limited to the vertical thickness of the fractured layer that is at least an order of magnitude smaller than the bedding plane (fig. F15). The maximum vertical extent of individual fractures measured in small-diameter boreholes for this study was about 6 ft (appendix 3N7, 3O2). This is an important aspect of borehole hydrogeology because the geometric relation between steeply-dipping fractures and a steeply-inclined borehole limits the thickness of the fractured layer (fig. F28). It also demonstrates that the 3D extent and hydraulic connection between steeply-dipping fractures in a fractured layer is difficult to determine from borehole BTV studies alone.

Reported transmissivity (T) values of deep bedrock vary significantly, commonly as much as three orders of magnitude among the different aquifers and discreet sections of a single aquifer (appendix 2F3, 2F4, 2F5, 2F6 and Morin and others, 1997; Lewis-Brown and dePaul, 2000; Lewis-Brown and others, 2004; Michalski, 2001; and Michalski, 2009). This varied character results from geological heterogeneity and from the different methods used for calculating T. For example, T values of an aquifer commonly are calculated from pumping tests based on the entire saturated interval penetrated by a well. It is important to note that these aquifer characteristics are only average values of a composite flow system consisting of many thin aquifers separated by some thick confining layers. Detailed hydrogeological studies using methods for determining intervals flows, such as HPFM studies and straddle packer tests produce more accurate determinations of aquifer characteristics for discrete WBZs. Parameter values of individual parts of the section should be determined and used for

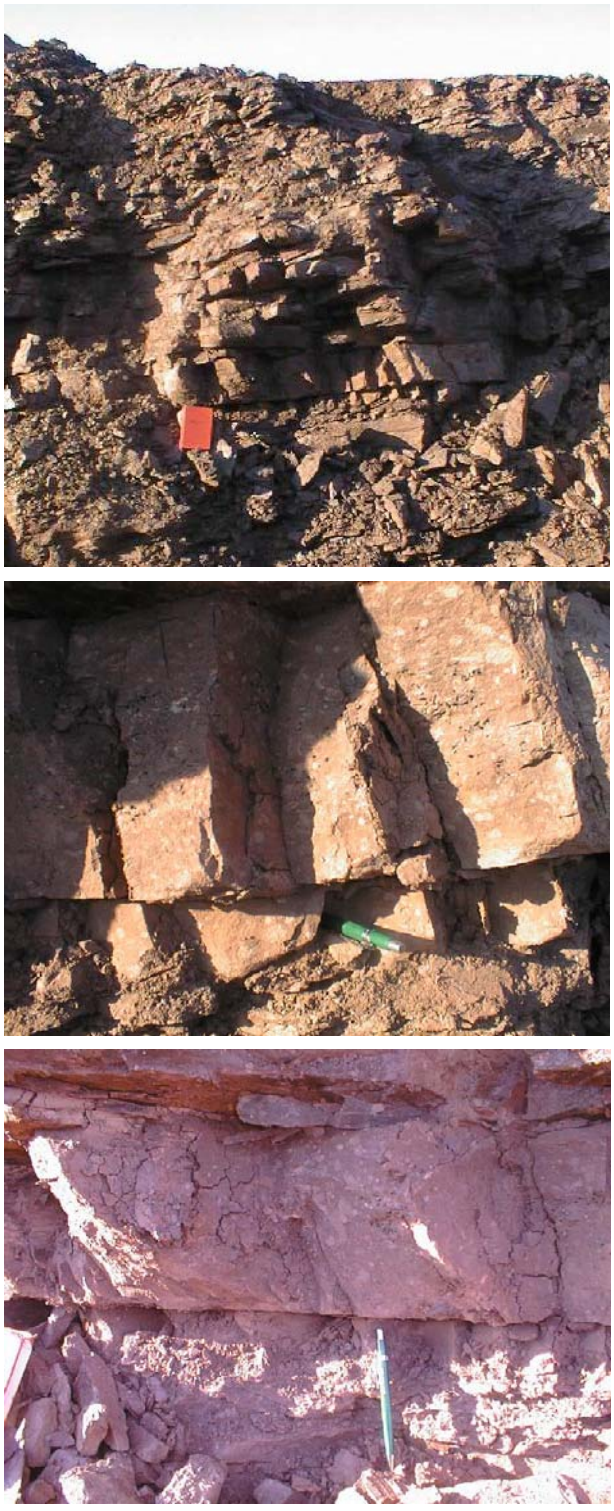

Figure F27. Bedrock excavations in the Passaic Formation during construction of the Heron Glen Golf Course, Hunterdon County (appendix 3K). Shortly after excavation, polygonal mudcracks formed along fracture walls in desiccated silt and clay residuum of siltstone and mudstone. This shows that silt and clay infilling shallow fractures originate directly from degradation and weathering of bedrock.

characterizing the distribution, fate, and transport of groundwater contaminants when possible. Average values based on large intervals of open borehole may result in underestimating T and therefore both the distribution and velocity of contaminants in highly transmissive units.

A benefit of recorded OPTV records is that they may help to constrain the vertical extent of the section for which aquifer parameters are required. Based on OPTV records for this study, the maximum vertical extent of any specific WBF intersected by a well is about 10 ft regardless of whether it is classified as large-aspect extension fractures or a thick gypsum-paleosol bed. This needs to be taken into consideration when assembling straddle packers for conducting environmentally sensitive hydrogeologic studies, because straddle-packer tests commonly employ assemblies having 20-ft of separation, possibly leading to underestimation of T values by a factor of at least two.

Cross flows in water wells in the Newark basin stem mostly from topographic irregularities at the land surface resulting from differential erosion of gently-dipping, layered strata. Ambient flow volumes measured in small-diameter water wells in the basin range from no measurable flow (NMF) to about 15 gpm in the Stockton aquifer, 8 gpm in the Brunswick aquifer, 5 gpm in basalt, and 1 gpm in the Lockatong Fm. and diabase (table F4). The 8 gpm measured in the Brunswick aquifer was from a 6-inch-diameter observation well located near two irrigation wells that were pumping at a combined rate of about 500 gpm (appendix 3K1). The 8 gpm value is therefore probably more than it would be under nonpumping conditions based on other studies where cross-flow rates for the same section were 2 to 6 times greater under pumping conditions in comparison to those for nonpumping conditions (appendix 3D5 and 3G6). Most of the gray beds in the Brunswick and Lockatong aquifers yield meager flows too low to detect using the NJGS HPFM, whereas the highest cross flows are from red beds in the Brunswick aquifer, particularly from the middle red zone, where gypsum paleosol is abundant. It is notable that the respective flows cited for each aquifer resemble the aquifer rankings in the basin (Herman and others, 1998); the Stockton (C-ranking) and Brunswick (C) aquifers produce the highest flows and high-capacity yields, followed in decreasing order by the Lockatong (D) and basalt (D), then diabase (E).

Hydrogeological framework characterization of red beds in the Brunswick formation needs to take into account the distribution of gypsum-soil beds with unconformity surfaces and dissolution-enhanced WBZs. These features are common in massive red mudstone and are important because their occurrence and geometry can diminish or enhance the ability of an aquifer to supply groundwater. Angular unconformities

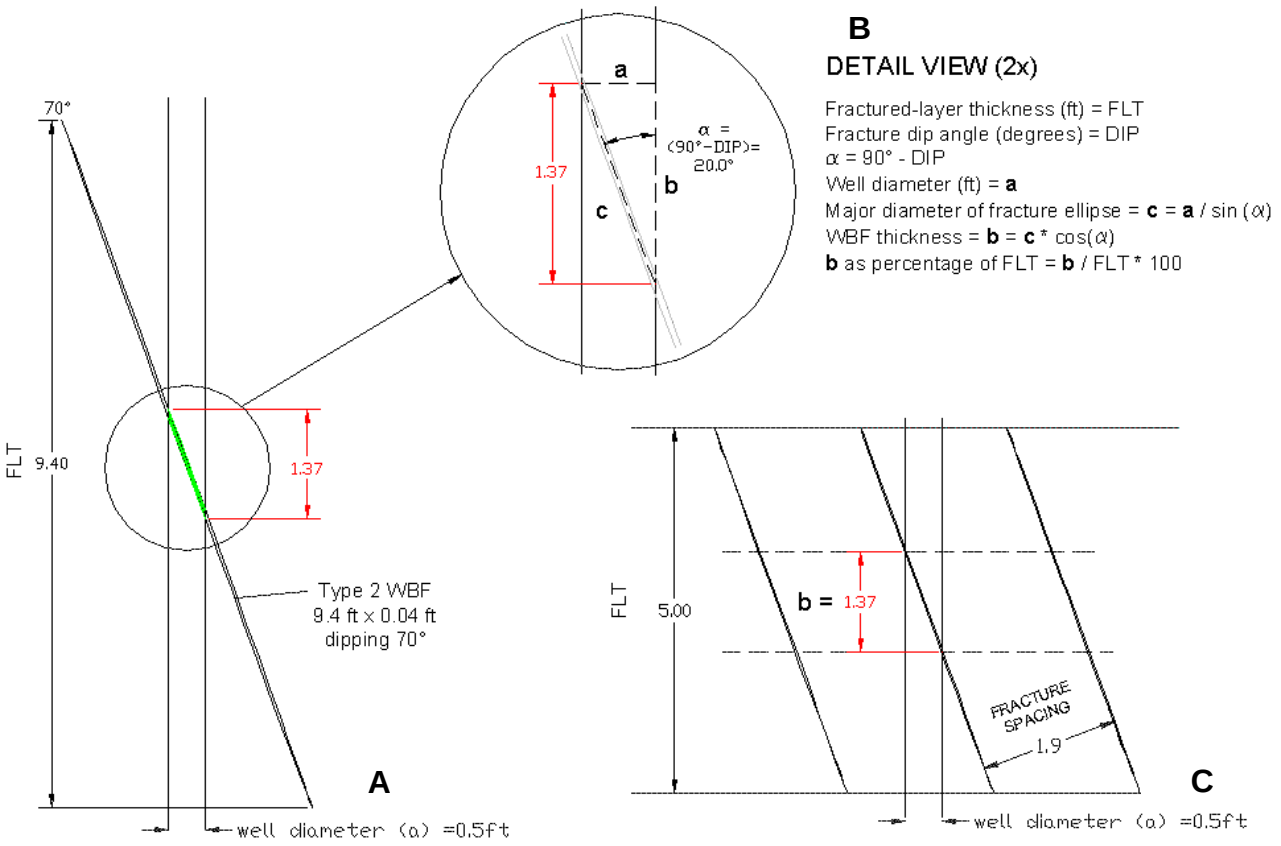

Figure 28. Profile views of dipping type 2 WBFs in relation to the thickness of fractured layers and a vertical well. A. A 9.4 ft-thick fractured layer penetrated by a 6-inch diameter well bisects one steeply-dipping and permeable extension fracture with a maximum, 4 mm-wide interstice. In this example, the measured thickness of the WBF in the borehole is only ~15% (1.37/9.40) the actual thickness of the fractured, permeable layer. B. Details of the geometric relationships for the approximate vertical thickness of the WBF (b), the diameter of the borehole (a) and the partial length of the fracture ellipse (c). C. A second example of a type 2 WBF dipping 70° with only a 5.0 ft fractured-layer thickness and a fracture-spacing of about 2.0 ft; a typical value mapped in the basin for medium-to thick sedimentary beds. In this example, the vertical thickness of the WBF is about 27% that of the permeable layer. Flow rates and contaminant concentrations for partially-penetrated type 2 WBFs are therefore apparent values that represent conditions for the entire fractured layer when fracture interstices are open and hydraulically conductive throughout the layer. Measured flow rates and analyte concentrations for a partially-penetrated type 2 WBF, or an interval containing such a feature, must be used with caution because of differences between the apparent (b) and true (FLT) thicknesses of the permeable unit; measured flow and constituent concentrations associated with a dipping, type 2 feature reflect conditions over a much thicker interval than directly sampled by a well. Similarly, if the well fails to penetrate such a feature, the interval may be misinterpreted as being impermeable and unpolluted.

can locally truncate paths of groundwater recharge to deep aquifers (appendix 3F4) and thereby diminish well yields, whereas conductive dissolution zones locally form high-yielding WBZs over distances of thousands of feet (appendix 3M7, 3D14, 3F3 and 3F4). Dissolution enhancement of gypsum-soil beds and fractured layers can result in highly productive aquifers capable of conveying groundwater pollution over great distance in relatively short time periods.

More work is needed to evaluate aquifer characteristics in areas of dense tectonic fractures near large-scale faults. In outcrops, multiple sets of tightly spaced fractures exhibit iridescent-blue manganese minerals coating fracture surfaces. Clearly, groundwater flow is vigorous in tectonically active areas and fault zones may contain anomalous groundwater that deviates geochemically from the LMAS groundwater flow model, at least to the extent that fractures exert primary hydrogeological control. If so, the horizontal component of hydraulic conductivity may be preferentially aligned along the strike of the fault rather than bedding strike if bedding and faults strike do not coincide. Nevertheless, stratigraphic bedding is the dominant control on the storage and movement of groundwater in most of the basin and the primary consideration in determining the direction of groundwater flow below the

weathered-bedrock interval.

Acknowledgements

Many people helped find and gain access to the project sites used for this research. In this regard, I thank Matt Mulhall, Penelope Althoff, Vince Uhl, Greg Bakeman, Frank Source, Nick Sodano, Carole Chatelain, Jill Dunphy, Marc Romanell, Greg Giles, Jason Pierce, Bay Weber, Jim Kinsell, Pierre LaCombe, Glen Carleton, Tony Hauk, Rob Sheneman, Dave Misiolek, Charles Dey, Roger Stewart, Michael Gornnert, Robert Weiss, David Stout, and Ken Luperi. I acknowledge and thank all homeowners who provided access to their domestic water-supply wells. Steve Laney provided a valuable review of the early manuscript and appendixes. Paul Sanders and Kevin Schick of the NJDEP provided program coordination and administered research funds used to support this work. Below I acknowledge the efforts and contributions of fellow NJGS employees. Many enjoyable field days were spent pulling and replacing water pumps and packer strings, and logging wells with Steve Spayd, John Curran and Gregg Steidl, Brian McCann, and Mark French. Michael Serfes and Jim Boyle contributed valuable discussions and insights with regard to hydrogeologic relationships and analyses. Joe Rich and Walter Marzulli provided surface elevation surveys for some projects. I thank Don Monteverde, Hugh Houghton, Jim Mitchell, and Seth Fankhauser of the NJGS for their use of their structural data and bedrock maps. Dave Hall, Robert Canace, Dave Pasiczynk, and Karl Muessig supervised these efforts and provided program support. I give special recognition and thanks to Irving, 'Butch' Grossman, and Bill Graff for providing thorough and helpful reviews of this manuscript. Butch's review, in particular, resulted in a much more presentable and clear report.

References

Ackermann, R.V., 1997, Spatial distribution of rift-related fractures: field observations, experimental modeling, and influence on drainage networks: Rutgers University Ph.D. dissertation, New Brunswick, New Jersey, 136 p.

Brown, J.C., and dePaul, V.T., 2000, Groundwater flow and distribution of volatile organic compounds, Rutgers University Busch Campus and vicinity, Piscataway township, New Jersey: U.S. Geological Survey Water-Resources Investigations Report 99-4256, 72 p.

Burton, W.C., and Ratcliffe, N.M., 1985, Attitude, movement history, and structure of cataclastic rocks of the Flemington fault--Results of core drilling near Oldwick, New Jersey: U.S. Geological Survey Miscellaneous Field Studies Map MF-1781.

Carlton, G.B., Welty, C., and Buxton, H.T., 1999, Design and analysis of tracer tests to determine effective porosity and dispersivity in fractured sedimentary rocks, Newark Basin, New Jersey: U.S. Geological Survey Water-Resources Investigations Report 98-4126, 80 p.

de Boer, J.Z., and Clifford, A.E., 1988, Mesozoic tectogenesis: Development and deformation of 'Newark' rift zones in the Appalachians (with special emphasis on the Hartford basin, Connecticut), *in* Manspeizer, Warren, ed., Triassic-Jurassic Rifting, Continental Breakup, and the Origin of the Atlantic Ocean and Passive Margin: Elsevier, New York, New York, p. 275-306.

Dietz, R.S., 1961, Continent and ocean basin evolution by spreading of the sea floor: Nature, v. 190, p. 854-857

Drake, A.A., Jr., Volkert, R.A., Monteverde, D.H., Herman, G.C., Houghton, H.H., and Parker, R.A., 1996, Bedrock geologic map of northern New Jersey: U.S. Geological Survey Miscellaneous Investigation Series Map I-2540-A, scale 1:100,000; 2 sheets.

Dula, W.F., 1991, Geometric models of listric normal faults and rollover folds: American Association of Petroleum Geologists Bulletin, v. 75, no. 10, p. 1609-1625.

Ghatge, S.L., 2004, Magnetic anomalies of New Jersey, N.J. Geological Survey Digital Geodata Series DGS04-3, ArcView shapefile coverage, scale 1:500,000.

Goldberg, D., Lupo, T., Caputi, M., Barton, C., and Seeber L., 2003. Stress regimes in the Newark basin rift: Evidence from core and downhole data: *in* LeTourneau, M., Olsen, P.E., eds., The great rift valleys of Pangea in eastern North America 1, Tectonics, Structure, and Volcanism, Chapter 7: Columbia University Press, New York, New York, p. 104-117.

Groshong, R.H., 1988, Low-temperature deformation mechanisms and their interpretation: Geological Society of America Bulletin, v. 100, p. 1329-1360.

Gross, M.R., 1993, The origin and spacing of cross joints: examples from the Monterey Formation, Santa Barbara Coastline, California: Journal of Structural Geology, v. 15, p. 737-751.

Herman, G.C., 1997, Digital mapping of fractures in the Mesozoic Newark basin, New Jersey: Developing a geological framework for interpreting movement of groundwater contaminants: Environmental Geosciences, v. 4, no. 2, p. 68-84.

Herman, G.C., 2000, ArcView 3.X Extension for making 2D and 3D structural geologic shapefiles: NJ Geological Survey Digital Geodata Series DGS00-5. Computer program for use with ESRI

ArcView 3.x Geographic Information System.

Herman, G.C., 2001a, ArcView 3.X Extension for making 2D and 3D structural geologic shapefiles: N.J. Geological Survey Digital Geodata Series DGS01-1. 1. Computer program for use with ESRI ArcView 3.x Geographic Information System.

Herman, G.C., 2001b, Hydrogeological framework of bedrock aquifers in the Newark basin, New Jersey: *in* LaCombe, P.J. and Herman, G.C., eds. Geology in Service to Public Health, Field Guide and Proceedings of the 18th Annual Meeting of the Geological Association of New Jersey, p. 6-45.

Herman, G.C., 2005, Joints and veins in the Newark basin, New Jersey, in regional tectonic perspective: *in* Gates, A. E., ed., Newark basin – View from the 21st Century: Field Guide and Proceedings of the 22nd Annual Meeting of the Geological Association of New Jersey, p. 75-116.

Herman, G.C., 2006, Field tests using a heat-pulse flow meter to determine its accuracy for flow measurements in bedrock wells: N.J. Geological Survey Technical Memorandum TM06-1, 8 p.

Herman, G.C., Canace, R.J., Stanford, S.D., Pristas, R.S., Sugarman, P.J., French, M.A., Hoffman, J.L., Serfes, M.S., and Mennel, W.J., 1998, Aquifers of New Jersey: N.J. Geological Survey Open-File Map 24, scale 1:500,000, 1 sheet.

Herpers, H., and Barksdale, H.C., 1951, Preliminary report on the geology and groundwater supply of the Newark, New Jersey, Area: N.J. Department of Conservation and Economic Development, Special Report 10, 52 p.

Hodgson, R.A., 1961, Regional study of jointing in Comb ridge-Navajo Mountain Area, Arizona and Utah: American Association of Petroleum Geologists Bulletin, v. 45, 1-38.

Hoffman, J.L., and Lieberman, S.E., 2000, New Jersey Water Withdrawals 1990-1996: N.J. Geological Survey Open-File Report OFR 00-1, 123p.

Houghton, H.F., 1990, Hydrogeology of the early Mesozoic rocks of the Newark basin, New Jersey, *in* Brown, J.O., and Kroll, R. L., eds. Aspects of Groundwater in New Jersey: Field Guide and Proceedings of the 7th Annual Meeting of the Geological Association of New Jersey, p. E1-E36.

Houghton, H.F., Herman, G.C., and Volkert, R.A., 1992, Igneous rocks of the Flemington Fault zone: Geochemistry, structure, and stratigraphy, in Puffer J.H. and Ragland, P.C., eds., Eastern North American Mesozoic Magmatism, Geological Society of America Special Paper 268, p. 219-232.

Huang, Q., and Angelier, J., 1989, Fracture spacing and its relation to bed thickness: Geological Magazine, v. 126, p. 355-362.

Kasabach, H.F., 1966, Geology and Groundwater Resources of Hunterdon County, New Jersey: N.J. Geological Survey Special report no. 24, 128 p.

Knapp, G.N., 1904, Underground waters of New Jersey, Wells drilled in 1903: Annual report of the State Geologist for 1903, N.J. Geological Survey, p. 73-93.

Kulander, B.R., Dean, S.L., and Ward, B.J., 1990, Fractured core analysis: Interpretation, logging, and use of natural and induced fractures in core: American Association of Petroleum Geologists Methods in Exploration Series, no. 8, Tulsa, Oklahoma, USA, 88 p.

Kummel, H.B., 1898, The Newark System or red sandstone belt: N.J. Geological Survey Annual Report of the State Geologist for the Year of 1897, p. 23-159.

Laney, S.E., 2005, Stop 4. Structure of the Hopewell fault, North segment, Belle Mead, N.J., *in* Gates, A.E., ed., Newark basin – View from the 21st Century: Field Guide and Proceedings of the 22nd Annual Meeting of the Geological Association of New Jersey, p. 145-159.

Laney, S.E., Husch, J.M., and Coffee, C.,1995, The petrology, geochemistry and structural analysis of late-stage dikes and veins in the Lambertville sill, Belle Mead, New Jersey: Northeastern Geology and Environmental Sciences, v. 17, no. 2., p. 130-145.

Lewis-Brown, J.C., and dePaul, V.T., 2000, Groundwater flow and distribution of volatile organic compounds, Rutgers University Busch campus and vicinity, Piscataway Township, New Jersey: U.S. Geological Survey Water-Resources Investigations Report 99-4256, 72 p.

Lewis-Brown, J.C., and Jacobsen, E., 1995, Hydrogeology and groundwater flow, fractured Mesozoic structural-basin rocks, Stony Brook, Bedens Brook, and Jacobs Creek drainage basins, west-central New Jersey: U.S. Geological Survey Water-Resources Investigations Report 94-4147, 83 p.

Lewis-Brown, J.C., Rice, D.E., Rosman, R., and Smith N.P., 2004, Hydrogeological framework, groundwater quality, and simulation of groundwater flow at the Fair Lawn well field Superfund site, Bergen County, New Jersey: U.S. Geological Survey Scientific Investigations Report 2004-5280, 109 p.

Lucas, M., Hull, J., and Manspeizer, W., 1988, A foreland-type fold and related structures of the Newark rift basin, *in* Manspeizer, W., ed., Triassic-Jurassic Rifting, Continental Breakup, and the Origin of the Atlantic Ocean and Passive Margin: Elsevier, New York, New York, p. 307-332.

Michalski, A., 1990, Hydrogeology of the Brunswick (Passaic) formation and implications for groundwater monitoring practice: Groundwater Monitoring Review, v. 10, no. 4, p.134-143.

Michalski, A., 2001, A practical approach to bedrock aquifer characterization in the Newark basin, *in*

LaCombe, P.J. and Herman, G.C., eds., Geology in Service to Public Health: Field Guide and Proceedings of the 18th Annual Meeting of the Geological Association of New Jersey p. 46-59.

Michalski, A., 2010, Hydrogeologic characterization of contaminated sites in the Newark basin: Selecting conceptual flow model and characterization tools, *in* Herman, G.C. and Serfes, M.E., eds., Contributions to the geology and hydrogeology of the Newark basin, Chapter D: N.J. Geological Survey Bulletin 77, Trenton, N.J., p. D1-D12.

Michalski, A., and Britton, R., 1997, The role of sedimentary bedding in the hydrogeology of sedimentary bedrock - Evidence from the Newark basin, New Jersey: Groundwater, v. 35, no. 2. p. 318-327.

Michalski, A., and Gerber, T., 1992, Fracture flow velocities in the Passaic Formation in light of interwell tracer tests: *in* Ashley, G.M. and Halsey, S.D, eds., Field Guide and Proceedings of the 9th Annual Meeting of the Geological Association of New Jersey, p. 1-7.

Michalski, A., and Klepp, G.M., 1990, Characterization of transmissive fractures by simple tracing of in-well flow: Groundwater, v. 28, no. 2, p. 191-198.

Monteverde, D.H., Stanford, S.D., and Volkert, R.A., 2003, Geologic Map of the Raritan Quadrangle, Hunterdon and Somerset Counties, New Jersey: N.J. Geological Survey Geologic Map Series GMS 03-2, scale 1:24,000.

Monteverde, D.H. and Volkert, R.A., 2005, Bedrock Geology of the Chatham Quadrangle, Morris, Somerset, and Union Counties, New Jersey, N.J. Geological Survey Geological Map Series Map GMS04-2, scale 1:24,000.

Morin, R.H., Carleton, G.B., and Poirier, S., 1997, Fractured-aquifer hydrogeology from geophysical logs; the Passaic Formation, New Jersey: Groundwater, v. 35, no. 2, p. 328-338.

Morin, R.H., Senior, L.A., and Decker, E.R., 2000, Fractured-aquifer hydrogeology from geophysical logs: Brunswick Group and Lockatong Formation, Pennsylvania: Groundwater, v. 38, no. 2, p. 182-192.

Narr, W., and Suppe, J., 1991, Joint spacing in sedimentary rocks: Journal of Structural Geology, v. 13, p. 1037-1048

NASA (National Aeronautics and Space Administration), 2009, GPS Time-series data: http://sideshow.jpl.nasa.gov/mbh/series.html.

Olsen, P.E., 1980, The latest Triassic and early Jurassic Formations of the Newark basin (Eastern North America, Newark Supergroup): Stratigraphy, structure, and correlation: New Jersey Academy of Sciences, v. 25, no. 2, p. 25-51.

Olsen, P.E., 1986, A 40-million year lake record of orbital climate forcing: Science, v. 234, p. 842-847.

Olsen, P.E., 1988, Continuity of strata in the Newark and Hartford Basins, *in* Froelich, A.J., and Robinson, G.P., Jr., eds., Studies of the Early Mesozoic Basins of the Eastern United States: U.S. Geological Survey Bulletin 1776, p. 6-18.

Olsen, P.E., Kent, D.V., Cornet, Bruce, Witte, W.K., and Schlische, R.W., 1996, High-resolution stratigraphy of the Newark rift basin (early Mesozoic, eastern North America): Geological Society of America Bulletin, v. 108, no. 1, p. 40-77.

Olsen, P.E., Withjack, M.O., and Schlische, R.W., 1992: Inversion as an integral part of rifting: An outcrop perspective from the Fundy basin, eastern North America: Eos-American Geophysical Union Transactions, v. 73, n. 43, p. 562.

Owens, J.P., and Sohl, N.F., 1969, Shelf and deltaic paleoenvironments in the Cretaceous-Tertiary Formations of the New Jersey Coastal Plain, *in* Subitzky, Seymour, ed., Geology of selected areas in New Jersey and Eastern Pennsylvania and guide book: Rutgers University Press, New Brunswick, New Jersey, p. 235-278.

Owens, J.P., Sugarman, P.J., Sohl, N.F., Parker, R.A., Houghton, H.F., Volkert, R.A., Drake, A.A., Jr., and Orndorff, R.C., 1998, Bedrock geologic map of central and southern New Jersey: U.S. Geological Survey Miscellaneous Investigation Series Map I-2540-B, scale 1:100,000; 3 sheets.

Pollard, D.P., and Aydin, A., 1988, Progress in understanding jointing over the past century: Geological Society of America Bulletin, v. 100, p. 1181-1024.

Parnell, J., and Monson, B., 1995, Paragenesis of hydrocarbon, metalliferous and other fluids in Newark Group basins, Eastern U.S.A., Institute of Mining and Metallurgy, Transactions, Section B: Applied Earth Science; v. 104, p. 136-144.

Ragan, D.M., 1985, Structural Geology; an Introduction to Geometric Techniques, 3rd Edition: John Wiley & Sons, Inc., New York, New York, 393 p.

Ramsay, J.G., and Huber, M. I., 1987, The techniques of modern structural geology, v. 2: Folds and fractures: Academic Press, London, England, 700 p.

Ratcliffe, N.M. 1980, Brittle faults (Ramapo fault) and phyllonitic ductile shear zones in basement rocks of the Ramapo seismic zone, New York and New Jersey, and their relationship to current seismicity, *in* Manspeizer, Warren, ed., Field studies of New Jersey geology and guide to field trips, 52nd annual meeting of the New York State Geological Association, p. 278-311.

Ratcliffe, N.M., Burton, W.C., D'Angelo, R.M., and Costain, J.K., 1986, Low-angle extensional faulting, reactivated mylonites, and seismic reflection geometry of the Newark basin margin in eastern Pennsylvania: Geology, v. 14, p. 766-770.

Ratcliffe, N.M., Burton, W.C., and Pavich, M.J., 1990,

Orientation, movement history, and cataclastic rocks of the Ramapo fault based on core drilling, and trenching along the western margin of the Newark basin near Bernardsville, New Jersey: U.S. Geological Survey Miscellaneous Investigation Series Map I-1982.

Retallack, G.J., 2001, Soils of the Past, and Introduction to Paleopedology: Blackwell Science Ltd., Osney Mead, Oxford, England, 404. P.

Sanders, J.E., 1963, Late Triassic tectonic history of northeastern United States: American Journal of Science, v. 261, p. 501-524.

Schlische, R.W., 1992, Structural and stratigraphic development of the Newark extensional basin, eastern North America: Evidence for the growth of the basin and its bounding structures: Geological Society of America Bulletin, v. 104, p. 1246-1263.

Schlische, R.W., and Olsen, P.E., 1988, Structural evolution of the Newark basin, *in* Husch, J. M., and Hozik, M.J., eds., Geology of the central Newark basin: Field guide and proceedings of the 5th Annual meeting of the Geological Association of New Jersey, p. 43-65.

Schlische, R.W., and Olsen, P.E., 1990, Quantitative filling model for continental extensional basins with application to the early Mesozoic rifts of eastern North America: Journal of Geology, v. 98, p. 135-155.

Serfes, M.E., 1994, Natural groundwater quality in bedrock of the Newark basin: N.J. Geological Survey Report GSR 35, 32 p.

Serfes, M.E., Spayd, S. E., Herman, G.C., and Monteverde, D. H., 2000, Arsenic occurrence, source and possible mobilization mechanisms in groundwater of the piedmont physiographic province in New Jersey: EOS, Transactions of the American Geophysical Union Fall Meeting, v. 81, no. 48, p. F525-H210-08.

Serfes, M.E., Spayd., S.E., Herman, G.C., 2005, The occurrence, sources, mobilization, and transport of groundwater in the Newark basin of New Jersey, *in* O'Day, P.A., Vlassopoulos, Meng, Xiaoguang, and Benning, L.G., eds., Advances in Arsenic Research; Integration of Experimental and Observational Studies and Implications for Mitigation, Chapter 13: American Chemical Society Symposium Series 915, Washington, District of Columbia, p. 175-190.

Smoot, J.P., and Olsen, P. E., 1985, Massive mudstones in basin analysis and paleoclimatic interpretation of the Newark Supergroup, *in* Robinson, G. R., and Froelich, A. J., eds., Proceedings of the second U.S. Geological Survey workshop on the Early Mesozoic basins of the Eastern United States: U. S. Geological Survey Circular 946., p. 29-33.

Smoot, J.P., and Olsen, P.E., 1988, Massive mudstones in basin analysis and paleoclimatic interpretations, *in* Manspeizer, W., ed., Triassic-Jurassic rifting, continental breakup, and the origin of the Atlantic Ocean and passive margins, Part A: , Elsevier, Amsterdam, The Netherlands, p. 249-274.

Smoot, J.P., and Olsen, P.E., 1994, Climatic cycles as sedimentary controls of rift-basin lacustrine deposits in the early Mesozoic Newark basin based on continuous core, *in* Lomando, T., and Harris, M., eds. Lacustrine depositional systems: Society of Economic Paleontologists and Mineralogists Core Workshop Notes, v. 19, p. 201-237.

Spayd, S.E., 1985, Movement of volatile organics through a fractured rock aquifer: Groundwater, v. 23, no. 4, p. 496-502.

Stanford, S.D., 2000, Overview of the glacial geology of New Jersey, *in* Harper, D. P. and Goldstein, F. R., eds., Glacial Geology of New Jersey: Field Guide and Proceedings for the 7th Annual Meeting of the Geological Association of New Jersey, p. II-1 to II-24.

Stanford, S.D., Ashley, G. M., and Brenner, G. J., 2001, Late Cenozoic fluvial stratigraphy of the New Jersey Piedmont: A record of glacioeustacy, planation, and incision on a low-relief passive margin: Journal of Geology, v. 109, p. 265-276.

Stanford, S.D., Monteverde, D.H., Volkert, R.A., Sugarman, P.J., and Brenner, G.J, 1998, Geology of the New Brunswick quadrangle, Middlesex and Somerset Counties, New Jersey: N.J. Geological Survey Open-file Map 23, scale 1:24,000 scale; 3 sheets.

Szabo, Z., Taylor, T.A., Payne, D.F., and Ivanchenko, T., 1997, Relation of hydrogeologic characteristics to distribution of radioactivity in groundwater, Newark basin, New Jersey: U.S. Geological Survey Water-Resources Investigations Report 95-4136, 134 p.

Tabakh, M. El, and Schreiber, B.C., 1998, Diagenesis of the Newark rift basin, Eastern North America: Sedimentology v. 45, p. 855-874.

Tabakh, M. El, Schreiber, B.C., and Warren, J.K., 1998, Origin of fibrous gypsum in the Newark basin, eastern North America: Journal of Sedimentary Research, v. 68, p. 88-99.

Tollo, R.P., and Gottfried, D., 1992, Petrochemistry of Jurassic basalt from eight drill cores, Newark basin, New Jersey: Implications for the volcanic petrogenesis of the Newark Supergroup, *in* Puffer, J. H. and Ragland, P. C., eds., Eastern North American Mesozoic Magmatism: Geological Society of America Special Paper 268, p. 233-259.

Van Houten, F.B., 1962, Cyclic sedimentation, Upper Triassic Lockatong Formation, central New Jersey and adjacent Pennsylvania: American Journal of Science, v. 260, p. 561-576.

Van Houten, F.B., 1965, Composition of Triassic Lockatong and associated formations of Newark Group, central New Jersey and adjacent

Pennsylvania: American Journal of Science, v. 263, p. 825-863

Vecchioli, J., 1965, Directional hydraulic behaviour of a fractured-shale aquifer in New Jersey: International Association of scientific hydrology; Symposium of Dubrovnik, Croatia, p. 318-326.

Vecchioli, J., Carswell, L.D., and Kasabach, H.F., 1969, Occurrence and movement of groundwater in the Brunswick Shale at a site near Trenton, New Jersey: U.S. Geological Survey Professional Paper 650-B, p. B154-B157.

Volkert, R.A., 2006, Bedrock Geologic map of the Paterson quadrangle, Passaic, Essex and Bergen Counties, New Jersey: N.J. Geological Survey Geologic Map Series GMS 06-6, scale 1: 24,000.

Weems, R.E., and Olsen, P.E., 1997, Synthesis and revision of groups within the Newark Supergroup, eastern North America: Geological Society of America Bulletin, v. 109, no. 2, p. 195-209.

Withjack, M.O., Islam, Q.T., and La Pointe, P.R., 1995, Normal faults and their hanging-wall deformation: An experimental study: American Association of Petroleum Geologists Bulletin, v.79, no. 1, p. 1-18.

Xiao, H., and Suppe, J., 1992, Origin of rollover: American Association of Petroleum Geologists Bulletin, v. 76, no. 4, p. 509-529.